



# Identification and validation of novel adipokines in mouse models for obesity and type 2 diabetes mellitus

INAUGURAL-DISSERTATION

Zur Erlangung des Doktorgrades  
der Mathematisch-Naturwissenschaftlichen Fakultät  
der Heinrich-Heine-Universität Düsseldorf

vorgelegt von  
Simon Göddeke  
aus Selm-Bork

2017

Diese Arbeit wurde angefertigt am

Deutschen Diabetes Zentrum  
Institut für klinische Biochemie und Pathobiochemie  
Leibniz Zentrum für Diabetes-Forschung

An der Heinrich Heine Universität Düsseldorf

Gedruckt mit der Genehmigung der  
Mathematischen-Naturwissenschaftlichen Fakultät der  
Heinrich-Heine-Universität Düsseldorf

Referent: Prof. Hadi Al-Hasani

Korreferent: Prof. Michael Feldbrügge

Tag der mündlichen Prüfung: 19.02.2018



Identification and validation of novel  
adipokines in mouse models for obesity and  
type 2 diabetes mellitus

INAUGURAL-DISSERTATION

Zur Erlangung des Doktorgrades  
der Mathematisch-Naturwissenschaftlichen Fakultät  
der Heinrich-Heine-Universität Düsseldorf

vorgelegt von  
Simon Göddeke  
aus Selm-Bork

2017

Diese Arbeit wurde angefertigt am

Deutschen Diabetes Zentrum  
Institut für klinische Biochemie und Pathobiochemie  
Leibniz Zentrum für Diabetes-Forschung

An der Heinrich Heine Universität Düsseldorf

Gedruckt mit der Genehmigung der  
Mathematischen-Naturwissenschaftlichen Fakultät der  
Heinrich-Heine-Universität Düsseldorf

Referent: Prof. Hadi Al-Hasani

Korreferent: Prof. Michael Feldbrügge

Tag der mündlichen Prüfung:

# Zusammenfassung

Die Prävalenz des Typ-2-Diabetes mellitus (T2DM) steigt seit den letzten Jahrzehnten kontinuierlich an und hat bis heute Ausmaße einer globalen Epidemie erreicht, wobei Fettleibigkeit den wichtigsten Risikofaktor für T2DM darstellt. Zusätzlich zur Funktion als Speicherorgan sekretiert das Fettgewebe Faktoren und Proteine (Adipokine), welche hormonähnliche Wirkung haben und zusammenfassend als „Sekretom“ bezeichnet werden. Eine Vergrößerung des Fettgewebes führt dazu, dass sich die Funktion der Adipozyten und deren Sekretionsprofil verändert.

Warum Fettleibigkeit manchmal keinerlei gesundheitliche Auswirkungen hat, in anderen Fällen jedoch zu erheblichen metabolischen Komplikationen führen kann, war die grundlegende Fragestellung dieser Arbeit. Dabei war die zentrale Hypothese, dass ein verändertes Fettgewebssekretom Auswirkungen auf den Energie- und Substratstoffwechsel hat und somit die Diabetessuszeptibilität modulieren kann.

Es wurde zunächst ein verbessertes Protokoll zur Analyse des Adipozytensekretoms entwickelt. Dadurch konnte die Probenqualität in Bezug auf Verunreinigung mit hoch abundanten Proteinen signifikant verbessert werden. In der nachfolgenden Proteomanalyse ermöglicht dies erst die Detektion von niedrig abundanten Adipokinen. Für diese Untersuchungen wurden geeignete Mausmodelle, die eine Diabetessuszeptibilität abbilden, verwendet. Ein monogenetischer Defekt im Leptin-Gen (*ob*) oder im Leptinrezeptor Gen (*db*) führt in Diabetes resistenten C57BL/6J (BL6) Mäusen nur zu Fettleibigkeit, wobei C57BL/Ks (BKS) Mäuse Fettleibigkeit in Kombination mit T2DM ausbilden.

Konditioniertes Medium von primären Adipozyten des viszeralen Fettgewebes (vWAT) von C57BL/6J (BL6) und C57BL/Ks (BKS) Mäusen wurde gewonnen und als Surrogat für das Fettgewebssekretom untersucht. Das Sekretom von Adipozyten der beiden Mausmodelle wurde mittels Tandem-Massenspektrometrie analysiert, um zu klären, ob diese Prädisposition im Sekretionsprofil verankert ist. Der Vergleich beider Modelle lieferte 35 signifikant regulierte Adipokine, wovon sechs Proteine noch nicht als Adipokine des weißen Fettgewebes beschrieben wurden. Die vergleichende Proteomanalyse wurde auf die jeweiligen Krankheitsmodelle für Fettleibigkeit (B6.Cg-Lep<sup>ob</sup>; *ob*) und T2DM (B6.BKS(D)-Lepr<sup>db</sup>; *db*) erweitert.

In dieser Arbeit konnte T-cadherin (CDH13) erstmals als reguliertes Adipokin identifiziert werden. Sowohl die Proteinabundanz als auch die mRNA Expression im vWAT waren geringer in beiden fettleibigen Mausmodellen. *In vitro* Experimente zeigten, dass die Expression von T-cadherin während der Fettzeldifferenzierung und somit steigendem Fettgehalt verringert wurde. Eine Abschwächung der T-cadherin Expression durch siRNA reduzierte jedoch die Expression von PPAR $\gamma$  und C/EBP $\alpha$ , was zu einer Verzögerung der Adipogenese und einer Verringerung des Fettgehalts im Adipozyten führte. Dies belegt, dass eine geringe T-cadherin Expression nicht

ursächlich für die Fettzellhypertrophie ist. Analysen von Fettgewebsbiopsien aus humanen Kohorten bestätigten eine geringere T-cadherin Abundanz im vWAT und darüber hinaus im Blutplasma fettleibiger Patienten im Vergleich zu schlanken Patienten. Die Gewichtsabnahme durch eine bariatrische Operation führte zu einer Erhöhung der T-cadherin Konzentration im Blut, die vergleichbar mit Werten der schon vorher schlanken Kontrollen war. Demnach eignet sich T-cadherin als Biomarker, der den Gesundheitsstatus des Fettgewebes widerspiegelt.

Darüberhinaus wurde das Sekretom im Zusammenhang mit bioaktiven Metaboliten untersucht. Der Einfluss von Diacylglycerolen (DAGs) auf die Insulinresistenz wurde schon in Leber und Pankreas nachgewiesen und dieser Zusammenhang sollte im Fettgewebe analysiert werden. Hierbei zeigte sich, dass db/db Mäuse generell höhere Gesamtmengen von DAGs aufwiesen als ob/ob Mäuse. Außerdem waren gesättigte Fettsäuren (C16:0 und C18:0) höher abundant in db/db als in BKS Mäusen. In ob/ob Mäusen war der Anteil von ungesättigten Fettsäuren (C16:1) höher als in den BL6 Mäusen. Mithilfe der Kombination von Proteomanalyse und klinischen Parametern (DAG Profil) wurden RNA-bindende Proteine identifiziert, die eine potenzielle Rolle in der metabolischen Kontrolle von Fettleibigkeit und Diabetes spielen könnten. Schlussendlich stellt diese Arbeit Sekretomdaten zur Verfügung, die zur Aufklärung der Pathogenese von Fettleibigkeit und T2DM beitragen können.

## Summary

The prevalence of Type-2-Diabetes mellitus has been rising in the last decades reaching dimensions of a global epidemic with obesity representing the main risk factor for T2DM. Besides having storage functions the adipose tissue has been described to act as an endocrine organ that secretes factors and proteins called “adipokines” which have hormone-like effects. The secretion pattern of the adipokines is changed during expansion of the adipose tissue and might be fundamental for the pathogenesis of obesity and T2DM.

In this work, a key question of metabolic research was addressed: What is the difference of obesity in healthy, unhealthy or even diabetic conditions? This question was investigated referring to the adipose tissue and whether the disease susceptibility can be found upon the level of the secretome. The basis of this thesis was the design of a protocol to generate conditioned medium from primary murine adipocytes. Here, a significant improvement of sample quality in terms of contamination with high abundant proteins and concentration of low-abundant proteins was accomplished which enables subsequent proteomic analyses. For these analyses suitable mouse models that resemble diabetes susceptibility were used. Both monogenic defects in either leptin (*ob*) or the leptin receptor (*db*) result in obesity in diabetes resistant C57BL/6J (BL6) mice, but lead to an obese diabetic phenotype in diabetes prone C57BL/Ks (BKS) mice.

Primary adipocyte conditioned medium (secretome) of C57BL/6J (BL6) and C57BL/Ks (BKS) mice was generated and analyzed via high resolution tandem mass spectrometry. The comparison of both secretomes yielded 35 adipokines to be differentially regulated between the mouse strains. Thereof, we were able to identify six proteins that had not been described as adipokines before. Secretomes of related disease mouse models for obesity (B6.Cg-Lep<sup>ob</sup>; *ob*) and diabetes (B6.BKS(D-Lepr<sup>db</sup>; *db*) were analyzed subsequently.

In this work, T-cadherin was identified as a novel adipokine. The T-cadherin protein as well as mRNA expression in the vWAT is consequently downregulated in the obese mouse models. *In vitro* studies showed that downregulation of T-cadherin expression lowered PPAR $\gamma$  and C/EBP $\alpha$  expression resulting in deceleration of adipogenesis and a decrease of lipid content of the adipocyte. Translational experiments in human cohorts confirmed the lower levels of T-cadherin expression in the vWAT as well as decreased circulating levels of T-cadherin in obese patients compared to lean controls. Bariatric surgery induced weight-loss re-established circulating T-cadherin comparable to lean control levels. The regulation of T-cadherin induces collateral effects in adipogenesis rather suggesting it as a biomarker for the health status of the adipose tissue.

Furthermore, the secretome was analyzed with regard to bioactive metabolites. The effects of Diacylglycerols (DAGs) on insulin resistance have been described in tissues like the liver or pancreas. Therefore, these interrelations were analyzed in the vWAT. Generally, a higher content of diacylglycerols (DAGs) in *db* mice compared to non-diabetic *ob* mice was detected.

Additionally, saturated fatty acids (C16:0 and C18:0) were identified to be higher abundant in db mice, whereas ob mice showed unsaturated C16:1 to be changed when compared to the respective controls. The combined analysis yielded novel interrelations of proteomic and lipidomic data, like RNA-binding proteins, that might play a role in metabolic control of obesity and diabetes. Especially the combination of proteomic analysis and clinical parameters (DAG profile) was demonstrated to be a useful add-on to receive new insights in the regulation of the secretome upon certain affections. Ultimately, this thesis provides secretome data that might contribute to the elucidation of the pathogenesis of obesity and T2DM.

## List of abbreviations

2D-DIGE	2 dimensional in gel electrophoresis
3T3-L1	murine fibroblast cell line
ADA	american diabetes association
AgRP	agouti related peptide
Akt	protein kinase b
AMPK	AMP-activated protein kinase
AP-1	activator protein 1
B10	C57Bl/10 mouse
BAT	brown adipose tissue
BBB	blood brain barrier
BFA	brefeldin A
BKS	C57BL/Ks
BL6	C57BL/6J
BMI	body mass index
C/EBP	CCAAT/Enhancer binding proteins
C2C12	murine myoblast cell line
CaCl <sub>2</sub>	calcium chloride
cAMP	cyclic AMP
CART	cocaine- and amphetamine regulated Transcript
CCL2	CC-chemokine ligand 2
CD36	cluster of differentiation 36 (fatty acid translocase 4)
CDH13	cadherin 13
CDK	cyclin dependent kinase
CREB	cAMP response element-binding protein
CVD	cardiovascular disease
DAG	diacylglycerol
DIO	diet induced obesity
DLK	protein delta homolog 1
DM	diabetes mellitus
EGF	epidermal growth factor
ELISA	enzyme-linked immunosorbent assay
ER	estradiol receptor
ERK1/2	extracellular signal–regulated kinase 1/2
ESI	electrospray ionisation
eWAT	epicardial adipose tissue
FABP	fatty acid binding protein
FAT	fatty acid translocase
FATP	fatty acid transport protein
FCS	fetal calf serum
FDR	false discovery rate
FFA	free fatty acid

FGF21	fibroblast growth factor 21
FoxO3a	forkhead-box-protein O3
GLUT	glucose transporter
GO	gene ontology database
GR	glucocorticoid receptor
GRP-78	78 kDa glucose-regulated protein
GSK-3 $\beta$	glycogen synthase kinase 3 $\beta$
HCC	hepatocellular carcinoma cell
HDL	high density lipoprotein
HIF-1 $\alpha$	hypoxia inducible factor 1 alpha
HMW	high molecular weight
HSL	hormone sensitive lipase
HUVEC	human umbilical vein endothelial cell
IDF	international diabetes federation
IGF	insulin like growth factor
IgG	immunoglobulin G
IL-6	interleukin 6
ILK	integrin linked kinase
IP3	inositoltrisphosphate
IPA	ingenuity pathway analysis
IRS	insulin receptor substrate
JAK2	janus kinase
KEGG	kyoto encyclopedia of genes and genomes
KLF	kruppel like factor
LC	liquid chromatography
LDL	low density lipoprotein
LEPRb	leptin receptor b
LPL	lipoprotein lipase
MAG	monoacylglycerol
MALDI-TOF	matrix assisted laser desorption ionization - time of flight
MC4R	melanocortin 4 receptor
MCP-1	monocyte chemotactic protein 1
MEF	mouse embryonic fibroblasts
MHO	metabolic healthy obese
Mrap2	melanocortin 2 receptor accessory protein 2
MS/MS	tandem mass spectrometry
mTOR	mammalian target of rapamycin
MUNW	metabolic unhealthy normal weight
NAFLD	non alcoholic fatty liver disease
NC	normal chow diet
NF $\kappa$ B	nuclear factor kappa B
nPKC	novel protein kinase C
NZO	new zealand obese
PBS	phosphate buffered saline
PDE-3B	phosphodiesterase 3b

PDGF	platelet derived growth factor
PGC-1 $\alpha$	Peroxisome proliferator-activated receptor gamma coactivator 1-alpha
PKA	protein kinase a
PL	pancreatic lipase
PLC	phospholipase C
POMC	proopiomelanocortin
PPAR $\gamma$	peroxisome proliferator-activated receptor gamma
Pref-1	preadipocyte factor 1
pWAT	perivascular adipose tissue
RER	respiratory exchange ratio
RhoA	ras homolog family member A
RNA	ribonucleic acid
scWAT	subcutaneous adipose tissue
shRNA	short hairpin RNA
siRNA	small interfering RNA
SREBP-1	sterol regulatory element binding protein 1
STAT	signal transducer and activator of transcription
STZ	streptozotozin
SVC	stromal vascular cells
T1DM	type 1 diabetes mellitus
T2DM	type 2 diabetes mellitus
TCF/LEF	T-cell factor/lymphoid enhancer factor
TNF	tumor necrose factor
VEGF	vascular endothelial growth factor
VLDL	very low density lipoprotein
vWAT	visceral white adipose tissue
WAT	white adipose tissue
WHO	world health organization

# Table of Contents

Zusammenfassung	I
Summary	III
List of abbreviations	V
Figures	X
1 General introduction	- 1 -
1.1 Diabetes - a global epidemic	- 1 -
1.1.1 Classification of T1/T2DM and the metabolic syndrome	- 2 -
1.1.2 Obesity as a risk factor for T2DM	- 3 -
1.1.3 Inheritance of the metabolic state	- 4 -
1.2 Adipose tissue	- 5 -
1.2.1 Adipogenesis	- 5 -
1.2.2 Lipid metabolism in general	- 7 -
1.2.3 Glucose uptake	- 8 -
1.2.4 Ectopic lipid storage / Glucolipotoxicity in the liver	- 9 -
1.3 Secretome – the concept of the “kines”	- 10 -
1.3.1 Adipokines in obesity/ T2DM	- 11 -
1.3.2 The generation of adipose tissue secretome	- 13 -
1.4 Mouse models in basic metabolic research	- 15 -
1.4.1 The history of ob and db	- 16 -
1.4.2 Disease susceptibility	- 17 -
1.4.3 BKS susceptibility	- 17 -
1.5 Thesis outline	- 18 -
2 General discussion	- 89 -
2.1 Analysis of high quality secretome	- 89 -
2.2 Proteomic analyses identify T-cadherin as a novel adipokine	- 91 -

2.3 T-cadherin function in cell growth and metabolism	- 92 -
2.4 T-cadherin regulation in the WAT and lipid metabolism	- 94 -
2.5 Comprehensive analysis of vWAT secretome	- 98 -
2.6 Perspectives	- 99 -
3. Further contributions	- 100 -
Article Z1: So close and yet so far: mitochondria and peroxisomes are one but with specific talents	- 100 -
Article Z2: Peroxisomes compensate hepatic lipid overflow in mice with fatty liver	- 101 -
Article Z3: Alteration of liver peroxisomal and mitochondrial functionality in the NZO mouse model of metabolic syndrome.	- 102 -
Article Z4 (submitted): Liver - to - adipose tissue de novo lipid synthesis ratio associates with adipokinome signatures and serum lipid levels in NAFLD mouse models.	- 103 -
Bibliography	- 105 -

## Figures

<b>FIGURE 1:</b> SCHEMATIC PROCESS OF ADIPOGENIC DIFFERENTIATION AND TRANSCRIPTIONAL STATUS OF THE CELLS.....	6
<b>FIGURE 2:</b> REGULATION OF ADIPOKINES IN THE LEAN (GREEN) AND THE OBESE (RED) STATE AND THEIR EFFECT ON INSULIN SENSITIVE TISSUES.....	11
<b>FIGURE 3:</b> 2-D GELS (STAINFREE) OF CONDITIONED MEDIUM FROM PRIMARY WAT ADIPOCYTES. (A) UNTREATED ADIPOCYTES; (B) ADIPOCYTES WASHED WITH 3 mM CaCl <sub>2</sub> .....	90
<b>FIGURE 4:</b> WORKFLOW SCHEME TO GENERATE SECRETOME SAMPLES FROM DIFFERENTIATED MOUSE ADIPOCYTES.....	90
<b>FIGURE 5:</b> INTERACTIONS OF T-CADHERIN.....	94
<b>FIGURE 6:</b> SCHEME OF T-CADHERIN ABUNDANCE DURING VWAT DIFFERENTIATION.....	97

# 1 General introduction

## 1.1 Diabetes - a global epidemic

Diabetes is nowadays considered as one of the biggest health risks with globally around 422 million people suffering from the disease in 2014 compared to 108 million patients in 1980 [3]. In the same period, worldwide prevalence almost doubled from 4.7 % to 8.5 %. According to the world health organization 1.6 million people died due to diabetes mellitus (DM) in 2015 [3]. This number has almost doubled since the year 2000 and by 2030 DM is estimated to become the 7th leading cause of death (<http://www.who.int/diabetes/global-report>). The number of patients suffering from type 1 diabetes mellitus (T1DM) is constantly increasing by 2-5% but the prevalence of DM in general doubled within the last 20 years [4, 5]. Because of the fact that about 10% of all patients suffer from T1DM, the rise in DM incidence is mainly due to an increase of type 2 diabetes mellitus (T2DM). Additionally, not all patients are aware of their disease. Based on estimations of the American Diabetes Society, 8.1 million diabetic Americans out of 29.1 million diabetics in total are undiagnosed ([www.diabetes.org](http://www.diabetes.org)). In the USA, the diabetes prevalence in seniors (65 years or older) remains high at about 26 % [6]. However, alarming is that the prevalence of younger diabetics (44-65 years) tripled in the last 20 years. In combination with the fact that the number of people (age 20 and older) diagnosed with prediabetes increased by about 8 % between 2010 and 2012 (in US) this demonstrates that the onset of the disease is shifting more and more to younger ages [6]. Besides being a health burden, DM is a threat to global economic welfare. In 2010 between 5-13 % (11.6 % in average) of global healthcare expenditures was spent on diabetes. According to extrapolations, 80 % of global healthcare spending will be covered by high-income states, although 80 % of diabetics will live in low- or middle-income countries [7]. Corresponding to the International Diabetes Federation (IDF) Diabetes Atlas 2010, the global spending on diabetes healthcare varied between 376 billion US\$ with the North American and European region paying about 320 billion US \$. Furthermore, it was estimated that health expenditures for diabetes will grow by 30 % to 34 % between 2010 and 2030, which is more than the assumed global population growth (28.6 %) among persons aged 20-79 years over the same period. This upcoming imbalance will be supported by the demographic trend of ageing and increasing urbanization [8]. In summary, all these numbers show that DM is a global health burden with onset at an ever-earlier age emphasizing that investigation of the mechanics of the disease is essential in order to stall this development.

### **1.1.1 Classification of T1/T2DM and the metabolic syndrome**

At first glance, T1DM, T2DM and the metabolic syndrome seem to be similar with hyperglycemia as one of the first recorded symptoms. According to fasting blood sugar, plasma concentrations of more than 126 mg/dl (7 mmol/l) classify patients as diabetic. This parameter alone is outdated and needs to be verified with the measurement of hemoglobin A1c (HbA1c). This long-term blood glucose determination is the gold standard of diabetes detection and is used for therapy control as well. A HbA1c of more than 6.5 % of the past 10-12 weeks is considered as the threshold for diabetes (WHO, IDF, ADA; [9]). Yet, this symptom alone is not sufficient to discriminate between T1DM and T2DM. The differential diagnosis is based on the general constitution of the patient and additional blood parameters. T1DM is defined as a chronic, immune-mediated disease that leads to beta cell failure with ensuing absolute lack of insulin. Therefore, serological detection of autoimmune markers or the measurement of genetic markers are required to validate T1DM.

The term of the metabolic syndrome is used very frequently in prediabetic conditions regarding the evaluation of plasma glucose levels. When fasting blood-glucose exceeds 100 mg/dl patients exhibit an impaired glucose tolerance which classifies them as prediabetic. Yet, definition-wise additional symptoms must be present to be diagnosed with metabolic syndrome. Abdominal girth of more than 94 cm in males or 80 cm in females is a prerequisite. Additionally, two of the following conditions have to be met: Elevated plasma triglycerides ( $\geq 150$  mg/dl), low HDL-cholesterol (male:  $\leq 40$  mg/dl; female:  $\leq 50$  mg/dl), hypertension (systolic:  $\geq 130$  mmHg; diastolic:  $\geq 85$  mmHg) or increased blood glucose levels ( $\geq 100$  mg/dl) (IDF, 2005; Diabetologie und Stoffwechsel 2014).

In the early stages of the disease, T2 diabetics show hyperinsulinemia and high c-peptide levels. However, long-term plasma glucose measurements are the best evidence for T2DM in combination with the general constitution. In contrast to T1DM, T2 diabetic patients are predominantly obese which mostly occurs before the manifestation of diabetes. Due to that correlation obesity is considered as the main risk factor to develop T2DM.

### **1.1.2 Obesity as a risk factor for T2DM**

Obesity or overweight represent the major risk factors for metabolic disorders. Both are measured by the body mass index (BMI) which describes a person's bodyweight in relation to his height ( $\text{kg/m}^2$ ); WHO). Overweight is characterized by a BMI between 25 and 30, whereas exceeding a BMI of 30 is defined as obesity. Although the assessment via BMI is a rough estimate it bears some pitfalls, because young children (<5 years) and professional athletes would easily be classified as overweight or obese. In such cases, it is more applicable to calculate the fat and lean mass in detail. Typically, obesity is marked by an increase in white adipose tissue (WAT) mass. Increased WAT usually includes more (hyperplasia) and bigger (hypertrophy) adipocytes. Obesity is considered as a major risk factor for many diseases like cardiovascular diseases (CVD), DM and musculoskeletal disorders [10]; [11]; [12]. In 2014, 39 % of adults worldwide (>18 years of age) were overweight and 13 % were obese per definition. These numbers have been rising in the last decades, even doubling between 1980 and 2014 (WHO). Obesity is often considered as a complication of the "rich" due to imbalance between physical activity and caloric intake. This imbalance might be influenced by a change in mobility with increased passive transportation, sedentary styles of work and urbanization, whereas simultaneously the energy-density of food increases. However, like T2DM, the incidence of obesity is also increasing in urbanized areas of low- and middle-income countries. In Africa, the number of overweight and obese children increased from 5.4 % to 10.6 % between 1990 and 2014 (Global Nutrition Report 2015 [13]; [14]; [15]; [16]. Although obesity is the undisputable major risk factor for metabolic diseases, some obese patients remain metabolically healthy lacking dyslipidemia and impaired glucose tolerance. Metabolically healthy obese (MHO) patients exhibit less visceral white adipose tissue (vWAT), smaller adipocytes and a reduced inflammatory profile but about 50% are supposed to turn into unhealthy obese patients longitudinally [17]; [18]. On the other hand, there are metabolically unhealthy normal weight (MUNW) patients. A recent study identified adipose tissue function as a crucial characteristic for metabolic implications [19].

Genetically, a few mutations are known that directly cause obesity. For example, a mutation of the melanocortin 2 receptor accessory protein 2 (Mrap2) gene leads to increased food consumption and weight gain due to subsequent absence of signaling via melanocortin 4 receptor (MC4R) in the brain. However, less than 5 % of all obese patients carry a monogenic mutation that might be causative. Although these genes are presumably not responsible for the obese epidemic, such findings shed light on pathways and interactions that might be crucial for the development of the disease.

### **1.1.3 Inheritance of the metabolic state**

In addition to genetic factors, environmental cues contribute to the disease pathogenesis. This influence might already start during gestation, in which the feeding status of the parents is handed down to the progeny by epigenetic modifications. It was recently demonstrated in mice that offspring of high fat diet (HFD) fed parents gain more weight upon a HFD feeding compared with offspring of normal chow (NC) fed parents [20]. Moreover, plasma insulin and glucose levels were increased in mice whose parents were fed a HFD. When only the male parent was supplemented with a HFD, the body weight of male offspring was increased and insulin and glucose levels were higher compared with mice whose mother was the only parent receiving a HFD [20]. This study proposes a key role for the father in the inheritance of the metabolic state in mice. Additionally, it was also shown that there is even a transgenerational inheritance of the metabolic state. Exposing either the male or female parent to a metabolic challenge (HFD or fasting period), alterations in both the F1 and F2 generation according to disease risks, metabolites and gene expression are observable [21]. Analogue correlations could be observed in several human studies. High parental BMI could be identified as a strong independent risk factor for childhood obesity and maternal BMI was even classified as a predictor of BMI z-scores in young children [22]; [23]; [24]; [25]; [26]. On the other hand, gestational fasting due to a famine influences offspring metabolic constitution as well. Studies demonstrated an increase in total cholesterol and triglycerides in female offspring while males were unaffected [27]. When caloric restriction during gestation was combined with subsequent high caloric intake by the offspring in the following, the effect was even boosted. Taken together, these findings support the hypothesis of epigenetic priming and disease susceptibility.

## 1.2 Adipose tissue

The white adipose tissue (WAT) is a lipid storage organ that stores excess nutritional energy like lipids and glucose in times of caloric surplus. By esterification to glycerol, fatty acids (FAs) are stored as triglycerides and during energy scarcity they are released back into circulation. Glucose is primarily used to form glycerol, because adipocytes do not express glycerol transporters, or it is transformed to glucose-6-phosphate and acetyl-CoA to finally form fatty acids. The WAT consists of many different depots and accumulated lipids can exert different effects on metabolism depending on the location of the depot. The two most prominent fat depots are the visceral adipose tissue (vWAT) and subcutaneous adipose tissue (scWAT). This generalization disregards the visceral adipose tissue as an umbrella term that describes all depots within the peritoneal cavity. All visceral depots are derived ontogenetically from a common progenitor and express Wilms' tumour gene (Wt1) whereas the subcutaneous depots are not [28]; [29]. The vWAT is supposed to exert detrimental effects promoting insulin resistance, glucose intolerance, dyslipidemia, hypertension and coronary artery disease [30]; [31]; [32]; [33]. Yet, the scWAT does not act harmful, it is rather described to have protective functions with regard to insulin resistance [34]; [35]. Moreover, Laplante et al. proposed that scWAT was more prone to a Peroxisome proliferator-activated receptor gamma (PPAR $\gamma$ ) agonist than vWAT leading to increased scWAT mass and reduced vWAT due to higher Lipoprotein lipase (LPL) activation in rodents. The treatment of T2D patients with rosiglitazone, a PPAR $\gamma$  agonist, increased subcutaneous but not visceral adipose tissue depots [36]. Studies have shown that losing scWAT by liposuction but maintaining vWAT mass does not improve insulin sensitivity and health [37]. However, losing vWAT mass leads to enhancement of metabolic parameters [38]. It was demonstrated that vWAT is reduced faster than the scWAT during moderate weight loss [39]; [40]. Additionally, the biggest improvement of metabolic parameters was observed in the early stages of weight loss (5-10 % of initial weight, [41]). However, the correlations of early weight loss due to fasting and amelioration of insulin sensitivity is still highly debated. Other studies rather correlate it to the loss of ectopic hepatic lipids and the concept of lipotoxicity, which is addressed later, than to a decrease of adipose tissue mass [42].

### 1.2.1 Adipogenesis

Because the vWAT is considered as detrimental and disease-causing, it is of interest to investigate its function and especially the secretome in diseased states. To be able to exert storage and secretion in a fully functional way the designated cells have to follow a differentiation process that comprises a specific course of events. Deteriorations of this process can cause metabolic implications like obesity, T2DM or liver disease [43]; [44]; [32]; [45]; [46].

Adipocytes emerge from mesenchymal stem cells (MSCs) which derive from the mesenchymal layer of the embryo. Extracellular cues make the cells lose their pluripotency thereby determining them as preadipocytes. When preadipocytes undergo growth arrest, the expression of two crucial factors is stimulated. Peroxisome proliferator-activated receptor gamma (PPAR $\gamma$ ) and CCAAT/enhancer binding protein alpha (C/EBP $\alpha$ ) induce the expression of all factors needed to continue adipocyte differentiation [47]; [48]. However, these two factors are not the first step in adipogenesis, but rather activator protein 1 (AP-1), signal transducer and activator of transcription 5 (STAT5), kruppel like factor 4 (KLF4) and KLF5 which induce the expression of C/EBP $\beta$  and C/EBP $\delta$ . The latter two induce sterol regulatory binding protein 1 (SREBP-1) and KLF15 leading to the final activation of PPAR $\gamma$  and C/EBP $\alpha$  [49].

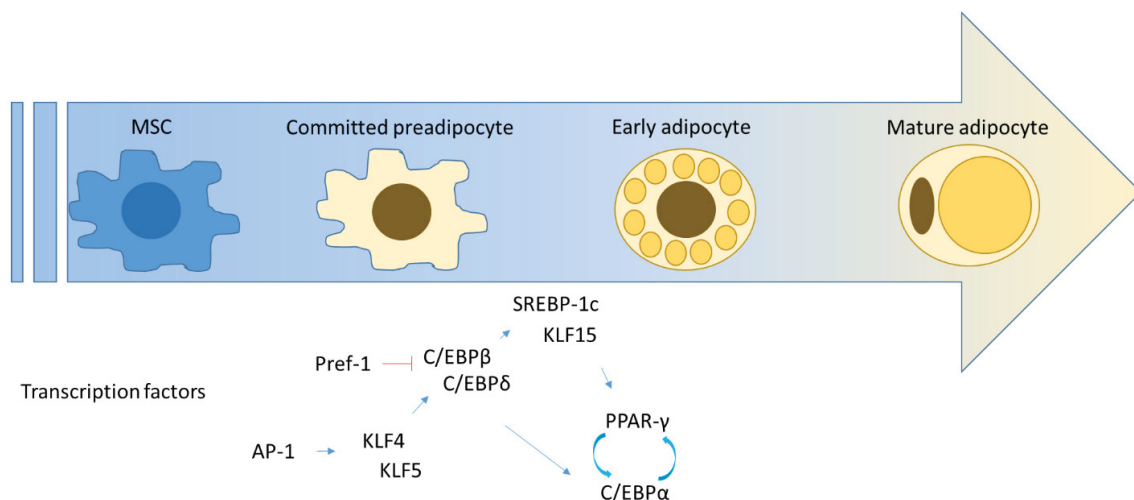


**Figure 1: Schematic process of adipogenic differentiation and transcriptional status of the cells.** The adipogenic program is induced by increased AP-1 expression in mesenchymal stem cells (MSC). Subsequent expression of KLF4 and KLF5 induce C/EBP- $\beta$  and - $\delta$  expression which commit the cell to the preadipocyte state. Downregulation of Pref-1 is crucial for subsequent adipogenesis. In line with C/EBP $\beta$  and  $\delta$ , activation of SREBP-1c and KLF15 expression causes induction of PPAR $\gamma$  and C/EBP $\alpha$ .

Regulation upon any level of this transcriptional cascade can crucially influence adipogenesis and obesity. Double-knockout mice of C/EBP $\beta$  and C/EBP $\delta$  have reduced WAT mass and decreased lipids in BAT. Additionally, embryonic fibroblast cells (MEFs) of these mice are not able to differentiate into mature adipocytes in response to hormonal stimulation [50]. This effect is probably due to absence of PPAR $\gamma$  and C/EBP $\alpha$  expression. Furthermore, blocking expression of the PPAR $\gamma$ 2 isoform in 3T3-L1 cells leads to a failure of adipogenesis, whereas restoring PPAR $\gamma$ 2 expression in PPAR $\gamma$  deficient cells reestablishes adipogenesis [51]. The disruption of initial steps of adipogenesis can lead to a total loss of white fat mass. Transgenic mice that express a dominant negative regulator of b-ZIP transcription factor binding within the adipose tissue do not develop white adipose tissue and less brown adipose tissue. The b-ZIP is needed for correct transcriptional activation of C/EBP $\alpha$  and C/EBP $\delta$ . This in turn leads to the manifestation of lipotrophic diabetes

with hyperlipidemic liver [52]. The lipodystrophic phenotype can also be observed in mice overexpressing nuclear SREBP-1c under the control of the adipose specific aP-2 promoter [53]. However, the same kind of overexpression of the SREBP-1a isoform leads to a completely different phenotype of mice showing fully differentiated adipocytes, no diabetes and only mild hepatic steatosis [54].

A key regulator of adipocyte differentiation is the transmembrane protein Pref-1 (in human) which is exclusively expressed in preadipocytes and its expression is diminished during ongoing adipogenesis [55]. Constitutive expression leads to inhibition of differentiation in 3T3-L1 preadipocytes and lipotrophy in aP2-mediated expression in mice [56]; [57]. In line with this, deletion leads to accelerated adiposity in mice [58]. Just like metabolic inheritance or obesity being inherited by males, paternal Pref-1 deficiency in mice led to accelerated adiposity in heterozygous offspring, but maternal deficiency did not [57]. Additionally, obese women exhibit fewer committed preadipocytes possibly due to a higher recruitment to adipogenesis or apoptosis [59].

### **1.2.2 Lipid metabolism**

The main task of adipose tissue is fatty acid synthesis, triglyceride storage and utilization. Following the ingestion, fat that usually occurs as triacylglycerides (TAGs) in the food is hydrolyzed by the pancreatic lipase (PL). Free fatty acids (FFA); diacylglycerides (DAGs) and monoacylglycerides (MAG) are released. These form micelles to be able to enter the enterocytes afterwards. Within the enterocyte, TAGs are reesterified again and chylomicrons are formed. These are secreted into the circulation and can be hydrolyzed by lipoprotein lipase (LPL) to enter target cells as monoacylglycerides or FA again. In case of an energetic surplus this happens in proximity of the adipose tissue. DAGs, MAGs and FAs are taken up by the tissue by fatty acid transport proteins with the help of membrane bound and cytosolic fatty acid binding proteins (FABPs). The fatty acid transport protein (FATP), plasma membrane fatty acid binding protein (pmFABP) and fatty acid translocase (FAT/CD36) are supposed to be the key players in this transport. Afterwards FAs are re-esterified to form TAGs and end up being stored in lipid droplets. During energetic scarcity lipolysis is induced so that FFAs can be utilized. TAGs are broken down by adipocyte triglyceride lipase (ATGL) into diacylglycerides and FFAs, the following step is the hydrolyzation of DAGs into MAGs and FFAs by hormone sensitive lipase (HSL) and the final enzyme monoglyceride lipase (MGL) releases the glycerol backbone and FFAs [60]. The latter enter the bloodstream to supply tissues with a lack of energy, whereas glycerol is principally taken up by the liver or kidney to rejoin the glycolysis or gluconeogenesis pathway. On the other hand, FAs can be utilized by  $\beta$ -oxidation in the mitochondria. Disruption of any stage in this network

can contribute to the development of obesity or T2DM [32]. The regulation of LPL is very complex and especially the ratio of skeletal muscle expressed LPL and adipose tissue LPL is crucial. Adipose LPL expression is upregulated with feeding and skeletal muscle LPL expression decreases. During exercise or low energy dense feeding the regulation is vice versa [61]; [62]. Insulin and glucose trigger LPL upregulation in adipose tissue [63]; [64], but interestingly fasting subsequent to an obese state increases the expression of LPL even more [65]; [66]. Diminished lipid uptake into the adipocyte generally ameliorates systemic insulin action. Deletion of whole-body CD36 in mice reduced lipid uptake into the adipocyte and increased insulin sensitivity but reduced inflammation in the adipose tissue [67]. However, CD36 seems not to be directly related to obesity but rather to metabolic complications like abnormal levels of FFA, HDL and LDL particles [68]; [69]. High density lipoprotein (HDL) and low density lipoprotein (LDL) transport cholesterol and fatty acids from peripheral tissues to the liver and vice versa respectively. Similarly, knockout of FABP4 and FABP5 results in increased insulin sensitivity [70]. Deletion of the FATP1, which is present in adipose tissue as well as skeletal muscle, did not improve overall insulin sensitivity, but in combination with a HFD the mice were protected from fat-induced insulin resistance [71]. A central aspect of the pathogenesis of insulin resistance, obesity and T2DM is probably represented by proteins that regulate lipolysis of TAGs within the adipose tissue [72]; [73]. In the insulin sensitive state, insulin inhibits lipolysis by activation of phosphodiesterase 3B (PDE-3B). PDE-3B hydrolyzes cAMP and inhibits activation of protein kinase A (PKA) so that phosphorylation of HSL does not take place. During insulin resistance there is no nutritional feedback or inhibiting cue for lipolysis what triggers FFA release. However, insulin resistance evoking higher lipolysis rates in adipocytes is highly debated, because there is no increase in HSL activation or basal lipolytic rate observable in the adipose tissue of obese humans [74]. When normalized to total body fat, lipolysis of obese and lean controls is even comparable [75]; [76]; [77]. On the other hand, larger adipocytes exhibit higher levels of cAMP resulting in higher basal lipolytic rates irrespective of insulin resistance [78]. Obesity is not definitely related to insulin resistance but rather to symptoms like ectopic lipid accumulation or adipose tissue inflammation which were demonstrated to induce cellular insulin resistance. Therefore, this relationship will be further addressed in the following chapters.

### **1.2.3 Glucose uptake**

In addition to the direct uptake of fatty acids to form triglycerides, adipocytes take up glucose in times of energy surplus. Postprandial glucose stimulates pancreatic secretion of insulin which binds to insulin receptors on respective tissues. The subsequent signaling cascade triggers phosphatidylinositol kinase (PI3K) activity which leads to the cell membrane presentation of glucose transporting proteins (GLUTs), primarily GLUT4 in the adipocyte [79]; [80]. Chronically

elevated glucose levels can only be partially overcome by glucose oxidation in skeletal muscle, but are rather compensated by increased glucose storage which can represent 60-70 % of total glucose uptake [81]. Glucose is either used to form glycerol, because adipocytes do not express glycerol transporters, or is transformed to glucose-6-phosphate and acetyl-CoA to finally form fatty acids. Although skeletal muscle is the main organ for acute glucose utilization, deteriorations of glucose uptake into the adipocyte have been shown to be involved in the manifestation of metabolic diseases [82]; [83]. Adipose-selective reduction of GLUT4 resulted in insulin resistance in muscle and liver although GLUT4 was preserved in these tissues [84]. Additionally, fat specific overexpression of GLUT4 was able to compensate for the skeletal muscle specific knockout in mice and to reverse whole body insulin resistance without restoring glucose transport in muscle [85]. Therefore, the glucose metabolism of the adipocyte has to be taken into account when insulin sensitivity is investigated.

#### **1.2.4 Ectopic lipid storage / Glucolipototoxicity in the liver**

In addition to the concept of a distending adipose tissue due to higher ingestion and the direct effects within the tissue, there are events taking place in other organs in parallel and subsequent to the adipose tissue enlargement. Unger *et al.* postulated as an initial idea of the concept of glucotoxicity that a continuous cellular surplus of glucose leads to depletion of insulin storage and due to that to decreasing glucose utilization in a downward spiral manner [86]. In the same way, the permanent exposition to lipids might lead to cellular lipotoxicity and affect the cell viability of pancreatic beta-cells, myocardium or skeletal muscle [87], [88]. Changes in osmolarity induce alterations in the fluidity of membranes and thus membrane-linked transport processes. This also severely affects cellular function and might lead to cell death. The combination of both leads to the concept of glucolipototoxicity, which eventually implies linkage of intracellular lipid content and composition to glucose levels [89]. Pathological cellular lipid accumulation in the liver is called non-alcoholic fatty liver disease (NAFLD) and clinical studies demonstrated an association with insulin resistance [90]. NAFLD is a very heterogeneous disease with a broad spectrum of histological indications and is considered as the hepatic manifestation of the metabolic syndrome. According to recent estimations of the WHO, two million patients are at risk of developing liver cirrhosis or liver associated diseases as a result of NAFLD or non-alcoholic hepatosteatosis [91]. In this regard, insulin resistance, adiposity and especially hypertriglyceridemia are named as the main risk factors. The increase of cellular hepatic lipid content can be based on disturbances of *de novo* lipid synthesis. In this context, the urgency of lipid clearance rises with increasing lipid content to circumvent cell damage. Typically, triglycerides are bound to ApoB transport proteins in the endoplasmic reticulum (ER) and assembled to very low density lipid (VLDL) particles that are secreted into the plasma. This

binding to ApoB is regulated by ApoB degradation in case of insufficient amount of cellular triglycerides, a process that is promoted by insulin/PI3K signaling [92]. Mitochondria typically use short-chain fatty acids as a substrate for  $\beta$ -oxidation whereas long-chain fatty acids have to be processed to C16-fatty acids by  $\beta$ -oxidation in peroxisomes. Mitochondrial function and oxidative capacity are diminished by chronic lipid excess [93]; [94]; [95]. Eventually, hyperglycemia can decrease insulin sensitivity and hypertriglyceridemia leads to hepatic dysfunction both amplifying their effects negatively.

### **1.3 Secretome – the concept of the “kines”**

The symptoms and the pathologic background of the metabolic syndrome are diverse. Because the reasons of the metabolic syndrome are often related to lifestyle and primarily nutrition, many investigations focus on the brain and hypothalamic regions. In addition to the pancreas, peripheral insulin-sensitive tissues like the liver, skeletal muscle and adipose tissue play a role in the pathogenesis of T2DM. Investigations do not only focus on them as solitary tissues but even on their complex, interconnected network which is generally summarized as inter-organ-crosstalk. This is primarily accomplished by factors that are secreted by the respective tissue and can exert hormone like effects. Depending on the secreting tissue they are called e.g. myo-, hepato-, or adipokines.

Interleukin-6 (IL-6) is a cytokine being secreted from many different cells and evoking various effects. However, nowadays it is primarily known as a myokine. The expression of IL-6 is upregulated in the contracting muscle fiber and the IL-6 protein is secreted upon muscle activity. It has anti-inflammatory effects and improves glucose uptake in the skeletal muscle [96]; [97]; [98]. As an endocrine effect, the infusion of IL-6 in humans led to lipolysis and fat oxidation in scWAT [99]. Additionally, IL-6 knockout mice show mature onset of obesity [100]. Energy expenditure could be increased by intracerebroventricular but not by intraperitoneal IL-6 infusion. This suggests a central effect of IL-6 on energy metabolism. In this context it was investigated whether blood borne IL-6 can cross the blood brain barrier (BBB) to have such effects, but only 16 % of the IL-6 remain intact after crossing the BBB [101]. Thus, centrally expressed IL-6 is the responsible cytokine to influence energy metabolism. In addition to that, many peripheral effects of IL-6 are known.

Fibroblast growth factor 21 (FGF21) has been described as a hepatokine [102]. Although it is also secreted by other tissues, the liver is contributing the most to circulating levels [102]. FGF21 was described to increase glucose uptake into skeletal muscle in the presence of insulin in humans [103] and to increase glucose uptake in 3T3-L1 cells and primary human adipocytes [104].

Overexpressing FGF21 was shown to lower blood glucose and plasma triglycerides in diabetic animals [105]. Systemic administration of FGF21 in diet induced obesity [106] and ob/ob mice led to a decrease in obesity due to an increase of energy expenditure [107].

Secretion of these factors is not restricted to a single organ but rather to several affecting each other in different ways. Regarding FGF-21, it was described not only to represent a hepatokine, but even a myo- and adipokine. Secreted by hepatocytes, FGF21 inhibits lipolysis in the WAT, myocytic FGF21 can protect against diet-induced obesity [106] and insulin resistance and adipocytic FGF21 induces browning of white adipose tissue [108].

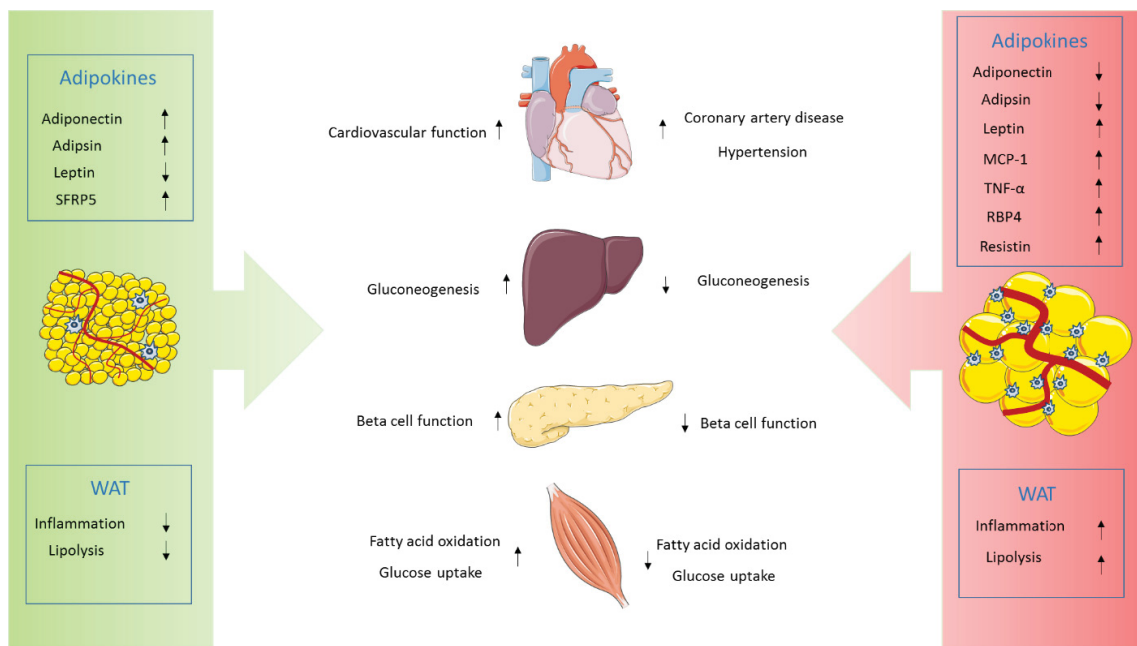


**Figure 2: Regulation of adipokines in the lean (green) and the obese (red) state and their effect on insulin sensitive tissues.** Ameliorating (arrow up) or deteriorating (arrow down) effects on the heart, liver, pancreas or skeletal muscle are illustrated by arrows.

### 1.3.1 Adipokines in obesity/ T2DM

Adipocytes can synthesize and secrete a number of enzymes, cytokines and hormones that affect energy metabolism [109]; [110]. The status of being overweight is mostly accompanied by a mixture of many other characteristics like mild inflammation, hyperglycemia or abnormalities in thermogenesis. The deleterious effects of obesity are often correlated with high vWAT mass. Due to higher lipolytic activity of this depot, increased amounts of fatty acids drain to the liver and can affect liver function [32]. However, being obese does not implicate secondary characteristics *per se*, but might rather be found in the alteration of the adipokine profile, the adipokinome [111]; [112]; [113].

After discovery of leptin being secreted from white adipose tissue in 1994 by Jeffrey Friedman, the latter became more recognized as an endocrine organ [114]. Leptin secretion increases with fat mass, transmits the energy status to the brain via POMC/CART neurons thereby regulating energy balance. Despite the fact that leptin is a central satiety signal, it was shown that obese patients exhibited increased levels of leptin in the circulation leading to the hypothesis of leptin resistance [115]. Many different results for the interaction of insulin and leptin have been reported. Initially, no short-term effect of insulin on leptin secretion was observable and on the other hand fasting neither acutely regulated leptin expression [116]; [117]; [118]; [119]. Within the following years of research the response of leptin secretion emerged to be regulated by the nutritional status of the patient but not due to diet in the short term [120], [121]. In rats leptin secretion increased due to a 96-hour supplementation of insulin. The increase was more directly related to glucose uptake which, when inhibited, led to an inhibition of leptin secretion [122]. Human patch clamp studies demonstrated that the amount of infused dextrose is related to serum leptin levels [123], because euglycemic-hyperinsulinemia clamp resulted in higher leptin response than hypoglycemic-hyperinsulinemic clamp.

Low-grade inflammation during obesity recruits cells of the innate and adaptive immune system to the adipose tissue [124]; [125]. TNF- $\alpha$  was identified as one of the first adipokines that is upregulated in obese animal models [126]; [127]. However, immune cells within the stromal-vascular fraction (SVF) release proinflammatory factors as well. Some studies even propose that the contribution to the release of certain adipokines is higher for certain stromal vascular cells (SVCs) than for adipocytes [128]. The inflammatory state links fat mass to insulin resistance and chemoattractant adipokines like monocyte chemoattractant protein 1 (MCP-1) might contribute to that scenario [129]. MCP-1 serum levels correlate with insulin resistance as diabetic patients have higher levels of MCP-1 [130]. Concomitantly, surgery-induced weight loss as a clinical diabetes treatment reduced circulating MCP-1 levels and ameliorated insulin sensitivity [131]. Referring to lipolysis and inflammatory state of enlarged adipose tissue, TNF- $\alpha$  can increase basal levels of adipocyte cAMP in rodents and reduce lipid droplet coating protein perilipin. Both effects lead to an increase of HSL activity and lipolysis [132]; [133]; [134]. Further, TNF- $\alpha$  upregulates MCP-1 in human preadipocytes and 3T3-L1 cells emphasizing the interaction of inflammation and adipokines [135]. In addition to adipocyte derived kines, immune cells can secrete factors that affect adipocyte function and contribute to the inflammation-induced insulin resistance [136]. Application of antiresistin IgG in diabetic obese rodents led to improved insulin sensitivity [137]. Although resistin is secreted at low levels in human adipocytes, the majority derives from monocytes and macrophages. Introduction of the human macrophage-deriving resistin into mice lacking adipocyte derived resistin led to a higher WAT inflammation, lipolysis and circulating free fatty acids [138]. Although the site of production differs between mice and men, the hormonal function is preserved.

Adiponectin was found to be exclusively secreted by adipocytes, but showed a negative correlation with adipose tissue mass. To date, it has been linked to several metabolic processes like peripheral insulin sensitivity and fatty acid oxidation [139]; [140]. As alluded to this topic before, local visceral adipose tissue depots might be involved in the association of CVD and obesity [141]. Two specific depots, the epicardial (eWAT) and the perivascular visceral adipose tissue (pWAT), are supposed to directly affect cardiac and vascular function [142]. In this regard, resistin was brought out to be associated with heart failure [143], whereas adiponectin was described to act cardioprotective [144].

Eckel *et al.* evaluated the relationship of proteins that are secreted from adipocytes as well as skeletal muscle, adipo-myokines. Depending on their secretory origin the adipo-myokines can exert different effects. A coin was used as a metaphorical illustration to describe their possible regulation. According to the percentage amount of skeletal muscle or adipose tissue in the body, the “coin flips” and the respective secretome is dominating in the body. This goes in line with the concept of MHO phenotype which describes normal adipose tissue function and absence of insulin resistance [145]; [146]. In contrast, the fact that lipodystrophic patients exhibit severe diabetes emphasizes the role of the adipose tissue as a normal functioning organ and balanced adipokine secretion in the preservation of metabolic health [147]; [148].

### **1.3.2 The description of the adipose tissue secretome**

To analyze a cell-specific secretome, the isolated cells are cultured for a defined period of time and the medium containing the secreted factors is considered as secretome. In this regard, the investigation contains many challenges and pitfalls. The processing of the tissue and isolation of pure adipocytes is the most essential step for all following experiments. In this work adipocyte secretome should be analyzed and the novel secreted factors that might play a role in pathologies like obesity and T2DM be investigated. Another challenge is to consider potential secretory mechanisms. The generation of secretome from untreated and Brefeldin A (BFA) treated cells is a chemical way to discriminate classical secretion from contamination or exocytosis respectively. A following comparison of both helps to identify commonly secreted proteins. However, this method does not register factors that reach the extracellular space in alternative routes, because BFA exclusively blocks major common secretion pathways [149]. Some factors like Dipeptidylpeptidase 4 (DDP4) are found in the extracellular space due to ectodomain shedding by metalloproteases which is also not blocked by BFA [150]. Furthermore some factors bypass the ER-golgi network or are translocated via lipidic pores into the extracellular space [151]. The hints for possible secretion can up to date only be evaluated by *in silico* analyses of the peptide sequences. Databases like SignalP or SecretomeP help to identify proteins within the secretome that are either classically secreted by a signal peptide (SignalP; [152]) or due to chemo-physical

properties (SecretomeP; [153]) which enable secretion with strong significance. Some studies have already pointed out that some factors that are not classically secreted are found within the secretome and should be considered as part of the secretome [154]. In addition to the type of secretome an additional processing step is important, because the detection of all factors is a big challenge. High abundant proteins like albumin can reflect up to 99 % of the secretome and some adipokines are found in a femtomolar range. Therefore an additional processing step is crucial to concentrate proteins of interest and deplete high abundant proteins to enable for MS/MS analysis [155-157]. So far, many different approaches have been conducted to gather the adipocyte secretome. However, because of the pitfalls mentioned above, the entity of identified adipokines is still growing and the adipocyte secretome is incompletely characterized. For a reliable detection of adipokines a combination of different methods like 2-D DIGE and ESI/MALDI-MS/MS emerged to be more suitable than using only one methodology. In 2002, the secretome of 3T3-L1 preadipocytes versus differentiated 3T3-L1 adipocytes was characterized using a combination of 1-DE and ESI-MS/MS [158]. At least for these cells, other combinations of techniques were tested in the following years mostly combining a gel-based method and one gel-free screening technology [159]; [160-162]. For the generation of adipocyte secretome, three different protocols have been used so far. Some groups use the complete WAT explants for cultivation [163]. Here, an appropriate representation of the whole adipose tissue secretome is achieved. Although it does not account for the in-depth adipocyte secretome, because all different kinds of cells contribute to the secretome, this methodology rather represents a physiological way to analyze the adipose tissue as a whole. The second strategy to generate adipocyte secretome is to isolate primary preadipocytes and differentiate them into adipocytes which offers pure adipocyte secretome. In terms of feasibility, most of the protocols for primary adipocyte culture focus on utilization of preadipocytes. They can be easily cultivated and used for treatments or co-cultivation experiments [164]. In this regard the choice of the adequate method is pivotal for the investigation of adipocyte or adipose tissue secretome and the identification of meaningful targets.

## 1.4 Mouse models in basic metabolic research

Animal models are used to investigate the impact of alterations of single genes with regard to the pathophysiology of diseases. Due to discoveries in basic research and identification of potential key players in the pathogenesis of a disease, respective genes can be modified *in vivo* to investigate their function in detail. Various knockouts are known so far that induce the development of obesity and insulin-independent diabetes. The modification of insulin signaling plays a central role in these models. The targeted systemic disruption of the insulin receptor (IR) leads to a severe form of diabetes with ketoacidosis, skeletal muscle hypotrophy and hepatic steatosis which results in neonatal death around day 7 [165]. By using the Cre/loxP system tissue specific knockouts can be generated and the function of insulin signaling can be investigated specifically [166]; [167]; [168]. In addition, there are artificial rodent models available with obese or diabetic phenotypes due to the knock in or overexpression of certain genes. Mice that overexpress c-Myc in beta cells under control of the rat insulin II promoter develop neonatal diabetes that is lethal at day three after birth due to increased beta cell apoptosis [169]. Transgenic mice that ubiquitously express the agouti related protein (AgRP), an orexigenic neuropeptide, exhibit hyperphagia, severe obesity and insulin resistance [170]. T1DM can easily be induced by treatment with chemical compounds like streptozotocin (STZ) or alloxan that destroy beta cells by necrosis [171]; [172]. Further, STZ can be applied in multiple low doses to induce a phenotype in mice that rather resembles T2DM [173]. Additionally, the chronic treatment with dexamethasone leads to insulin resistance and disturbed lipid metabolism when combined with HFD feeding [174].

In addition to man-made modifications there are natural spontaneous mutations leading to mice that develop phenotypes similar to human T2DM. The New Zealand Obese (NZO/HILt) mouse is a suitable polygenic mouse model for T2DM. Both sexes become severely obese upon a standard diet and exhibit impaired glucose tolerance, but only males develop T2DM like diabetes. Various congenic lines were bred from the NZO mouse to further analyze quantitative trait loci (QTL) that contribute to the complex phenotype [175]; [176].

The Lep<sup>ob</sup> / Lep<sup>ob</sup> (ob/ob) mouse lacks functional leptin due to an autosomal recessive mutation in the leptin gene (Lep<sup>ob</sup>). The nonsense mutation changing an arginine into a stop codon leads to a biologically inactive protein. On the other hand, the Lep<sup>db</sup> / Lep<sup>db</sup> (db/db) mouse carries an autosomal recessive loss of function mutation in the long form of the leptin receptor (Ob-Rb). This leads to an overproduction of extracellular leptin, but lack of intracellular leptin-action through Ob-Rb. However the phenotypes of these mice are not due to the monogenic defects in the leptin or the leptin receptor gene, but rather fixed in the genetic background strains. The background strain for the ob/ob mouse is C57Bl/6J (BL6) and the background of the db/db mice is C57Bl/Ks (BKS).

### **1.4.1 Diabetes susceptibility of ob and db mutations in mice**

The ob/ob mouse was discovered in 1950 [177]. The mutation is described as being inherited as an “autosomal recessive unit with complete penetrance”. Additional investigations showed that these mice are severely obese and exhibit hyperglycemia, glycosuria, increased size of islets of langerhans and decreased life span. But even when fed a high-fat diet these mice are protected from developing diabetes [178]. The db/db mouse was described in 1966 as phenotypically similar to the ob/ob mouse but with early onset of diabetes and shortened life-span. The characteristics were obesity, hyperglycemia and non-fertility. Following studies then revealed that leptin-deficient ob/ob mice that were bred on the BKS background developed diabetes, whereas ob/ob mice on a BL6 background did not [179]. The latter only exhibited obesity, transient hyperglycemia and hypertrophy of islets with resulting hyperinsulinemia. It was proposed that the hyper- or atrophy of the islets is due to the interaction of the db and ob gene with modifiers of the genetic background rather than relying especially on the specific mutant. In the following years, Coleman unraveled the genetic basis of the ob and db mouse strains by conducting parabiosis experiments. Parabiosis is typically achieved by surgical conjunction of different organisms to combine their physiological systems, here the circulation of both mouse models. This experiment resulted in the obese partner (ob/ob) becoming hypoglycemic and dying due to starvation. Though the diabetic partner (db/db) was unaffected by the experiment. This led to the hypothesis that the obese mice have normal satiety centers that are sensitive to a satiety factor produced by the diabetes mouse [180]. This factor was identified as leptin in 1994 showing that the ob mutation represents a nonsense mutation, resulting in a truncated, inactive protein. On the other hand, it was shown that the db/db mouse exhibits a glycine to threonine mutation in the leptin receptor gene on chromosome 4 resulting in abnormal mRNA splicing and the subsequent production of a nonfunctional Ob-Rb (LEPRb) protein [181]. This is the only isoform out of six (Ra-Rf) that has a longer cytoplasmic part containing the complete JAK2/STAT domains. Investigations of the function of the short leptin receptor isoforms did not contribute novel insights regarding energy metabolism. Only the whole-body knockdown of all leptin receptor isoforms led to a slight increase in respiratory exchange ratio (RER) and body temperature [182], [183]. BKS and BL6 mice are lean and phenotypically healthy. Upon the genetic challenge by ob or db mutation mice become only diabetic on the BKS but not on the BL6 background. However, very little is known about the responsible gene interactions. Up to today it is known that BKS is a composite of BL6 and DBA strains but also contain alleles from 129 and B10 mice and an unidentified mouse strain [184]. Thus, the crucial gene/ genetic interaction needs to be elucidated.

### 1.4.2 Disease susceptibility

Diseases can occur due to single genetic errors but many pathologies start to develop because of the conjunction of several factors. These include age, gender and environmental factors like chemicals or pathogens. Yet, the handling of those factors is different in every body. Because the exposition and/or duration to such can lead to the onset of a disease, these parameters are considered as risk factors (e.g. increasing age, sex, smoking, obesity) [185]; [186]; [187]; [188]; [189]; [190]. In most cases the timing and causation of a disease are dependent on the interplay of both risk factors and genetic prevalence. The genetic prevalence or susceptibility reflects a genetic make-up that does not obligatorily lead to a disease and is often not even noticed as long as no health disadvantages are present. Some diseases, like cardiovascular problems or T2DM, tend to cluster in families affecting more than one generation without a clear pattern like monogenic diseases [191]; [192]; [193]; [194].

Therefore, it is of big interest to identify the strongest disease risk factors according to lifestyle, but furthermore finding susceptibility genes or even epigenetic modifications that might increase or decrease the risk.

### 1.4.3 BKS susceptibility

Neither ob nor db mutation alone are responsible for the phenotype of the B6.Cg-Lepr<sup>ob</sup> or BKS.Cg-Lepr<sup>db</sup> mice, but rather the background strains are crucial. Up to date, it is not fully elucidated how BKS susceptibility for diabetes arises. Both ob and db mice on either background become hyperphagic and, at least transiently (ob), hyperglycemic. BL6 develop pancreatic hyperplasia and hypertrophy, whereas beta cells of BKS mice become apoptotic. This difference in beta cell proliferative capacity was shown to be twice as high in BL6 as in BKS [195]. Additional experiments showed that there is not a defect in beta cell proliferative activity in BKS in general. Mice with a defect in the carboxypeptidase E (*Cpe<sup>fat</sup>*) gene bred on the Ks background did not show beta cell atrophy but rather hyperplasia and hypertrophy [196]. It was concluded, that the atrophy of beta cells is a secondary effect to hyperglycemia [196]. This was supported by experiments showing that hypertrophy/-plasia can be restored if hyperglycemia is reduced by estrogen therapy [197].

## 1.5 Thesis outline:

Because of continuously increasing prevalence of T2DM and other obesity associated diseases, our interest was to investigate the role of the white adipose tissue as an endocrine organ in energy metabolism. The adipokinome and its modulations especially during obesity are incompletely understood. In this work, the underlying hypothesis was that the secretome might contain factors that are crucial for the development of obesity or T2DM. Therefore, the measurement of the entire adipocyte secretome is fundamental to understand the role in the development of metabolic diseases.

This thesis addresses the characterization of the adipose tissue secretome utilizing established mouse models for obesity and T2DM. This procedure is a crucial step that needs to be precise and reproducible. Subsequent analysis of the adipokinomes, identification of novel adipokines and the final analysis of promising novel targets provides the basis to investigate putative functions within the adipose tissue and disease pathophysiology (Study 1-4).

In the following the aims and key questions of the publications included in this thesis are summarized:

- Study 1: The list of adipokines has been growing in the last years, however a bias is still present due to the identification of contaminant proteins when tissue-specific secretomes are generated. Therefore, an improved workflow for the generation of high-quality secretome samples from primary murine adipocytes was developed [198].
- Study 2: Using the established protocol, conditioned media (secretomes) of adipocytes deriving from murine visceral white adipose tissue were generated. The mouse strains C57BL/6 and C57BL/Ks are lean and healthy. However, breeding single gene mutations (ob and db) on these backgrounds, the progeny become either obese or obese and diabetic which depends crucially on the underlying background strain. The reasons for this genetic susceptibility are not known. To address this, the adipocyte-derived secretomes of BKS and BL6 mice was investigated using liquid chromatography (LC)-electrospray ionization (ESI)-MS/MS. The composition of the adipokines was analyzed to address the hypothesis: Adipokines that are regulated between the mouse models might play a role in strain-specific disease susceptibility [199].
- Study 3: Following the identification of T-cadherin as a novel adipokine, the objective of this study was to investigate the protein abundance within the adipocyte secretome and the expression in total visceral adipose tissue. Furthermore, it was investigated whether T-cadherin levels in vWAT and in the circulation are affected by obesity in mouse models. T-cadherin has been described in terms of proliferation and migration before. Therefore, the 3T3-L1 cell line was used to confirm the hypothesis that T-cadherin might affect adipogenesis. As a translational approach, human plasma and adipose tissue biopsies were

investigated to investigate whether T-cadherin is regulated in human obesity or diabetes and if it is affected by bariatric surgery-induced weight loss.

- Study 4: As a follow-up study, the secretome of obese mouse models (ob/ob and db/db) was characterized. The adipokinome data were compared with different databases (KEGG, GO and IPA) to monitor possible pathway regulations. Upon the theory of diabetogenic lipids, the profiles of diacylglycerols (DAG) within the vWAT were analyzed. The aim of this study was whether the combination of protein and lipid data is useful to receive new insights into the significance of vWAT in obesity and T2DM.

In Studies Z1, Z2, Z3 and Z4- which are not included in this thesis - my contribution was limited to the execution of single experiments.

List of publications related to the thesis:

- **Study 1:** Göddeke S, Kotzka J, Lehr S: Investigating the adipose tissue secretome: a protocol to generate high-quality samples appropriate for comprehensive proteomic profiling. *Methods Mol Biol.* (2015); 1295:43-53. **Contributions: p. 29**
- **Study 2:** Hartwig S, Göddeke S, Poschmann G, Dicken HD, Jacob S, Nitzgen U, Passlack W, Stühler K, Ouwens DM, Al-Hasani, H, Knebel B, Kotzka J, Lehr S: Identification of novel adipokines differential regulated in C57BL/Ks and C57BL/6. *Arch Physiol Biochem* (2014) Dec;120(5):208-15. **Contributions: p. 41**
- **Study 3:** Göddeke S, Knebel B, Fahlbusch P, Hörbelt T, Poschmann G, van de Velde F, Benninghoff T, Al-Hasani H, Jacob S, Van Nieuwenhove Y, Lapauw B, Lehr S, Ouwens DM, Kotzka J: CDH13 abundance interferes with adipocyte differentiation and is a novel biomarker for healthy status of fat tissue. (In revision 11/2017; *International Journal of Obesity*). **Contributions: p. 65**
- **Study 4:** Knebel B, Goeddeke S, Poschmann G, Markgraf DF, Jacob S, Nitzgen U, Passlack W, Preuss C, Dicken HD, Stühler K, Hartwig S, Lehr S, Kotzka J. Novel insights into the adipokinome of obese and obese/diabetic mouse models. *Int J Mol Sci* 2017, 18, doi: 10.3390/ijms18091928. **Contributions: p. 88**
- Study Z1: Knebel B, Hartwig S, Haas J, Lehr S, Goeddeke S, Susanto F, Bohne L, Jacob S, Koellmer C, Nitzgen U, Müller-Wieland D, Kotzka J: Peroxisomes compensate hepatic lipid overflow in mice with fatty liver. *Biochim Biophys Acta* (2015) Jul; 1851(7):965-976.
- Study Z2: Hartwig S, Knebel B, Goeddeke S, Koellmer C, Jacob S, Nitzgen U, Passlack W, Schiller M, Dicken HD, Haas J, Müller-Wieland D, Lehr S, Kotzka J: So close and yet so far: mitochondria and peroxisomes are one but with specific talents. *Arch Physiol Biochem* (2013) Jul; 119(3): 126-35.
- Study Z3: Knebel B, Göddeke S, Hörbelt T, Fahlbusch P, Al-Hasani H, Jacob S, Koellmer C, Nitzgen U, Schiller M, Lehr S, Kotzka J: Alteration of liver peroxisomal and mitochondrial functionality in the NZO mouse model of metabolic syndrome. (Accepted 10/2017; *Proteomics Clinical Applications*)
- Study Z4 (submitted): Birgit Knebel, Gereon Poschmann, Simon Goeddeke, Cora Weigert, Jan Krumsiek, Parviz Gomari, Kai Stühler, Sonja Hartwig, Sylvia Jacob, Ulrike Kettel, Dirk Müller-Wieland, Stefan Lehr, Jörg Kotzka: Liver - to - adipose tissue *de novo* lipid synthesis ratio associates with adipokinome signatures and serum lipid levels in NAFLD mouse models.

# Study 1: Investigating the Adipose Tissue Secretome: A Protocol to Generate High-Quality Samples Appropriate for Comprehensive Proteomic Profiling

Published in *Methods Mol Biol.* 2015;1295:4353.

Simon Göddeke<sup>1</sup>, Jörg Kotzka<sup>1</sup> and Stefan Lehr<sup>1</sup>

<sup>1</sup> Institute of Clinical Biochemistry and Pathobiochemistry, German Diabetes Center at the Heinrich-Heine-University Duesseldorf, Leibniz Center for Diabetes Research, Aufm Hennekamp 65, 40225 Duesseldorf, Germany

## Abstract

**In this chapter, we describe in detail how to prepare a sample containing the complete entity of secretion products from murine primary adipocytes, which are suitable for comprehensive and sensitive secretome analysis. The underlying protocol should be seen as a starting point guiding through critical steps of the complex workflow in order to approximate to the real secretome in the context of different sample types used for the diverse research questions the protocol has to be carefully adjusted.**

## Keywords:

Secretome analysis, Adipokines, Murine adipose tissue, Preadipocytes

## 1 Introduction

Obesity, which is favored by imbalanced energy supply and energy consumption coupled with a sedentary lifestyle is considered as an epidemic disease and represents a burden for almost all societies (1). Therefore, overweight today is the major risk factor for developing various metabolic complications such as insulin resistance, type 2 diabetes, non-alcoholic liver disease, and cardiovascular diseases (2–6).

Over the last decade we have learned that adipose tissue, besides its predominant role

within energy homeostasis also represents a major endocrine organ, releasing a wide variety of signaling and mediator proteins. These so-called adipokines seem to be causally involved in the development of a wide variety of metabolic diseases. Over the last years, several attempts have been made to characterize the adipokines by utilizing diverse proteomic profiling approaches. This has led to a catalog of adipokines comprising several hundred potentially secreted peptides and proteins (7). Nevertheless, the limited overlap of identified adipokines in published studies impressively illustrates that the analysis of tissue-specific secretomes is an extreme challenging business. Within the complex workflow including sample preparation, concentration, proteomic profiling and extensive bioinformatics, the most striking point is to discriminate the real secretome from contaminating proteins. Therefore, a meaningful characterization inalienable starts with high-quality samples and requires a reproducible processing as crucial points for successful identification of secreted proteins. Particularly during sample collection and culturing processes considerable contaminations could occur from different sources, e.g. release of cellular proteins due to cell damage or contamination of high-abundant proteins derived from culture, i.e. FCS. Due to the fact that the expected concentrations of adipokines are low (pg to ng/ml), artificial

proteins have the potential to shift the dynamic range of the secretome sample dramatically. In the light of these possible pitfalls, a careful evaluation of sample preparation and culture setup to minimize contamination are the most crucial steps in order to obtain relevant secretome data (7, 8).

## 2 Materials

### 2.1 General Hardware and Consumables

1. Incubator (37 °C; 5 % CO<sub>2</sub>; 95 % humidity).
2. Sterile cell culture bench.
3. Centrifuge.
4. Ultracentrifuge.
5. Laboratory scissors (double sharpened); 145 mm.
6. Scalpel grip Nr. 4 L.
7. Scalpel blades Nr. 22.
8. Forceps.
9. 6-Well-culture plates.
10. Polypropylene (PP) centrifugation tubes, 15 ml.
11. Polypropylene (PP) centrifugation tubes, 50 ml.
12. Sterile serological pipettes, 10 ml.
13. Glass funnel, Pasteur pipettes.
14. Incubation rotator.
15. Steam-sanitizer.
16. Special accuracy scale.

### 2.2 Tissue Biopsies

1. Hank's Balanced Salt Solution (HBSS) w/o Calcium and Magnesium (pH 7.4).

### 2.3 Isolation of Preadipocytes

1. Cell Strainer, 70 µm, Nylon (BD Falcon). Mesh, 150 µm).
3. Mesh, 75 µm.
4. Syringe filters, 25 µm.
5. Special accuracy scale.
6. Collagenase (NB8, Clostridium Histolyticum).
7. Phosphate buffered saline (PBS) w/o Calcium and Magnesium, sterile.
8. Collagenase solution (750 U collagenase/g adipose tissue): 250 U/ml in HBSS (pH 7.4) (see **Note 1**) supplemented with 3 mM CaCl<sub>2</sub> (see **Note 2**) and 4 mM glucose. Sterile filtration (10 ml syringe), G26 cannula (1½"), sterile syringe filters (0.2 µm, 33 mm).
9. HBSS to dilute the collagenase: add CaCl<sub>2</sub> (3 mM).
10. Erythrocyte lysis buffer: 8.29 g/l NH<sub>4</sub>Cl, 0.99 g/l K<sub>2</sub>HPO<sub>4</sub>, 0.04 g/l EDTA, pH 7.3 sterile filtration.
11. Basal medium: DMEM/F-12 (17.5 mM glucose), 1.25 g/l NaHCO<sub>3</sub>, 16 mg/l Biotin, 8 mg/l Calcium- D-pantothenate, pH 7.3, sterile filtration. Before use add 5 ml/l Gentamycin.
12. Basal medium w/o phenol-red: DMEM, w/o phenol red, w/o FCS, 10 pmol/ml insulin. Before use add 5 ml/l Gentamycin.

### 2.4 Differentiation of Preadipocytes

1. Vacuum filtration unit, 500 ml (0.22 µm).
2. Ethylenediaminetetraacetic acid (EDTA) solution pH 8.0 (1 mg/ml).
3. Dulbecco's Modified Eagle's Medium/F-12 (DMEM/F-12, 17.5 mM glucose).
4. Phosphate buffered saline (PBS) w/o Calcium and Magnesium, sterile.
5. Cultivation medium: Basalmedium (Subheading 2.3, item 12), 10 % FCS, 5 ml/l Gentamycin.

6. Troglitazon (TZO) stock solution: Solve 5 mg in 1 ml Dimethylsulfoxide (DMSO).

7. Differentiation medium #1 (for 50 ml) (see **Note 3**): 50 ml basal medium (Subheading 2.3, item 12), 5 µl TZO stock solution (see **Note 4**), 25 µl Apo-Transferrin stock solution, 100 µl Hydrocortisol stock solution, 5 µl T3 stock solution, 150 µl insulin stock solution.

8. Differentiation medium #2: Differentiation medium #1 w/o TZO, supplement with 10 % FCS.

9. Apo-Transferrin stock solution: Solve 50 mg in 1 ml ddH<sub>2</sub>O.

10. Hydrocortisol stock solution (50 µg/ml): Solve 1 mg in 1 ml EtOH<sub>abs</sub> and dilute in basal medium w/o phenol-red.

11. Trijodthyronin (T3) stock solution (20 µg/ml): Solve 5 mg in 1 ml 1 N NaOH and dilute in ddH<sub>2</sub>O.

12. Insulin stock solution (=10<sup>-4</sup> M): Solve 5 mg in 860 µl 0.01 N HCl and dilute in 10 ml ddH<sub>2</sub>O.

### 2.5 Quality Control of Differentiation by Oil Red O Protocol

1. Oil Red O stock solution: Mix stock solution in 15 ml PP centrifugation tubes with ddH<sub>2</sub>O (6:4, v/v) and incubate for at least 2 h at room temperature in the dark. Filtrate the solution before use and centrifuge for 10 min at 3,200 × g.

2. Hemalaun solution: Dissolve Hematoxylin in ddH<sub>2</sub>O (1 mg/ml) and add sodium iodate (0.2 mg/ml) and potassium sulfate (50 mg/ml) while agitating (see **Note 5**). After mixing add chloride-hydrate (50 mg/ml) and crystalline citric acid (1 mg/ml) (see **Note 6**).

3. Fixation solution: Mix 15 ml Picric acid with 5 ml Formol (37 %) and 1 ml acetic acid (100 %).

4. Oil Red O stock solution: 0.3 g Oil Red O solve in 100 ml isoproanol (99 %) (see **Note 7**).

### 2.6 Collecting Secreted Peptides/ Proteins

1. Mesh, 50 µm.

2. Ethylendiaminetetraacetic acid (EDTA) solution pH 8.0 (1 mg/ml).

3. Phosphate buffered saline (PBS) w/o Calcium and Magnesium, sterile.

### 2.7 Concentration via Centrifugal Filter Concentrator

1. Centrifugal filter concentrator (Amicon Ultra 15.3 kDa).

## 3 Methods

In this chapter we describe in detail how to prepare a specimen, containing the complete entity of secretion products from murine primary adipocytes, which are suitable for comprehensive and sensitive secretome analysis. The underlying protocol should be seen as a starting point guiding through critical steps of the complex workflow in order to approximate to the real secretome in the context of different sample types used for the diverse research questions the protocol has to be carefully adjusted (Fig. 1).

### 3.1 Tissue Biopsies

1. On the day of surgery, after a 6 h fast, mice are sacrificed and adipose tissue specimens are obtained from the subcutaneous, visceral or brown depots.

2. Harvest the tissue as a whole part, not in small pieces.

3. Tissue specimens were immediately transferred in HBSS and transported on ice to the laboratory (see **Note 8**).

### 3.2 Isolation of Preadipocytes (Fig. 2, 3 and 4)

1. Dissect tissue from fibrous material and visible blood vessels and cut into fragments of ~ 5–10 mg (see **Note 9**).

2. Transfer the mashy tissue in a 50 ml tube and add collagenase mixture (see **Note 10**).

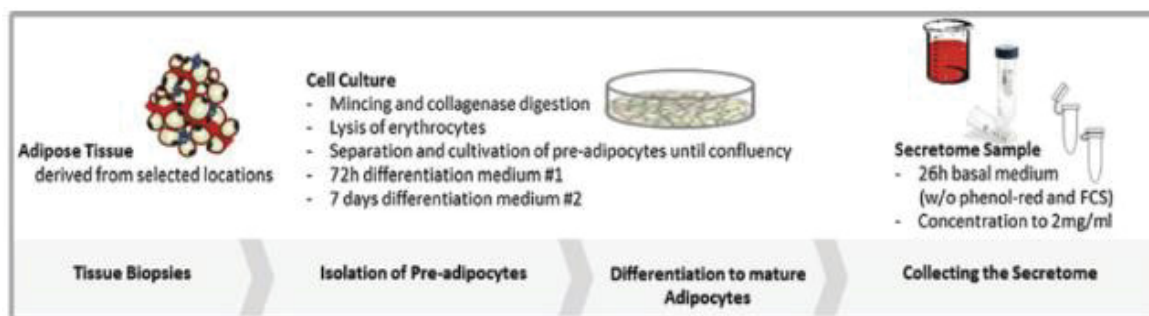


**Fig. 1:** Workflow scheme to generate secretome sample from differentiated mouse adipocytes

3. Incubate fat tissue fragments with vigorous shaking (250 cycles/min) for at least 30 min at 37 °C.

4. Centrifugation: 5 min,  $240 \times g$ , RT (see **Note 11**).

5. Re-suspend the pellet in HBSS (1:10, v/v).

6. The supernatant, more precisely the floating mature adipocytes, is harvested and transferred to another 50 ml tube with a Pasteur pipette (see **Note 12**).

7. Stop collagenase reaction by adding of 0.01 M EDTA solution (1:10, v/v) (see **Note 13**).

8. Mix the solution thoroughly by carefully shaking the tube (at least 5 times).

9. Centrifugation: 5 min,  $240 \times g$ , 4 °C.

10. Discard the supernatant by aspiration and re-suspend the pellet in HBSS (1:10, v/v).

11. Pool both pellets (steps 5 and 10), i.e. the stromal-vascular cell fraction, and transfer the cell suspension in a 50 ml tube.

12. Add erythrocyte-lysis buffer (1:10, v/v) and incubate after mixing the suspension on ice 10 min at longest (see **Note 14**).

13. Thereafter the tube is filled up to 50 ml with HBSS.

14. Centrifugation: 5 min,  $240 \times g$ , 4 °C.

15. Discard the supernatant by aspiration and re-suspend the pellet in basal medium (1:10, v/v).

16. This suspension is filtered without pressure through a 150  $\mu\text{m}$  filter (Image 3).

17. Thereafter flow-through is filtered without pressure through another filter (75  $\mu\text{m}$ ) (see **Note 15**).

18. Centrifuge the flow-through: 5 min,  $240 \times g$ , 4 °C (see **Note 16**).

19. Discard the supernatant by aspiration and resuspend the pellet in DMEM/F-12 medium supplemented with 20 % FCS (1:1, v/v) (see **Note 17**).

20. Inoculate the cells into a 35 mm dish at a density of approx. 50,000 cells/cm<sup>2</sup>.

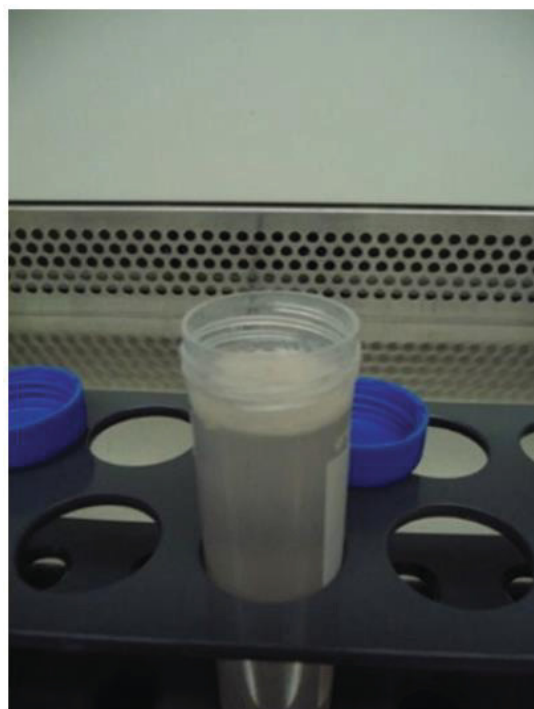


**Fig. 2:** Digested and centrifuged adipose tissue resulting in floating mature adipocytes

### 3.3 Differentiation of Pre-adipocytes

1. Incubate the cells in a humidified 5 % CO<sub>2</sub> atmosphere at 37 °C.
2. Incubate the cells in cultivation medium until reaching confluence.
3. After that the cells are repeatedly washed with 1× PBS to remove non-adhering material and incubated in differentiation medium #1 for another 3 days. 4. Thereafter the cells are washed with 1× PBS to remove non-adhering material and incubated in differentiation medium #2 (see **Note 18**).
5. The cells are differentiated after at least 7 days.
6. The mature adipocytes can now be cultivated for up to 14 days before becoming apoptotic.
7. In the phase of establishment a lipid staining with oil red is recommended.

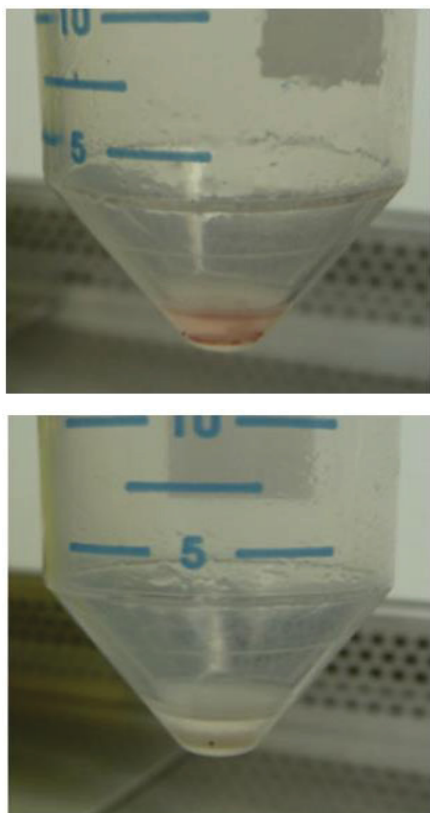


**Fig. 3:** Adipocyte-free pellet before [1] and after erythrocyte lysis (lower ; the pellet should be white and free of erythrocytes)

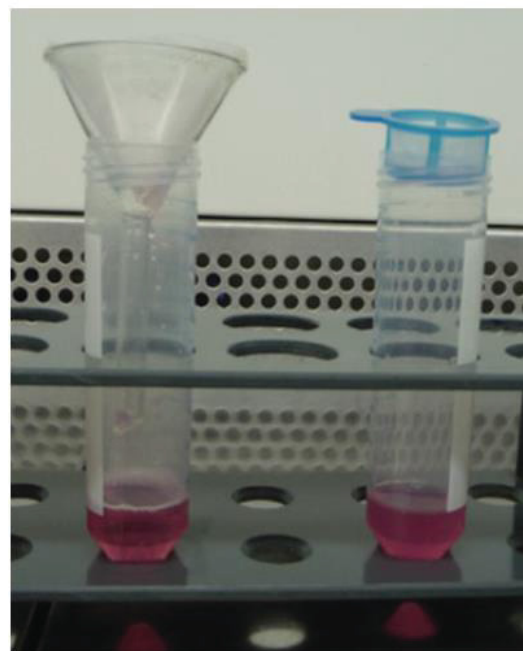


**Fig. 4:** 150 µm filter (left) and 75 µm mesh (right)

### 3.4 Quality Control of Differentiation by Oil Red O Protocol (Fig. 5)

Oil Red O protocol is an assay performed to detect mature adipocytes in histological visualization of fat cells by staining neutral fat

1. Soak off the culture medium and wash the cells very gently with 1× PBS two times.
2. Discard the supernatant by aspiration and add the fixation solution.
3. Incubate at RT for 2 h (see **Note 19**).
4. Discard the fixation solution and wash with 1× PBS two times (see **Note 20**).
5. Accordingly incubate the cells in 40 % isopropyl alcohol for 5 min.
6. Discard the isopropyl solution and add the Oil Red O solution.
7. Incubate at RT for 15 min (see **Note 21**).
8. Discard the Oil Red O solution and perform a short incubation (~5 s) in isopropyl alcohol.
9. Discard the isopropyl solution and subsequently wash briefly with ddH<sub>2</sub>O.

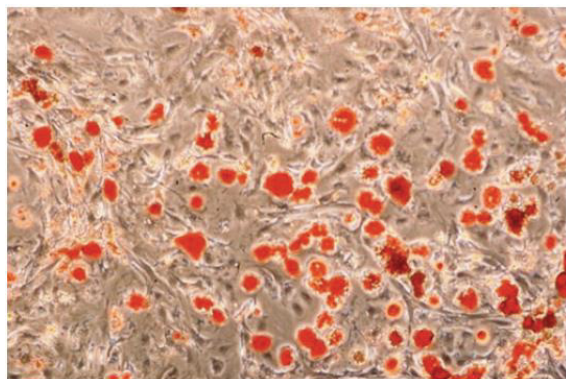


**Fig. 5:** Oil Red O staining of differentiated pre-adipocytes ( $\times 400$ )

10. The wet cells are incubated with the hemalaun solution for 2 min (see **Note 22**).

11. Afterwards the staining solution is discarded and tap water is added (see **Note 23**).

### 3.5 Collecting Secreted Peptides/ Proteins

1. Wash the differentiated pre-adipocytes (mature adipocytes) carefully two times with  $1\times$  PBS supplemented with 3 mM  $\text{CaCl}_2$  (see **Note 24**).

2. Thereafter add basal medium w/o phenol-red and incubate for 4 h.

3. Wash the cells carefully two times with  $1\times$  PBS supplemented with 3 mM  $\text{CaCl}_2$ .

4. Add basal medium w/o phenol-red and incubate the cells for 26 h.

5. Collect the supernatant in 15 ml polypropylene tube and centrifuge for 30 min at  $4,900 \times g$ ,  $4^\circ\text{C}$ .

6. Transfer the supernatant to another tube, determine the protein concentration and add EDTA solution and protease inhibitors ( $1\times$ ).

7. Concentrate the supernatants with filter concentrator to a protein concentration of  $2 \mu\text{g}/\mu\text{l}$  and store it at  $-80^\circ\text{C}$ .

### 3.6 Concentration via Centrifugal Filter Concentrator

1. The samples are centrifuged for 45 min at  $85,000 \times g$  and  $4^\circ\text{C}$  to get rid of remaining cell debris.

2. The supernatants were transferred to a filter concentrator with small pore size (3 kDa) (see **Note 25**).

3. Centrifuge at  $4,000\times g$  and  $4^\circ\text{C}$  to a final volume of 100  $\mu\text{l}$  (see **Note 26**).

The secretome sample now is appropriate for comprehensive targeted and non-targeted proteomic profiling. Complexity and sample quality could be evaluated, for example, by

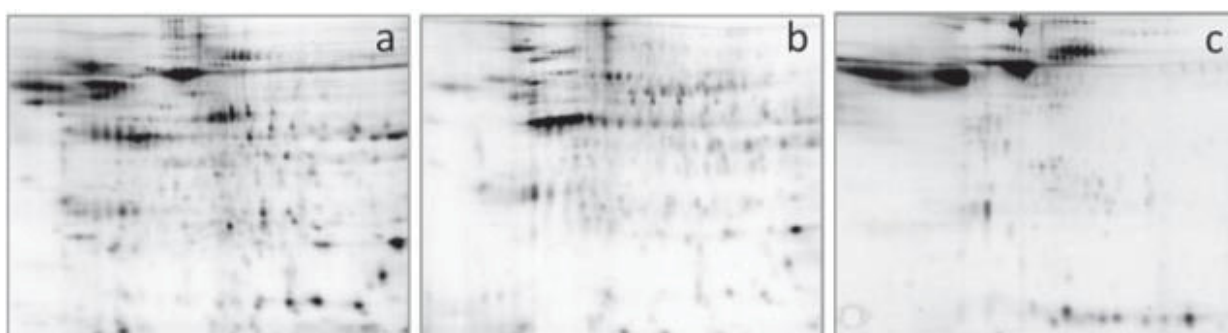


**Fig. 6:** Visualization and quality control of secretome samples using 2-dimensional gel electrophoresis. Aliquots (40  $\mu\text{g}$  protein each) of (a) secretome of differentiated, primary adipocytes, (b) total lysate of differentiated primary adipocytes and (c) Fetal Calf Serum (FCS). Samples were separated by 2-dimensional gel electrophoresis according to the 2D-ToGo workflow [9] standard operation procedure established in our group. Accordingly, in the first dimension samples in ReadyPrep Sample Buffer (8 M urea, 3 % CHAPS, 50 mM DTT, 0.2 % (w/v) Bio-Lyte 3/10 ampholytes) were separated by isoelectric focusing [2] using pH 3–10 linear ReadyStrip IPGstrips (pH 3–10, 11 cm) performed on a Protean i12<sup>TM</sup> electrophoresis unit (Bio-Rad) and in the second dimension by SDS-PAGE using Criterion<sup>TM</sup> TGX Stainfree<sup>TM</sup> Any KD precast gels (Bio-Rad). After electrophoretic separation spot pattern were acquired and documented without further staining, using a ChemiDoc<sup>TM</sup> MP (Bio-Rad) equipped with Image Lab Software.

2-DE (Fig. 6), which provides a powerful and reproducible profiling tool.

### Notes

1. Consider the unique activity of each collagenase-charge: e.g. PZU activity of 1.0 = 1,000 U/mg. When weighing the collagenase wearing a surgical mask is recommended.
2. The  $\text{CaCl}_2$  is crucial for activation of the collagenase.
3. Do not use this medium for more than a week.
4. TZO must be diluted in DMSO, not in aqueous solvent.
5. The solution should get a violet-blue staining.
6. The mixture should get a red-violet staining, filtrate the solution with a 150  $\mu\text{m}$  paper filter before use.
7. Only use the solution for 1–2 weeks until precipitation.
8. The buffer has to be freshly prepared, sterile filtered and stored on ice.
9. For rough dissection the use of a forceps and medical scissors is recommended. Therefore, you mince the adipose tissue, e.g. in a weighing pan.
10. Collagenase mixture  
= tissue/collagenase solution (1:1, v/v).
11. In all of the following centrifugation steps, the use of a swing-out rotor is necessary to ensure adequate separation of the fractions.
12. At this point harvested adipocytes can be used for further analysis. On the one hand, it is possible to generate secretome from the floating mature adipocytes and furthermore they can be used for Western blot and qPCR analyses.
13. Do not use a solution of more than 0.5 M of EDTA, because otherwise cells tend to clot. Using serum/FCS is not efficient enough to stop the collagenase reaction.
14. This step is crucial to remove contaminating erythrocytes. It is recommended to monitor the reaction, because ammonium chloride might damage the cells when incubating too long.
15. Both filtering steps are needed to isolate the pre-adipocytes, because using only a single step/mesh might end up with plugging of the mesh and less yield of pre-adipocytes.
16. Never centrifuge for more than 10 min, because the cells are destroyed otherwise.
17. If not planned to work on parallel with the mature adipocytes.
18. This medium was changed every 2–3 days, until full differentiation.
19. This incubation step can be elongated up to 24 h if needed.
20. Wash until the yellowish dye of the washing buffer is extincted.
21. The incubation time depends upon the staining. Better monitor with microscope.
22. For visualizing of the nucleus cells can stained with hemalaun.
23. Use enough water to cover all the cells. Use tap water to ensure presence of  $\text{HO}^-$  ions which activate the metal-hematoxylin complex. The incubation will probably take longer than 10 min until blue staining.
24. The addition of  $\text{CaCl}_2$  is crucial to wash away the FCS totally. This enables a subsequent 2D gel analysis. Wash very carefully, because attachment of cells is not very strong.
25. The use of a 3 kDa filter is of importance to ensure retaining all kinds of proteins in the solution.
26. The retention recovery performance of the filters is  $\sim 90\%$  so that an additional concentration step of the flow-through might be useful.

## References

1. Misra A, Khurana L (2008) Obesity and the metabolic syndrome in developing countries. *J Clin Endocrinol Metab* 93:9–30
2. Alberti KG, Eckel RH, Grundy SM et al (2009) Harmonizing the metabolic syndrome: a joint interim statement of the International Diabetes Federation Task Force on Epidemiology and Prevention; National Heart, Lung, and Blood Institute; American Heart Association; World Heart Federation; International Atherosclerosis Society; and International Association for the Study of Obesity. *Circulation* 120:1640–1645
3. Golay A, Ybarra J (2005) Link between obesity and type 2 diabetes. *Best Pract Res Clin Endocrinol Metab* 19:649–663
4. Moore JB (2010) Non-alcoholic fatty liver disease: the hepatic consequence of obesity and the metabolic syndrome. *Proc Nutr Soc* 69:211–220
5. Despres JP, Lemieux I, Bergeron J et al (2008) Abdominal obesity and the metabolic syndrome: contribution to global cardiometabolic risk. *Arterioscler Thromb Vasc Biol* 28: 1039–1049
6. Hauner H, Petruschke T, Russ M et al (1995) Effects of tumour necrosis factor alpha (TNF alpha) on glucose transport and lipid metabolism of newly-differentiated human fat cells in cell culture. *Diabetologia* 38:764–771
7. Lehr S, Hartwig S, Sell H (2012) Adipokines: a treasure trove for the discovery of biomarkers for metabolic disorders. *Proteomics Clin Appl* 6:1–11
8. Brown KJ, Formolo CA, Seol H et al (2012) Advances in the proteomic investigation of the cell secretome. *Expert Rev Proteomics* 9: 337–345
9. Posch A, Franz T, Hartwig S et al (2013) 2D-ToGo workflow: increasing feasibility and reproducibility of 2-dimensional gel electrophoresis. *Arch Physiol Biochem* 119:108–113

Journal: Methods in Molecular Biology

Impact factor: 0.79

Contribution: Conceived / designed experiments: 80 %

Performed experiments: 100 %

Analysed data: ø

Wrote the manuscript: 100 %

Contributed to discussion: ø

Author: 1st author

## Study 2: Identification of novel adipokines differential regulated in C57BL/Ks and C57BL/6

Published in Arch Physiol Biochem. 2014 Dec;120(5):208-15.

Sonja Hartwig<sup>1,2\*</sup>, Simon Goeddeke<sup>1,2\*</sup>, Gereon Poschmann<sup>3\*</sup>, Hans-Dieter Dicken<sup>4</sup>,  
Sylvia Jacob<sup>1</sup>, Ulrike Nitzgen<sup>1</sup>, Waltraud Passlack<sup>1</sup>, Kai Stühler<sup>3</sup>, D. Margriet Ouwens<sup>1,2,5</sup>,  
Hadi Al-Hasani<sup>1,2</sup>, Birgit Knebel<sup>1,2</sup>, Jörg Kotzka<sup>1,2</sup>, and Stefan Lehr<sup>1,2</sup>

<sup>1</sup>Institute of Clinical Biochemistry and Pathobiochemistry, German Diabetes Center at the Heinrich-Heine-University Duesseldorf, Leibniz Center for Diabetes Research, Duesseldorf, Germany,

<sup>2</sup>German Center for Diabetes Research (DZD), Partner Duesseldorf, Germany,

<sup>3</sup>Heinrich-Heine-University Duesseldorf, Molecular Proteomics Laboratory, Biomedizinisches Forschungszentrum (BMFZ), Duesseldorf, Germany,

<sup>4</sup>Multimedia Center, Heinrich-Heine-University Duesseldorf, Duesseldorf, Germany, and

<sup>5</sup>Department of Endocrinology, Ghent University Hospital, Ghent, Belgium

### Abstract

Visceral adiposity is associated with metabolic disorders, but little is known on the underlying pathophysiological mechanism. One possible link might be the release of various signaling and mediator proteins, named adipokines. Our hypothesis was that dependent on genetic background factors are released which might trigger a primary disease susceptibility. This study characterizes the adipokines released from visceral adipose tissue from two metabolic healthy mouse strains, i.e. C57BL/Ks (BKS) and C57BL/6 (C57), of which the former genetic background is more sensitive to develop diabetes following metabolic challenge. Using liquid chromatography (LC)-electrospray ionization (ESI)-MS/MS, a reference map comprising 597 adipokines was generated (<http://www.diabetesityprot.org>). Thirty-five adipokines, including six not previously described ones, were differentially released between the mouse strains. Most notable is the reduced release of the adiponectin-binding protein T-Cadherin (CAD13) in BKS mice. This observation highlights the importance of secretome profiling in unravelling the

**complex interplay between genetic diversity and lifestyle.**

### Keywords

Adipokine, label free proteomic profiling, visceral fat

### Introduction

Over the last decade adipose tissue has been pointed out as an active endocrine organ. It plays a crucial role in inter-organ communication by releasing a wide variety of signalling- and mediator-proteins, named adipokines (Lehr *et al.*, 2012a; Romacho *et al.*, 2014; Scherer, 2006). Alterations of adipokine secretion are thought to be involved in the pathogenesis of the obesity-related metabolic disturbances, including diabetes (Flehmig *et al.*, 2014; Wronkowitz *et al.*, 2014). However, the manifestation of metabolic disorders is dependent on genetic background, and the abundance of a released factor might be the trigger for primary disease susceptibility. The increase of adipose tissue, especially of the metabolic relevant visceral fat depot, is known to be associated with insulin resistance and cardiovascular disease (Despres & Lemieux, 2006; Mathieu *et al.*, 2009). Visceral adipose tissue has the adverse effect of higher lipolysis rates resulting in an increased

release of fatty acids into the portal vein, draining to the liver (Guilherme *et al.*, 2008). In addition, cytokines or adipokines differentially released from visceral fat may function as inter-organ signalling mediators to govern these processes (Bruun *et al.*, 2005; Motoshima *et al.*, 2002; van Harmelen, *et al.*, 1998). A recent survey catalogues the complex nature of the adipokinome by more than 600 potential adipokines (Lehr *et al.*, 2012b). The limited overlap of identified adipokines among previous reported studies, probably due to differences in the experimental setting and profiling techniques, indicates that the known adipose tissue secretome is still incomplete. Furthermore, most adipokine profiling studies have been conducted on subcutaneous adipose tissue, whereas the visceral adipose tissue depot is generally considered more important for metabolic control. To identify novel disease-related adipokines, we characterized the visceral adipose tissue secretome from two closely related, well characterized and metabolically healthy mouse strains, i.e. C57BL/Ks (BKS) and C57BL/6 (C57) by combining state-of-the-art protein identification and quantification tools. The striking difference between these commonly used experimental “wild-type” mouse strains is, that in response to metabolic stress transgenic mice breed on a BKS genetic background are prone to develop diabetes in contrast to animals bred on a C57 genetic background (Coleman & Hummel 1975; Hummel *et al.*, 1972). The advantage of inbred experimental mouse models is the minimized biological variations within each strain due to genetically homology. Selecting such mouse strains for secretome analysis maximizes sample uniformity and reproducibility necessary for successful secretome profiling and downstream validation approaches. In this investigation we define the unbiased secretome of murine visceral adipose tissue. To the best of our knowledge we identified 116 novel adipokines. Furthermore, 35 adipokines were significantly different in quantitative comparison analysis of the two metabolically healthy control mouse strains. Only one of these proteins, i.e. T-Cadherin, was categorized as SP+ (exhibiting a secretory peptide) and assigned as a novel adipokine. Interestingly, this putative

adipokine is involved in the regulation of adiponectin and may help to understand the strain specific metabolic differences.

## Experimental procedures

### *Animals*

C57BL/Ks (BKS) and C57BL/6 (C57) mice were bred and maintained in colonies of three animals in our animal facility (12 h light/dark cycle; 22 °C±1 °C, 50 %±5 % humidity). Mice were fed ad libitum with standard laboratory chow (13.7 MJ/kg: 53 % carbohydrate, 36 % protein, 11 % fat (Sniff, Soest, Germany)) and had free access to water. All mice were sacrificed at the age of 17 weeks by CO<sub>2</sub> asphyxiation. The Animal Care Committees of the University Duesseldorf approved animal care and procedure (Approval # 50.05-240- 35/06).

### *Preparation of mature murine adipocytes and sample preparation for secretome analysis.*

Male C57BL/Ks (n=5; age: 119±2 d, body weight: 26.77±1.91 g; blood glucose: 133.29±26.51 mg/dl; triglyceride: 127.5±20.45 mg/dl) and C57BL/6 (n=5; age 119±2 d, body weight: 28.08±2.85 g; blood glucose: 149.33±29.14 mg/dl; triglyceride: 113.67±3.06 mg/dl) were sacrificed after 6 h food restriction and the perirenal fraction of visceral adipose tissue was dissected. Mature adipocytes were isolated by collagenase digestion, cultured for 24 h and the secretome was harvested as previously described (Göddeke *et al.*, 2014). Secretome samples were centrifuged (80.000 g, 20 min, 4 °C), and supernatants were concentrated with a cut-off mass of 3000 Dalton to a final volume of 200 ml (Amicon\_ Ultra 15 centrifugal filter devices, Millipore, Billerica, USA). Protein concentrations were measured using Advanced Protein Assay (Cytoskeleton, Denver, USA) and concentrated samples (mg/ml range) were stored as aliquots at -80 °C until use.

### *Secretome profiling by liquid chromatography*

(LC)-electrospray ionization (ESI)-MS/MS. Adipose tissue secretome samples of BKS and C57 mice (each n=5) were tryptically digested and analysed using LC-ESI mass spectrometry. Samples (5 mg) were focused on a 4 to 12 % polyacrylamide bis-tris gel

(Life Technologies, Darmstadt, Germany). After silver staining, protein bands were cut, de-stained (15 mM Na<sub>2</sub>S<sub>2</sub>O<sub>3</sub>, 50 mM K<sub>3</sub>[Fe(CN)<sub>6</sub>]), reduced (10 mM DTT, 50 mM (NH<sub>4</sub>)HCO<sub>3</sub>) alkylated (50 mM C<sub>2</sub>H<sub>4</sub>INO, 50 mM NH<sub>4</sub>HCO<sub>3</sub>) and proteins were digested overnight (0.1 mg trypsin, 50 mM NH<sub>4</sub>HCO<sub>3</sub>) (Serva, Heidelberg, Germany). For LC-MS/MS analyses, peptides were extracted from the gel with 1:1 (v/v) 0.1 % TFA/ acetonitrile and after removal of acetonitrile 500 ng peptides subjected to liquid chromatography. An Ultimate 3000 Rapid Separation liquid chromatography system (Dionex/Thermo Scientific, Idstein, Germany) was used for peptide separation. After injection, peptides were pre-concentrated on an Acclaim PepMap100 trap column (3 mm C<sup>18</sup> particle size, 100 Å pore size, 75 mm inner diameter, 2 cm length, Dionex/Thermo Scientific, Dreieich, Germany) at a flow rate of 6 ml/min using 0.1 % (v/v) TFA as mobile phase. After 10 min, peptides were separated on an analytical column (Acclaim PepMapRSLC, 2 mm C<sup>18</sup> particle size, 100 Å pore size, 75 mm inner diameter, 25cm length, Dionex/Thermo Scientific) at 60 °C using a 2 h gradient from 4 to 40% solvent B (solvent A: 0.1 % (v/v) formic acid in water, solvent B: 0.1 % (v/v) formic acid, 84 % (v/v) acetonitrile in water) at a flow rate of 300 nl/min. Mass spectrometry was carried out on an Orbitrap Elite high resolution instrument (Thermo Scientific, Bremen, Germany) operated in positive mode and equipped with a nano electrospray ionization source. Capillary temperature was set to 275 °C and source voltage to 1.4 kV. Survey scans were carried out in the orbitrap analyzer over a mass range from 350 to 1700 m/z at a resolution of 60,000 (at 400 m/z). The target value for the automatic gain control was 1,000,000 and the maximum fill time 200 ms. The 20 most intense 2+ and 3+ charged peptide ions (minimal signal intensity 500) were isolated, transferred to the linear ion trap (LTQ) part of the instrument and fragmented using collision induced dissociation (CID). Peptide fragments were analysed with a maximal fill time of 300 ms and automatic gain control target value of 10,000. The available mass range was 200–2000 m/z at a resolution of 5,400 (at 400 m/z). Already

fragmented ions were excluded from fragmentation for 45 sec.

### Data analyses

Raw files were processed for protein and peptide identification using Proteome Discoverer (version 1.4.1.14, Thermo Scientific, Dreieich, Germany) connected to a Mascot server (version 2.4.1, Matrix sciences, London, UK) with default parameters for spectrum selection. Searches were carried out using 16,620 mouse sequences from the Swiss-Prot part of UniProtKB (release May 2014) applying the following parameters: mass tolerance precursor: 10 ppm (Orbitrap), mass tolerance fragment spectra: 0.4 Da (linear ion trap), trypsin specific cleavage (maximum of one missed cleavage site), fixed modification: carbamidomethyl, variable modifications: methionine oxidation and N-terminal acetylation. For peptide and protein acceptance, the “fixed value PSM validator” was used. Only peptides with high confidence (false discovery rate (FDR) 51 %) were used for protein assembly. For the comparison of the two mouse strains, only proteins with a minimum of two peptide spectrum matches (PSMs) were considered. Log<sub>2</sub> PSM values were used for hierarchical clustering using R (version 3.1.0, R Foundation for Statistical Computing, Vienna, Austria), and calculation of significant different proteins using FDR controlled Welch t-tests (FDR=5 %, S0=0.8), implemented in the Perseus software package (version 1.4.0.20, Max Planck Institute for Biochemistry, Munich, Germany). Results were visualized using OriginPro 8.5 (OriginLab Corporation, Northampton, MA, USA).

### Prediction and annotation of secretory proteins.

Secretory protein prediction and functional annotation was done using different independent methods. First, protein information of all identified proteins was extracted from the Swiss-Prot database (<http://www.uniprot.org/>). To assess secretory properties, protein sequences were analysed by SignalP 4.1 (Petersen *et al.*, 2011; <http://www.cbs.dtu.dk/services/SignalP/>) and SecretomeP 2.0.

(Bendtsen *et al.*, 2004; <http://www.cbs.dtu.dk/services/SecretomeP/>). Literature screening was performed with NCBI/Pubmed (<http://www.ncbi.nlm.nih.gov/pubmed>).

## Results

We have chosen two close related, well characterized and metabolic healthy mouse strains, i.e. C57BL/Ks (BKS) and C57BL/6 (C57) for secretome analyses of isolated adipocytes derived from visceral adipose tissue by mass spectrometry.

### Visceral adipokinome of BKS.

To define the secretome from visceral adipose tissue of BKS mice, secretome samples were collected from five different males to account for biological variability. Specimens were prepared according to our standardized secretome preparation protocol (Göddeke *et al.*, 2014) and subsequently analysed separately by high resolution ESI-LC-MS/MS utilizing an Orbitrap Elite instrument. Acquired spectra were used to search Swiss-Prot protein database (Release May 2014) by Mascot search engine. For reliable protein identification by mass spectrometry solely peptides with high confidence (false discovery rate (FDR) 51 %) were used for protein assembly. We identified 1230 unique proteins in the secretome of visceral adipocytes from the BKS strain (Supplemental Table 1). For further data analysis exclusively proteins were considered which were identified in at least four out of the five biological replicates with a minimum of two peptides for each replicate. This reduced the number of potential adipokines released from visceral adipose tissue of BKS mice to 520 proteins (Supplemental Table 2). Subsequent analysis of these proteins identified 133 proteins which exhibit secretory signal peptides (SP+) and 179 which assigned to non-classical alternative signal peptide-independent secretion mechanisms (SP-) (Supplemental Table 2). The remaining 208 proteins [201] did not show secretory properties according to this computational filtering. Additionally a literature comparison with 11 former adipose tissue secretome profiling studies was also applied to the 520 identified proteins. In a nutshell,

of the identified 520 proteins from BKS secretome 312 (60 %) were previously predicted as secretory and 154 (30 %) were not described in former profiling studies.

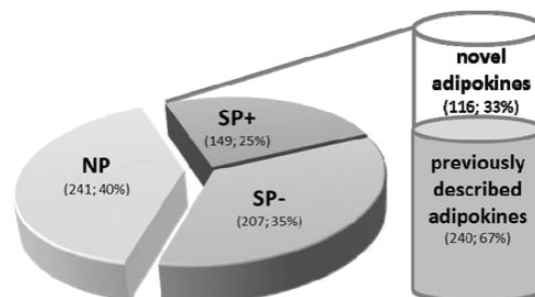


Figure 1. Murine adipose tissue secretome. Distribution of identified proteins to their secretory properties (SP+, signal positive; SP-, secretome positive; NP, non-putative secretory protein). Overlap with previous secretome profiling studies. Number and percentage of proteins are indicated (see also Supplemental Tables 2, 4 and 5).

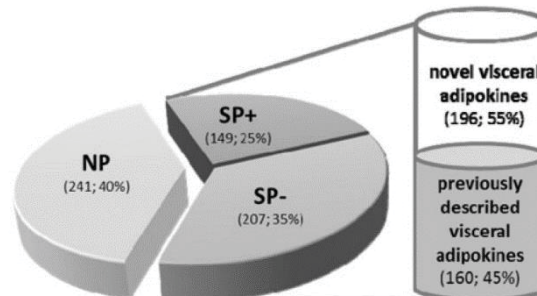


Figure 2. Visceral adipose tissue secretome. Distribution of identified proteins to their secretory properties (SP+, signalP positive; SP-, secretomeP positive; NP, non-putative secretory protein). Overlap with previous secretome profiling studies focusing on the visceral depot. Number and percentage of proteins are indicated (see also Supplemental Table 5).

### Visceral adipokinome of C57

Characterization of the secretory profile from visceral adipocytes from C57 mice resulted in the identification of 1268 non-redundant proteins (Supplemental Table 3). With the restriction of two peptides present for each protein and presence in a minimum of four out of five biological replicates, 494

non-redundant proteins remained (Supplemental Table 4). Of these, 293 (60 %) could be assigned as secretory proteins (126 SP+, 167 SP- and 201 NP). Literature comparison revealed that 367 (74 %) proteins were already described in former studies (Supplemental Table 4).

#### **Reference map for visceral adipose tissue secretome.**

To generate a reference secretome map for murine visceral adipose tissue, the identified proteins achieved from BKS and C57 were compiled. This list is open to the public on our tissue specific secretome database ([www.diabesityprot.org](http://www.diabesityprot.org)). The final list comprises 597 proteins being identified in the secretome from mature visceral adipocytes (Supplemental Table 5). The bioinformatics prediction revealed 75% (149 SP+ and 207 SP-) potential secretory proteins (Figure 1). Literature Comparison of these 356 potential secretory proteins, revealed 240 (67 %) proteins previously assigned to adipose tissue secretome, so we identified 116 proteins as potential novel adipokines. When literature data were restricted to secretomes from visceral origin, the overlap with previously published studies is only 45 % (160 adipokines), whereas 196 adipokines are first assigned to be released from especially visceral adipose tissue (Figure 2) in this study.

#### **Quantitative comparison of BKS and C57 adipose tissue secretomes.**

To examine whether there are quantitative differences between the adipokine release of BKS and C57 we applied a proteome-wide label-free quantification approach based on spectral counting. For calculation of valid differences in protein quantities between the mice strains, only those proteins from the reference map were considered, that were consistently identified in all specimens of the study. The resulting 314 proteins were applied to hierarchical clustering and analyses of these 10 independent datasets derived from two mouse strains with five replicates each, show two main clusters reflecting the genotype (Figure 3). To dissect quantitative alterations between secretomes of both strains, the protein amount differences were calculated using FDR

controlled Welch t-tests. Proteins meeting the set thresholds for being significant different are indicated in the volcano plot (Figure 4) and listed in Table 1. Assigning the proteins to their secretory properties, identified 35 putative adipokines (8 SP+, 27 SP-) discriminating between BKS and C57. Matching with the literature reveals 6 novel adipokines. Of those, only T-Cadherin was assigned a secretory peptide (Table 1) for classical secretion and the secretion levels in BKS are significantly lower.

## **Discussion**

The detailed characterization of the adipose tissue secretome, especially of the visceral fat depot, is essential to understand the role of adipokines in inter-organ communication and their contribution to the pathogenesis of metabolic diseases like cardiovascular diseases or insulin resistance (Guilherme *et al.*, 2008; Mathieu *et al.*, 2009). We have investigated the proteins released by Visceral adipose tissue from two metabolically healthy, commonly used experimental “wild-type” mouse strains, i.e. C57 and BKS. Both genetic backgrounds differentially favor the susceptibility to disease progression under metabolic pressure. In the present study, profiling the proteins secreted by isolated mature visceral adipocytes in a label free LC-MS/MS proteomic approach (Higgs *et al.*, 2008) resulted in the identification of 520 and 494 non-redundant proteins in BKS and C57, respectively. It should be noted that shotgun proteomic approaches, aiming to identify as many proteins as possible, entail that in a single run more than 100,000 detectable peptide species elute at the LC level (Michalski *et al.*, 2011). Although recent developments allow the identification of up to several thousand proteins in a single LC-MS/MS run, the high number of peptides derived from complex samples is still challenging. It has to be considered that coverage of common ions between different samples can be impacted by multiple factors like sample preparation, column conditions, instrument sensitivity and calibration (Houel *et al.*, 2010; Schulze & Usadel 2010; Wenger *et al.*, 2010; Wasinger *et al.*, 2013), especially for low intensity signals. Accordingly missing detection of peptides by a shotgun mass spectrometry approach

does not necessarily mean that the corresponding protein is absent. To reduce false discovery due to these technical limitations, only proteins with a minimum of four out of five identification rate in the replicates were used to define the murine visceral adipose tissue secretomes. For any quantitative comparison between the two genotypes we further restricted our analyses to those proteins that were consistently detectable in all biological replicates. As in our previous reports, we used a stringent computational filtering with known databases (SignalP 4.1, SecretomeP 2.0) to assess whether the identified proteins exhibit secretory properties (Hartwig *et al.*, 2014; Lehr *et al.*, 2012a). When comparing the resulting reference map for murine visceral adipose tissue with previous studies aimed at characterizing the adipose tissue secretome, irrespective of species and depot examined, 240 out of the 356 proteins in the reference map were previously assigned as adipokines (Alvarez-Llamas *et al.*, 2007; Celis *et al.*, 2005; Chen *et al.*, 2005; Kim *et al.*, 2010; Lee *et al.*, 2010; Lehr *et al.*, 2012a; Mutch *et al.*, 2009; Roca-Rivada *et al.*, 2011; Rosenow *et al.*, 2010; Zhong *et al.*, 2010; Zvonic *et al.*, 2007). Thus although 67% of the identified proteins have been previously identified as adipokine, our approach also resulted in the

116 potential novel adipokines. The identification of an unexpected high number of novel adipokines stresses the advantage of restrictive experimental settings, i.e. minimizing the biological variability in the samples due to the utilization of inbred, thus genetically homologous mouse strains and the standardized sample approach in addition to an unbiased analyses technique. Ranking our results more specifically to previous reports of adipokines secreted from the visceral fat depot (Alvarez-Llamas *et al.*, 2007; Chen *et al.*, 2005; Roca-Rivada *et al.*, 2011) results in an overlap of 45% with published proteomic studies.

Consequently, the 196 novel adipokines identified in our study, more than doubles the number of known proteins assigned to be released from the visceral fat depot. This clearly indicates the need for further investigations in order to generate a more complete picture of the highly complex depot-specific secretion signatures. Another advantage of our standardized approach is the direct and quantifiable comparability of results achieved from both inbred mouse strains. Quantification of protein abundances were calculated on basis of the acquired mass spectra. Hierarchical clustering verified the high over-all similarity between the biological replicates, as this is the prerequisite for quantitative analysis of genotype specific protein signatures.

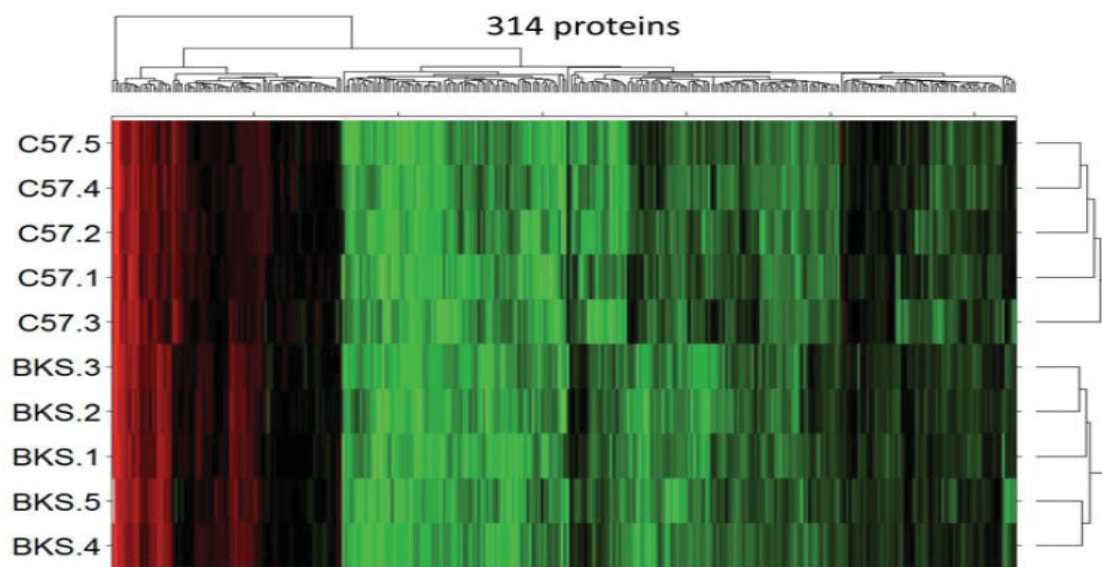


Figure 3. Hierarchical clustering. The presented heat map includes hierarchical clustering endograms for 314 protein intensities to visualize the inter-individual comparison of the dedicated secretomes derived from C57BL/Ks (BKS) and C57BL/6 (C57). The unsupervised clustering (dendrogram, right side) reveals phenotype specificity.

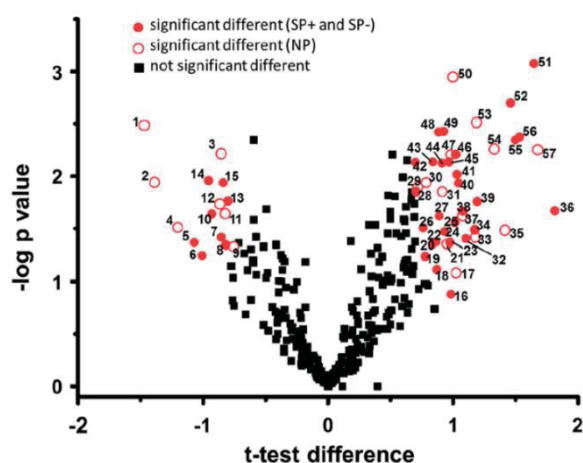


Figure 4. Comparison of visceral adipose tissue secretome signatures derived from C57BL/Ks (BKS) and C57BL/6 (C57). Differences of protein abundances were calculated using FDR controlled Welch t-tests (FDR $\leq$ 5%, S0 $\leq$ 0.8) displayed as volcano plot (Supplemental Table 6). Significant differences are highlighted in red (numbering according to Table 1; red dots: SP+, SP-; red circles: NP; black rectangles: not significant different).

Here 35 mouse strain specific adipokines with six newly described adipokines were identified in this study. According to our hypothesis, the gradual differences in the secretion of adipokines specific proteins for each mouse strain, reflects variations that might account for the different susceptibility to favour obesity and/or diabetic phenotypes under metabolic challenge. Although BKS and C57 mice are phenotypically healthy, the differential susceptibility to develop a primary metabolic phenotype is best demonstrated in mouse strains bred on these genetic backgrounds, e.g. the ob/ob mouse model with a mutation in the leptin gene. The metabolic phenotype of these mice differs by the genetic background strain used (BKS.Cg-Lep<sup>ob</sup> vs. B6.Cg-Lep<sup>ob</sup>) (Coleman & Hummel 1975; Hummel *et al.*, 1972). On C57 background ob/ob mice are prone to develop obesity, but show normoglycaemia and no regression of islets. In contrast, on BKS background ob/ob mice develop early overt hyperglycaemia, hyperinsulinaemia and at least pancreatic islet degeneration in addition to obesity leading to a diabetic phenotype. In line with this, the risk of db/db mice, a mouse model with a mutation in the leptin receptor gene (BKS.Cg-Lepr<sup>db</sup> vs. B6.Cg-Lepr<sup>db</sup>), on BKS genetic background to develop diabetes is severely increased,

whereas mice on C57 background are protected from developing diabetes. So, BKS and C57 mouse strains differ in the primary disease susceptibility, and any further metabolically alteration, e.g. dysfunctional leptin signalling, will give a trigger or “second-hit” to develop metabolic pathologies. At the molecular level, a differential adipokine secretion pattern might be a possibility to initiate and mediate systemic metabolic alterations. The differentially secreted adipokines identified in this study might be involved in this process. In this context one candidate of interest is T-Cadherin (Cadherin 13, CDH13), which is significantly less abundant in the secretome of BKS mice. T-Cadherin is involved in lipid metabolism by specifically binding LDL (Causeret *et al.*, 2005), primarily in lipid rafts (Philippova *et al.*, 2006). Furthermore hexameric adiponectin and high molecular weight (HMW) adiponectin are ligands for T-cadherin (Seino *et al.*, 2007). T-Cadherin is involved in adiponectin-dependent anti-atherogenic actions (Seino *et al.*, 2007) and might affect the HMW/total adiponectin ratio associated with insulin resistance, obesity and cardiovascular diseases (Kudrjashova *et al.*, 2002). In addition CDH13 gene variants are linked to cancer, blood pressure, blood lipid levels, metabolic syndrome, type 2 diabetes, and ischemic stroke in genome-wide association studies (Parker-Duffen *et al.*, 2013). The observations that T-cadherin is correlated with an overall ameliorated metabolic profile including glucose homeostasis and insulin resistance may give a first hint to address the basis for the different susceptibility for metabolic disorders in metabolically healthy background strains BKS and C57.

## Conclusion

Taken together the current study discloses a secretome reference map for murine visceral adipose tissue (<http://www.diabesityprot.org>), contributing to our understanding of the complex secretory capacity of the visceral adipose tissue. Using quantitative proteomic profiling, secretomes of the metabolically healthy background strains BKS and C57 differ by 35 adipokines, of which T-Cadherin levels may be involved in

developing different susceptibility for metabolic disorders. Based on these identifications additional basic research have to clarify the role of adipokine release patterns in order to understand their involvement in the pathophysiology of multifactorial metabolic diseases.

#### **Acknowledgements**

This work was supported by the Ministry of Science and Research of the State of North Rhine-Westphalia (MIWF NRW) and the German Federal Ministry of Health (BMG). This study was supported in part by a grant from the German Federal Ministry of Education and Research (BMBF) to the German Center for Diabetes Research (DZDe. V.).

#### **Declaration of interest**

The authors report no declaration of interest.

Table 1. Proteins exhibit significant quantitative differences between BKS and C57 mice.

Accession	Name	No. in Figure 3	Proportion
<b>Proteins that exhibiting a secretory peptide (SP+)</b>			
Q9WTR5	Cadherin-13	42	BKS <C57
P28653	Biglycan <sup>a</sup>	18	BKS <C57
Q04857	Collagen alpha-1(VI) chain <sup>b,cfghik</sup>	28	BKS <C57
P04186	Complement factor B <sup>acik</sup>	16	BKS <C57
P51885	Lumican <sup>cfghik</sup>	41	BKS <C57
O88322	Nidogen-2 <sup>chjk</sup>	44	BKS <C57
Q91ZX7	Prolow-density lipoprotein receptor-related protein 1 <sup>chk</sup>	8	BKS >C57
P82198	Transforming growth factor-beta-induced protein ig-h3 <sup>cfghik</sup>	36	BKS <C57
<b>Proteins that putative being secreted via non-classical pathways (SP-)</b>			
O35945	Aldehyde dehydrogenase, cytosolic 1	27	BKS <C57
P34914	Bifunctional epoxide hydrolase 2	19	BKS <C57
Q9CWJ9	Bifunctional purine biosynthesis protein PURH	22	BKS <C57
Q61753	D-3-phosphoglycerate dehydrogenase	55	BKS <C57
Q9WVL0	Maleylacetoacetate isomerase	56	BKS <C57
Q8QZS1	3-hydroxyisobutyryl-CoA hydrolase <sup>i</sup>	32	BKS <C57
Q8BWT1	3-ketoacyl-CoA thiolase <sup>ci</sup>	46	BKS <C57
P35979	60S ribosomal protein L12 <sup>hij</sup>	13	BKS >C57
P50247	Adenosylhomocysteinase <sup>jk</sup>	7	BKS >C57
Q9WTP6	Adenylate kinase 2 <sup>fk</sup>	25	BKS <C57
P07356	Annexin A2 <sup>b,cfghik</sup>	40	BKS <C57
Q91V92	ATP-citrate synthase <sup>ghk</sup>	38	BKS <C57
P62204	Calmodulin <sup>a,hi,ik</sup>	52	BKS <C57
P42125	Enoyl-CoA delta isomerase 1 <sup>k</sup>	23	BKS <C57
P97807	Fumarate hydratase <sup>ck</sup>	49	BKS <C57
P51855	Glutathione synthetase <sup>ck</sup>	20	BKS <C57
P13707	Glycerol-3-phosphate dehydrogenase [NAD(+)] <sup>b,cd,fg,hjk</sup>	26	BKS <C57
Q9CPV4	Glyoxalase domain-containing protein 4 <sup>l</sup>	14	BKS <C57
P02088	Hemoglobin subunit beta-1 <sup>ab,cfj</sup>	15	BKS >C57
Q61425	Hydroxyacyl-coenzyme A dehydrogenase <sup>ac,df,gi</sup>	48	BKS <C57
P01872	Ig mu chain C region secreted form <sup>ck</sup>	43	BKS <C57
Q9DCJ9	N-acetylneuraminase <sup>l</sup>	10	BKS >C57
P99029	Peroxioredoxin-5 <sup>fg,hjk</sup>	45	BKS <C57
O54724	Polymerase I and transcript release factor <sup>af,gh</sup>	24	BKS <C57
Q01730	Ras suppressor protein 1 <sup>af</sup>	39	BKS <C57
Q9WVA4	Transgelin-2 <sup>fg,hijk</sup>	6	BKS >C57
P20152	Vimentin <sup>ab,cfghijk</sup>	51	BKS <C57
<b>Proteins that putative being not secreted (NP)</b>			
P63038	60kDa heat shock protein <sup>af,gi</sup>	34	BKS <C57
Q9DCD0	6-phosphogluconate dehydrogenase <sup>cfghk</sup>	53	BKS <C57
Q8QZR5	Alanine aminotransferase 1 <sup>ci</sup>	37	BKS <C57
P28474	Alcohol dehydrogenase class-3 <sup>bc</sup>	11	BKS >C57
P48036	Annexin A5 <sup>h,shj</sup>	33	BKS <C57
P05201	Aspartate aminotransferase <sup>k</sup>	9	BKS >C57
Q8BH61	Coagulation factor XIII A chain <sup>c</sup>	50	BKS <C57
P10126	Elongation factor 1-alpha 1 <sup>b,df,ghik</sup>	21	BKS <C57
P19096	Fatty acid synthase <sup>ac,fg,hjk</sup>	47	BKS <C57
P29391	Ferritin light chain 1 <sup>b,hdj</sup>	31	BKS <C57
Q80X90	Filamin-B <sup>hij</sup>	1	BKS >C57
Q9CPU0	Lactoylglutathione lyase <sup>b,cf</sup>	12	BKS >C57
Q8VDD5	Myosin-9 <sup>h</sup>	4	BKS >C57
P06801	NADP-dependent malic enzyme <sup>ac,df,ghik</sup>	35	BKS <C57
Q9QXS1	Plectin <sup>fhik</sup>	2	BKS >C57
P48678	Prelamin-A/C <sup>fhik</sup>	3	BKS >C57
Q9R1P4	Proteasome subunit alpha type-1 <sup>cd,fhj</sup>	5	BKS >C57
Q05920	Pyruvate carboxylase <sup>i</sup>	54	BKS <C57
Q9D0K2	Succinyl-CoA:3-ketoacid coenzyme A transferase 1 <sup>j</sup>	57	BKS <C57
P40142	Transketolase <sup>ab,cfghijk</sup>	29	BKS <C57
Q91ZJ5	UTP - glucose-1-phosphate uridylyltransferase <sup>b,chk</sup>	30	BKS <C57

Literature previously described in: <sup>a</sup>Chen et al. (2005); <sup>b</sup>Celis et al. (2005); <sup>c</sup>Alvarez-Llamas et al. (2007); <sup>d</sup>Zvonic et al. (2007); <sup>e</sup>Mutch et al. (2009); <sup>f</sup>Kim et al. (2010); <sup>g</sup>Rosenow et al. (2010); <sup>h</sup>Zhong et al. (2010); <sup>i</sup>Lee et al. (2010); <sup>j</sup>Roca-Rivada et al. (2011); <sup>k</sup>Lehr et al. (2012b).

## References

1. Alvarez-Llamas G, Szalowska E, de Vries MP, *et al.* (2007). Characterization of the human visceral adipose tissue secretome. *Mol Cell Proteomics*, 6:589–600.
2. Bendtsen JD, Jensen LJ, Blom, N, *et al.* (2004). Feature based prediction of non-classical and leaderless protein secretion. *Protein Eng Des Sel*, 17:349–56.
3. Bruun JM, Lihn AS, Pedersen SB, Richelsen B. (2005). Monocyte chemoattractant protein-1 release is higher in visceral than subcutaneous human adipose tissue (AT): implication of macrophages resident in the AT. *J Clin Endocrinol Metab*, 90:2282–9.
4. Causeret M, Taulet N, Comunale F, *et al.* (2005). N-cadherin association with lipid rafts regulates its dynamic assembly at cell-cell junctions in C2C12 myoblasts. *Mol Biol Cell*, 16:2168–80.
5. Celis JE, Moreira JM, Cabezon T, *et al.* (2005). Identification of extracellular and intracellular signaling components of the mammary adipose tissue and its interstitial fluid in high risk breast cancer patients: toward dissecting the molecular circuitry of epithelial adipocyte stromal cell interactions. *Mol Cell Proteomics*, 4:492–522.
6. Chen X, Cushman SW, Pannell LK, Hess S. (2005). Quantitative proteomic analysis of the secretory proteins from rat adipose cells using a 2D liquid chromatography-MS/MS approach. *J Proteome Res*, 4:570–7.
7. Coleman DL, Hummel KP. (1975). Symposium IV: Diabetic syndrome in animals. Influence of genetic background on the expression of mutations at the diabetes locus in the mouse. II. Studies on background modifiers. *Isr J Med Sci*, 11:708–13.
8. Despres JP, Lemieux I. (2006). Abdominal obesity and metabolic syndrome. *Nature*, 444:881–7. Flehmig G, Scholz M, Kloting N, *et al.* (2014). Identification of adipokine clusters related to parameters of fat mass, insulin sensitivity and inflammation. *PLoS One*, 9:e99785.
9. Göddeke S, Kotzka J, Lehr S. (2014). Investigating the adipose tissue secretome: A protocol to generate high quality samples appropriate for comprehensive proteomic profiling. *Methods Mol Biol*, [in press].
10. Guilherme A, Virbasius JV, Puri V, Czech MP. (2008). Adipocyte dysfunctions linking obesity to insulin resistance and type 2 diabetes. *Nat Rev Mol Cell Biol*, 9:367–77.
11. Hartwig S, Raschke S, Knebel B, *et al.* (2014). Secretome profiling of primary human skeletal muscle cells. *Biochim Biophys Acta*, 1844:1011–17.
12. Higgs RE, Knierman MD, Gelfanova V, *et al.* (2008). Label-free LC-MS method for the identification of biomarkers. *Methods Mol Biol*, 428, 209–30.
13. Houel S, Abernathy R, Renganathan K, *et al.* (2010). Quantifying the impact of chimera MS/MS spectra on peptide identification in largescale proteomics studies. *J Proteome Res*, 9:4152–60.
14. Hummel KP, Coleman DL, Lane PW. (1972). The influence of genetic background on expression of mutations at the diabetes locus in the mouse. I. C57BL-KsJ and C57BL-6J strains. *Biochem Genet*, 7:1–13.
15. Kim J, Choi YS, Lim S, *et al.* (2010). Comparative analysis of the secretory proteome of human adipose stromal vascular fraction cells during adipogenesis. *Proteomics*, 10:394–405.
16. Kudrjashova E, Bashtrikov P, Bochkov V, *et al.* (2002). Expression of adhesion molecule T-cadherin is increased during neointima formation in experimental restenosis. *Histochem Cell Biol*, 118:281–90.
17. Lee MJ, Kim J, Kim MY, *et al.* (2010). Proteomic analysis of tumor necrosis factor-alpha-induced secretome of human adipose tissue-derived mesenchymal stem cells. *J Proteome Res*, 9:1754–62.
18. Lehr S, Hartwig S, Lamers D, *et al.* (2012a). Identification and validation of novel adipokines released from primary human adipocytes. *Mol Cell Proteomics*, 11:M111.
19. Lehr S, Hartwig S, Sell H. (2012b). Adipokines: a treasure trove for the discovery of biomarkers for metabolic

- disorders. *Proteomics Clin Appl*, 6:91–101.
20. Mathieu P, Poirier P, Pibarot P, *et al.* (2009). Visceral obesity: the link among inflammation, hypertension, and cardiovascular disease. *Hypertension*, 53:577–84.
  21. Michalski A, Cox J, Mann M. (2011). More than 100,000 detectable peptide species elute in single shotgun proteomics runs but the majority is inaccessible to data-dependent LC-MS/MS. *J Proteome Res*, 10:1785–93.
  22. Motoshima H, Wu X, Sinha MK, *et al.* (2002). Differential regulation of adiponectin secretion from cultured human omental and subcutaneous adipocytes: effects of insulin and rosiglitazone. *J Clin Endocrinol Metab*, 87:5662–7.
  23. Mutch DM, Rouault C, Keophipath M, *et al.* (2009). Using gene expression to predict the secretome of differentiating human preadipocytes. *Int J Obes (Lond)*, 33:354–63.
  24. Parker-Duffen JL, Nakamura K, Silver M, *et al.* (2013). T-cadherin is essential for adiponectin-mediated revascularization. *J Biol Chem*, 288:24886–97.
  25. Petersen TN, Brunak S, von Heijne G, Nielsen H. (2011). SignalP 4.0: discriminating signal peptides from transmembrane regions. *Nature Methods*, 8, 785–6.
  26. Philippova M, Banfi A, Ivanov D, *et al.* (2006). Atypical GPI-anchored T-cadherin stimulates angiogenesis *in vitro* and *in vivo*. *Arterioscler Thromb Vasc Biol*, 26:2222–30.
  27. Roca-Rivada A, Alonso J, Al-Massadi O, *et al.* (2011). Secretome analysis of rat adipose tissues shows location-specific roles for each depot type. *J Proteomics*, 74:1068–79.
  28. Romacho T, Elsen M, Rohrborn D, Eckel J. (2014). Adipose tissue and its role in organ crosstalk. *Acta Physiol (Oxf)*, 210:733–53.
  29. Rosenow A, Arrey TN, Bouwman FG, *et al.* (2010). Identification of novel human adipocyte secreted proteins by using SGBS cells. *J Proteome Res*, 9:5389–401.
  30. Scherer PE. (2006). Adipose tissue: from lipid storage compartment to endocrine organ. *Diabetes*, 55:1537–45.
  31. Schulze WX, Usadel B. (2010). Quantitation in mass-spectrometry based proteomics. *Annu Rev Plant Biol*, 61:491–516.
  32. Seino Y, Hirose H, Saito I, Itoh H. (2007). High molecular weight multimer form of adiponectin as a useful marker to evaluate insulin resistance and metabolic syndrome in Japanese men. *Metabolism*, 56:1493–9.
  33. van Harmelen V, Reynisdottir S, Eriksson P, *et al.* (1998). Leptin secretion from subcutaneous and visceral adipose tissue in women. *Diabetes*, 47:913–17.
  34. Wasinger VC, Zeng M, Yau Y. (2013). Current status and advances in quantitative proteomic mass spectrometry. *Int J Proteomics*, 2013, Article ID: 180605.
  35. Wenger C, Phanstiel D, Coon J. (2010). A real-time data acquisition method for improved protein quantitation on hybrid mass spectrometers. *Proceedings of the 58th ASMS Conference on Mass Spectrometry and Allied Topics*, 2010 May 23–27; Salt Lake City, UT.
  36. Wronkowitz N, Romacho T, Sell H, Eckel J. (2014). Adipose tissue dysfunction and inflammation in cardiovascular disease. *Front Horm Res*, 43:79–92.
  37. Zhong J, Krawczyk SA, Chaerkady R, *et al.* (2010). Temporal profiling of the secretome during adipogenesis in humans. *J Proteome Res*, 9:5228–38.
  38. Zvonic S, Lefevre M, Kilroy G, *et al.* (2007). Secretome of primary cultures of human adipose-derived stem cells: modulation of serpins by adipogenesis. *Mol Cell Proteomics*, 6:18–28.

Journal: Archives of Physiology and Biochemistry

Impact factor: 1.09

Contribution: Conceived / designed experiments: 75 %

Performed experiments: 50 %

Analysed data: 75 %

Wrote the manuscript: 50 %

Contributed to discussion: ø

Author: 1st author (shared)

# Study 3: CDH13 abundance interferes with adipocyte differentiation and is a novel biomarker for adipose tissue health.

In revision 11/17, Int J Obesity

Simon Göttsche<sup>1,2,#</sup>, Birgit Knebel<sup>1,2,#</sup>, Pia Fahlbusch<sup>1,2</sup>, Tina Hörbelt<sup>1,2</sup>, Gereon Poschmann<sup>3</sup>, Frederique van de Velde<sup>4</sup>, Tim Benninghoff<sup>1,2</sup>, Hadi Al-Hasani<sup>1,2</sup>, Sylvia Jacob<sup>1,2</sup>, Yves Van Nieuwenhove<sup>5</sup>, Bruno Lapauw<sup>4</sup>, Stefan Lehr<sup>1,2</sup>, D. Margriet Ouwens<sup>1,2,4</sup> and Jörg Kotzka<sup>1,2,\*</sup>

1 Institute of Clinical Biochemistry and Pathobiochemistry, German Diabetes Center at the Heinrich-Heine-University Duesseldorf, Leibniz Center for Diabetes Research, Aufm Hennekamp 65, 40225 Duesseldorf, Germany

2 German Center of Diabetes Research Partner, Duesseldorf, Germany

3 Heinrich-Heine-University Duesseldorf, Molecular Proteomics Laboratory, Biomedizinisches Forschungszentrum (BMFZ), Duesseldorf, Germany

4 Department of Endocrinology, Ghent University Hospital, Ghent, Belgium

5 Department of Gastrointestinal Surgery, Ghent University Hospital, Ghent, Belgium

## Abstract

CDH13, an atypical member of the cadherin superfamily, has been identified in adipocyte secretomes of lean mouse models. This study shows that CDH13 protein abundance and visceral adipose tissue mRNA levels were decreased in obese mouse models. *In vitro* studies in 3T3-L1 adipocytes indicate that CDH13 affects lipid metabolism during adipogenesis, but not in mature adipocytes. Specifically, CDH13 knockdown during adipogenesis reduced fatty acid uptake and lipid content in developing adipocytes. Furthermore, CDH13 depletion during adipogenesis lowered the induction of *PPAR $\gamma$*  and *C/EBP $\alpha$*  expression. These observations are of pathophysiological impact since visceral adipose tissue *CDH13* mRNA and circulating CDH13 levels were decreased in morbidly obese men compared to normal-weight controls. Weight-loss induced by bariatric surgery restored circulating CDH13 to levels found in normal-weight controls. In conclusion, CDH13 is a marker for plasticity of fat

tissue that might reflect the health status of adipose tissue.

## Introduction

Obesity is caused by imbalance between energy supply and energy expenditure. The caloric surplus is stored in white adipose tissue, which needs to remodel to cope with increasing storage capacities and to prevent lipid accumulation in non-adipose tissue ultimately resulting in lipotoxicity and impaired function of these tissues (Unger 2010). Adipose tissue can either rearrange by hypertrophy, thus increasing the lipid storage capacity per cell, or by hyperplasia, i.e. differentiation of adipocyte progenitor cells to mature adipocytes. Adipose tissue is complex and consists of mature lipid-storing adipocytes, the stromal vascular fraction of adipocyte precursor cells, macrophages, fibroblasts, and other cell types needed for innervation and vascularization. Of interest for adipose tissue functionality are adipocyte precursors, mainly originating from mesodermal ancestor cells or the vasculature which are capable to differentiate to mature adipocytes (Tang and Lane, 2012, Gupta *et al.*, 2012). First, progenitor cells are

determined to differentiation. In this phase, the cell is not distinguishable from the fibroblastic precursor and the differentiation cascade, mainly triggered by sequential transcription factor activation, is already initiated. This is followed by the initiation of transcriptional patterns for genes needed for all specific functions of mature adipocytes (Zhuang *et al.*, 2016). A hallmark of adipocyte precursors is PPAR $\gamma$  expression, which seems to be necessary for determination and the full differentiation process. Recently, we have identified CDH13 in murine adipose tissue derived secretomes (Hartwig *et al.*, 2014). CDH13, an atypical member of cadherin superfamily also known as T-cadherin, is a cell surface protein with a glycosyl phosphatidyl inositol (GPI)-anchor but no transmembrane or cytoplasmic domain. Although there is no intracellular signal transducing domain, CDH13 interacts with integrins and acts as adiponectin receptor in cell developmental processes, various cancers and neurological diseases, suggesting that CDH13 may also participate in differentiation (Killen *et al.*, 2017; Fukuda *et al.*, 2017; Dasen *et al.*, 2016). This study aimed at detailing the role of CDH13 in adipose tissue. The observation that CDH13 abundance differs in mouse models according to their susceptibility to develop metabolic disorders (Hartwig *et al.*, 2014) prompted us to investigate whether (i) CDH13 levels in adipose tissue and the circulation are affected by obesity in mouse models and humans, (ii) CDH13 interferes with the differentiation potential of adipocytes and (iii) CDH13 levels are restored by weight loss in humans.

## Results

### Role of CDH13 in adipocyte differentiation

We previously showed in a comparative analysis of adipose tissue secretomes from lean mouse models that the abundance of CDH13 was lower when the tissue was derived from a mouse model prone to develop future obesity (Hartwig *et al.*, 2014). In line with this observation, both the release of CDH13 from adipose tissue as well as the mRNA levels in adipose tissue were lower in obese mice (obob (C57BL/6lep $^{-/-}$ ); dbdb (C57BL/KSllep $^{-/-}$ ))

versus the corresponding lean strains (C57 (C57BL/6); BKS (C57BL/KS)) (Figure 1A, 1B). In order to investigate the role of CDH13 we used an established *in vitro* model for adipocyte differentiation 3T3-L1. The addition of recombinant CDH13 in a concentration comparable to physiological concentrations prior to the induction of adipocyte differentiation (d-1) neither interfered with *axin-2* expression (Figure 1C), a defined endpoint of CDH13/integrin mediated *Wnt*-signaling pathways (Duñach *et al.*, 2017), nor with PPAR $\gamma$  mRNA induction during adipocyte differentiation (Figure 1D). Thus, although identified as factor released from adipose tissue, CDH13 does not seem to elicit an autocrine effect on adipocytes. We next examined the effects on factors implicated in the regulation of adipocyte differentiation. During adipogenesis, CDH13 mRNA expression was highest in progenitor cells (d0), decreased in intermediate cells during differentiation (d4) and was barely detectable in mature 3T3-adipocytes (d9) (Figure 1E). Furthermore, the exposure of pre-adipocytes to palmitate or troglitazone lowered CDH13 mRNA levels at least by 50 %, respectively. Hydrocortisone increased CDH13 expression by 30 %, whereas insulin had no effect (Figure 1F). Although CDH13 expression in mature adipocytes was markedly lower versus precursor cells (Figure 1G), all stimuli examined caused a further reduction in the amount of CDH13 expressed in mature adipocytes. This raised the possibility that CDH13 may interfere with adipocyte differentiation. We next examined whether CDH13 depletion at various stages during adipogenesis (d0, d4, d7) results in physiological alterations of the mature cells (d9) (Figure 2). The increase of insulin-induced glucose uptake during adipocyte differentiation was not influenced by CDH13 depletion (Figure 2A). In contrast, CDH13 depletion reduced fatty acid (FA) uptake in pre-adipocytes and most significantly during adipocyte differentiation (d4) (Figure 2B). Nevertheless, in mature adipocytes a further reduction of CDH13 did not affect FA uptake (Figure 2B). In parallel, CDH13 depletion on given time points interfered with cellular FA content at d9, i.e. depletion in pre-adipocytes and small adipocytes

resulted in much lower lipid content (Figure 2C). Accordingly, depletion of CDH13 mRNA prior to induction of differentiation resulted in decreased *PPAR $\gamma$*  expression, which persists until day 4 of differentiation (Figure 2D). Finally, CDH13 reduction in mature adipocytes did not interfere with isoproterenol induced lipolysis (Figure 2E). We also examined whether CDH13 knockdown at various stages of adipocyte maturation impacted on the expression of key transcription factors involved in adipocyte differentiation, such as *C/EBP $\alpha$* , *PPAR $\gamma$*  or *SREBP-1c* (Zhuang *et al.* 2016). The siRNA-mediated knockdown of CDH13 at all time points during adipocyte maturation effectively lowered CDH13 expression (Figure 3). CDH13 knockdown in pre-adipocytes prior (d0) and during differentiation (d4) depleted the expression of *PPAR $\gamma$*  and *C/EBP $\alpha$*  compared to untreated cells. Silencing CDH13 in mature adipocytes did not affect *PPAR $\gamma$*  and *C/EBP $\alpha$*  expression (Figure 3). The levels of *SREBP-1c*, needed for adipocyte maturation, were not affected by CDH13 knockdown at d0 and d4. CDH13 knockdown in mature adipocytes caused a two-fold increase in *SREBP-1c* levels compared to untreated cells (Figure 3). Although CDH13 reduced FA uptake during differentiation, the expression patterns of various lipid transporters *CD36*, *perilipin*, *FABP4*, were unaffected (Supplement Figure 1).

#### **CDH levels in humans: impact of obesity and weight loss**

Both, circulating CDH13 protein levels and visceral adipose tissue CDH13 mRNA expression were decreased in morbidly obese men compared to normalweight controls (Figure 4A, 4B). The presence of type 2 diabetes did not lead to a further decrease in CDH13 levels (Figure 4A, 4B). In the entire study group, circulating CDH13 was negatively associated to BMI (r: -0.263), fat mass (-0.528), and positively associated to adiponectin (0.403), LDL-C (0.183), or HDL-C (0.236). Correlation to fat mass (-0.509) was also seen in obese participants and fat cell size was negatively correlated in the entire group and the obese diabetic patients (SAT: -0.293, -0.571; VAT: -0.344, -0.427). HDL-C (0.327) and LDL-C (0.373) correlated positively in

obese but not diabetic patients. The correlations with fat mass, adiponectin and HDL-C remained significant in regression models after adjusting to age, or age and BMI. *CDH13* mRNA expression in visceral adipose tissue showed a trend to associate negatively with BMI (-0.180 (0.084)) in the entire study group. The association to HDL-C (-0.370) was also observed for *CDH13* mRNA levels in visceral adipose tissue, and remained significant after adjusting for age, or age and BMI in obese men without diabetes (Supplement table 1). In line with the notion that CDH13 in fat tissue is a marker for the plasticity of the tissue, *PPAR $\gamma$*  but not *C/EBP $\alpha$*  expression was positively related to *CDH13* mRNA expression (Figure 4 C). The correlation of *PPAR $\gamma$*  remained significant if corrected for age, or age and BMI (Supplement table 1). Support to this view was given by investigating of patients before and after bariatric surgery weight control management. Here circulating CDH13 levels were restored to levels of normal-weight controls (Figure 4D).

## **Discussion**

We show that CDH13 is reduced in obesity in mice and men, and can be restored to levels of normal-weight persons following weight reduction. The physiological alterations observed in the study indicate no CDH13 interference with mature adipocyte functionality, rather favor a differentiation delay. The key observation of our study was that reduction of CDH13 amount in adipocyte precursor cells to the level of a mature adipocyte results in reduction of *PPAR $\gamma$*  expression in differentiating adipocytes, as well as in pre-adipocytes which were naive for differentiation triggers. This points towards CDH13 as a marker for fat tissue plasticity. There is increasing knowledge that adipose tissue remodeling is a regulation principle of metabolic healthy and diseased stages, but also the outcome of weight loss, including surgery. Adipose stem cells differentiate in response to adipocyte hypertrophy or released factors to induce visceral adipose tissue hyperplasia (Matsushita and Dzau, 2017). This process depends on extracellular matrix remodeling, the number of adipocyte precursors and coordinated terminal differentiation as critical factors (Muir *et al.*, 2017). For the

mechanistic investigations in this study, we used the established 3T3-L1 cell system to monitor differentiation of fibroblasts-like pre-adipocytes to lipid loaded mature adipocytes. We observed, that key genes for adipogenesis determination (*PPAR $\gamma$* ) and differentiation initiation (*C/EBP $\alpha$* ) are restrained by diminished CDH13 concentration and gene expression needed for terminal cell maturation i.e. *SREBP-1c* is increased. *PPAR $\gamma$*  expression is a hallmark of all adipocyte precursor cells and is central in determination to differentiation, initiation of a transcription cascade in differentiating adipocytes, and governs proliferation and turnover. With a sufficient *PPAR $\gamma$*  level, differentiation is initiated in precursor cells 10 and a transcriptional cascade including *C/EBP $\alpha$*  is activated (Tang and Lane, 2012; Zhuang *et al.* 2016; Siersbæk *et al.*, 2012). If determination to the differentiation process depends on a thrifty *PPAR $\gamma$*  concentration, according to our observation, CDH13 levels in adipocyte precursor cells seem to interfere at this stage with the initiation of adipocyte terminal differentiation due to reduced *PPAR $\gamma$*  expression. Here, we show that CDH13 mRNA is expressed in human visceral adipose tissue, according to our finding of CDH13 in murine adipose tissue secretomes (Hartwig *et al.*, 2014). The pathophysiological impact was given due to the differential abundance of circulating CDH13 in a study collective of morbidly obese men and lean controls. The most striking observation in the context of CDH13 as a marker for adipose tissue with healthy, thus hyperplastic capabilities, is the fact, that the concentration of circulating CDH13 is restored to levels comparable to normal-weight controls in morbid obese men following caloric uptake restriction by surgery weight control management. FA and insulin reduce CDH13 expression in pre-adipocytes or adipocytes. Based on these results, one can speculate that affluent lipids and metabolic active hormones as insulin hampers CDH13 to achieve levels necessary for adipocyte precursor determination to differentiation in states of obesity. This is favored by the finding that restriction of food consumption by bariatric surgery restores circulating CDH13 levels. This is also in line with the association of CDH13 variants to adiponectin and metabolic traits, but not to visceral fat mass (Kitamoto *et al.*, 2016).

Taken together, our data indicate that CDH13 amount is crucial during adipocyte differentiation process. We do not believe that CDH13 is directly involved in the process, rather it seems to reflect a valuable marker for the potential of a cell to differentiate to a terminal stage, thus the plasticity of an individual's fat tissue. So, the higher the CDH13 level, the more plastic the individuals' fat tissue still is, and therefore capable to adapt to metabolic surplus. CDH13, although identified in the secretome of adipose tissue does not qualify as a classical adipokine. It rather is a cell surface protein which is released from the cells by shedding-like mechanisms (Dasgupta *et al.*, 2005, Conant *et al.*, 2015). The presence of CDH13 might interfere with the settling of precursor cells, thus maintaining motility. If environmental conditions favor differentiation, the loss of CDH13 facilitates the integration of the newly differentiating cell into the cell-bound. For this, CDH13 might be implicated in cell adhesion processes in an antiadhesion fashion, as suggested in cancers, metastatic outgrowth, or other cadherin superfamily proteins (Hollingsworth & Swanson, 2004, Bosserhoff, 2014, Lackey *et al.*, 2014). This, in combination with the model suggested by Fujishima (Fujishima *et al.*, 2017) favors CDH13 cell surface presentation and release into cell environment hampers direct cell-cell contact. In turn, based on observations on cadherin superfamily (Dasgupta *et al.*, 2005, Conant *et al.*, 2015), shedding of CDH13 due to reduced expression would favor cell/cell contact, determine differentiation and thus cells form tissues. We are aware of the fact that there are limitations of the study. Next to the physiological investigations, we restricted the analyses to gene expression experiments in 3T3-L1. Another bias is the fact that only men were included in the clinical investigations, so caution should be taken to extrapolate to the general population. In conclusion, CDH13 is a marker for the dynamic of fat tissue to differentiate pre-adipocytes in adipose tissue. High levels of CDH13 indicate the potential of preadipocytes to adipocyte maturation, therefore act as a marker for metabolic active adipose tissue with the potential of increasing lipid storage capacity according to metabolic needs.

### Author's contribution

S.G., P.F., T.H., T.B., G.P., S.J. and performed experiments. S.G., B.K., and J.K.: designed experiments. S.G., B.K., D.M.O., and J.K.: analyzed data. FvdV: recruited patients for the clinical samples, collected and processed samples, supervised serum analysis, maintained clinical records. YvN and BL: supervised clinical study, recruited patients, reviewed manuscript. S.G., B.K., D.M.O and J.K.: wrote the manuscript. H.A-H. and S.L.: contributed to discussion. J.K. is the guarantor of the work.

### Acknowledgements

The work was supported by the German Diabetes Center (DDZ), which is funded by the German Federal Ministry of Health and the Ministry of Innovation, Science, Research and Technology of the state North Rhine-Westphalia. This study was supported in part by a grant from the German Federal Ministry of Education and Research (BMBF) to the German Center for Diabetes Research (DZD e. V.).

### Conflict of interest

The authors state no conflict of interests.

### Contact for reagent and resource sharing

Further information and requests for reagents may be directed to and will be fulfilled by the Lead Contact, Jorg Kotzka (jkotzka@ddz.uni-duesseldorf.de).

## Experimental model and subject details

### Mouse models

The Animal Care Committee of the University Duesseldorf approved all animal care and procedures (Approval#50.05-240-35/06). C57BL/6 (C57), C57BL/KS (BKS), C57BL/KS.Cg-Leprdb/db (db/db) and C57BL/KS.Cg- Lepob/ob (ob/ob) mice were bred and maintained in a regular 12 h light/dark cycle ( $22 \pm 1$  °C,  $50 \pm 5$  % humidity), with free access to water and standard laboratory food (Ssniff, Soest, Germany). Mice (n=5 each genotype) were sacrificed by CO<sub>2</sub> asphyxiation at 14 weeks of age after 6 h food restriction and visceral

adipose tissue was removed (Hartwig *et al.*, 2014, Knebel *et al.*, 2015).

### Patient collective

The study protocols were validated by the Ethical Review Board of Ghent University Hospital (Clinical Registration no NCT00740194 and B67020084018) and conducted according to the Declaration of Helsinki. Written informed consent was given by the patients. Both studies including acquisition of adipocyte derived parameters were described in detail (Ruijge *et al.*, 2012; Bekaert *et al.*, 2015). The morbidly obese men were scheduled for gastric banding or gastric bypass surgery, whereas the normal-weight men were scheduled for elective surgery in the abdominal region. Before surgery, a blood sample was collected after overnight fasting, and stored as aliquots at -80 °C until analysis. During surgery, visceral adipose tissue biopsies were collected, immediately frozen in liquid nitrogen, and stored at -80 °C until analysis. For analysis of CDH13 serum levels and CDH13 mRNA expression 37 normal-weight men and 109 morbidly obese men, including 51 type 2 diabetes patients, were introduced from the Obster Study in our investigation. Supplement Table 2 summarizes relevant clinical parameters for the present investigations.

## Method details

### CDH13 in mouse adipocyte secretomes

Preparation of mature murine adipocytes and sample preparation for secretome analysis of adipose tissue of C57 and BKS was described in detail (Hartwig *et al.*, 2014). Data of dbdb and obob mice were acquired in parallel, although not subject of initial report. In brief, mature adipocytes were isolated by collagenase digestion, cultured for 2 days and secretome samples were harvested as described (Göddeke *et al.*, 2015). Samples were tryptically digested, separated by LC-ESI (Ultimate3000, ThermoScientific, Bremen, Germany), followed by untargeted mass spectrometry (Orbitrap, ThermoScientific) and peptide identification (Proteome Discoverer v.1.4.1.14, ThermoScientific) as described

(Hartwig *et al.*, 2014). For the comparison of mouse strains, Log<sub>2</sub> PSM values were used.

### CDH13 serum levels in human study participants

Circulating CDH13 levels were determined in fasting serum samples using a RayBio® Human Cadherin 13 ELISA Kit (RayBiotech, Norcross, USA), with 40 pg/ml detection limit, 10 % intra-assay CV % and 12 % inter-assay CV %.

### Cell culture

For differentiation from fibroblasts to adipocytes, 3T3-L1 mouse fibroblast cells (Cl- 173, ATCC, USA) cells were grown to confluence and incubated with differentiation medium #1 (DMEM, 11mM glucose, 1 µg/ml troglitazone, 25 µg/ml human Apo- Transferrin, 100 µM hydrocortisone, 2 ng/ml T3, 300 nM insulin (Sigma-Aldrich)). On day 4 differentiation medium #1 was changed to medium #2 (medium #1 without troglitazone, 10 % FCS) and cells were cultured for additional 4 days (Goeddeke *et al.*, 2015).

### CDH13 regulation

3T3-L1 fibroblasts or mature adipocytes were serum starved (24 h) (5.5 mM glucose, 0 % FCS) and incubated with 800 µM PA, 400 µM PO, 100 nM isoproterenol, 1 µg/ml troglitazone, 100 µM hydrocortisone, or 300 nM insulin for 24 h, prior to harvesting.

### CDH13 administration and CDH13 knockdown

3T3-L1 fibroblasts were grown to confluence (day 0), or differentiated to adipocytes (until day 4 or day 7). For investigations with ectopic CDH13 recombinant protein (5 µg/ml = 70 nmol, R&D Systems, Wiesbaden, Germany) was added for 24 h before harvesting of cells. For CDH13 knockdown, cells were lipofected with 50 nM non-target (NT) or 50 nM CDH13 siRNAs (Dharmacon®, GE Healthcare, Freiburg, Germany) per well (24 h, MEM-□ (LifeTechnologies)) following manufacturers' recommendations. CDH13 knockdown was either performed prior to differentiation (d0), during differentiation (d4) or in mature 3T3-L1

cells (d7), as indicated in the respective figure legends.

### Gene Expression Analyses

For gene expression analyses in 3T3-L1 cells, all qPCRs were performed with the cDNA equivalent of 20 ng total RNA and gene-specific probes using 18S RNA as internal standard (RNeasy protocol, Qiagen, Hilden, Germany; Assay on Demand™, ThermoFisher, Darmstadt, Germany) as described (Knebel *et al.*, 2015; Kotzka *et al.*, 2010). For gene expression analysis in human visceral adipose tissue biopsies, total RNA was extracted from 100 mg frozen biopsies (RNeasy lipid tissue kit, Qiacube workstation (Qiagen)). Oligo-dT primed reverse transcription of 500 ng RNA and QPCR was performed using GoScript™, and GoTaq® Master Mix (Promega). The expression of *CDH13*, *PPARγ* and *C/EBPα* was calculated after normalization for the geomean against reference genes (*RPS18*, *YWHAZ*, and *UBE2D2*) (QbasePlus, 2.6; Biogazelle, Ghent, Belgium). All qPCRs were run on a StepOne Plus System (ThermoFisher).

### Glucose uptake in 3T3-L1-cells

Prior to assay, transfected cells were washed (Krebs-Ringer-HEPES buffer (KRH), 0.2 % BSA) and incubated in DMEM 5.5 mM glucose (1 % BSA) for 2 hours. Cells were washed and treated with either KRH/BSA (1 %) or KRH/BSA (1 %) supplemented with 100nM insulin (20 min) followed by 10 min incubation with 50 µl (KRH/BSA (1 %), 2 mM 2-[3H]-Deoxy-D-glucose (2-DOG), 0,02 µCi/µl). Cells were washed with ice-cold KRH/BSA (0.2 %) and lysed. Cell-incorporated glucose was determined in cell lysates by scintillation counting and normalized to protein concentration.

### Analysis of cellular fatty acid uptake

Cells were transfected with either NT or CDH13 siRNA (d0, d4, d7). Cells were washed with KRH/BSA buffer (0.1 %). Cells were pre-incubated in DMEM 11 mM glucose (1 % BSA) (2 h), washed with KRH/BSA (0.1 %) and once with KRH and were incubated with KRH (40 µmol/l BSA) (30 min.). For palmitate incubation, cells were treated with KRH (2.5 µM BSA, 5 µM

3H-palmitate (0.5  $\mu$ Ci, FA:BSA=2), 500  $\mu$ M palmitate (Sigma-Aldrich)) or KRH (2.5  $\mu$ M BSA, 450  $\mu$ M palmitate) (5 min., 37 °C). Cells were washed with ice-cold KRH/BSA (0.1 %) and lysed. Cell-incorporated fatty acids were determined in cell lysates by scintillation counting and normalized to protein concentration.

### Oil-Red-O lipid staining

Quantitation of lipid content of differentiated 3T3-L1-cells by Oil-Red-O was performed as described (Kotzka *et al.*, 2010). Measurement was performed at OD 500 nm.

### Lipolysis assay

At day 7 of differentiation (d7) lipolysis assay was performed following the instructions of manufacturer (Lipolysis Colorimetric Assay Kit; Sigma-Aldrich).

### Statistical Methods

Statistical analyses were performed in GraphPad Prism 5.0 and SPSS 22 (IBM). Data are given as mean  $\pm$  standard deviation [102] and data were directly compared with an unpaired Student's t test. For paired samples of the bariatric study, we used a paired Student-t test. Figure legends indicate the statistical tests applied.

### References

1. Bekaert, M., Van Nieuwenhove, Y., Calders, P., Cuvelier, C.A., Batens, A.H., Kaufman, J.M., Ouwens, D.M., Ruige, J.B. (2015). Determinants of testosterone levels in human male obesity. *Endocrine*. 50, 202-211.
2. Bosserhoff AK, Ellmann L, Quast AS, Eberle J, Boyle GM, Kuphal S. (2014). Loss of T-cadherin (CDH-13) regulates AKT signaling and desensitizes cells to apoptosis in melanoma. *Mol Carcinog*. 53, 635-647.
3. Conant, K., Daniele, S., Bozzelli, P.L., Abdi, T., Edwards, A., Szklarczyk, A., Olchefske, I., Ottenheimer, D., Maguire-Zeiss, K. (2017). Matrix metalloproteinase activity stimulates N-cadherin shedding and the soluble Ncadherin ectodomain promotes classical microglial activation. *J Neuroinflammation*. doi: 10.1186/s12974-017-0827-4
4. Dasen, B., Vlajnic, T., Mengus, C., Ruiz, C., Bubendorf, L., Spagnoli, G., Wyler, S., Erne, P., Resink, T.J., Philippova, M. (2016). T-cadherin in prostate cancer: relationship with cancer progression, differentiation and drug resistance. *J Pathol Clin Res*. 3, 44-57.
5. Dasgupta, A., Hughey, R., Lancin, P., Larue, L., Moghe, P.V. (2005). Ecadherin synergistically induces hepatospecific phenotype and maturation of embryonic stem cells in conjunction with hepatotrophic factors. *Biotechnol Bioeng*. 92, 257-266.
6. Denzel, M.S., Scimia, M.C., Zumstein, P.M., Walsh, K., Ruiz-Lozano, P., Ranscht, B. (2010). T-cadherin is critical for adiponectin-mediated cardioprotection in mice. *J Clin Invest* 120, 4342-4352.
7. Duñach, M., Del Valle-Pérez, B., García de Herreros, A. (2017). p120-catenin in canonical Wnt signaling. *Crit Rev Biochem Mol Biol*. 52 327-339.
8. Fujishima, Y., Maeda, N., Matsuda, K., Masuda, S., Mori, T., Fukuda, S., Sekimoto, R., Yamaoka, M., Obata, Y., Kita, S., *et al.* (2017). Adiponectin association with T-cadherin protects against neointima proliferation and atherosclerosis. *FASEB J*. 31, 1571-1583.
9. Fukuda, S., Kita, S., Obata, Y., Fujishima, Y., Nagao, H., Masuda, S., Tanaka, Y., Nishizawa, H., Funahashi, T., Takagi, J., *et al.* (2017). The unique prodomain of T-cadherin plays a key role in adiponectin binding with the essential extracellular cadherin repeats 1 and 2. *J Biol Chem*. doi: 10.1074/jbc.M117.780734.
10. Göddeke, S., Kotzka, J., Lehr, S. (2015). Investigating the adipose tissue secretome: a protocol to generate high-quality samples appropriate for comprehensive proteomic profiling. *Methods Mol Biol*. 1295, 43-53.
11. Gupta, R.K., Mepani, R.J., Kleiner, S., Lo, J.C., Khandekar, M.J., Cohen, P., Frontini, A., Bhowmick, D.C., Ye, L., Cinti S., *et al.* (2012). Zfp423 expression identifies committed preadipocytes and localizes to adipose endothelial and perivascular cells. *Cell Metab*. 15, 230-239.
12. Hartwig, S., Goeddeke, S., Poschmann, G., Dicken, H.D., Jacob, S., Nitzgen, U., Passlack, W., Stühler, K., Ouwens, D.M., Al-Hasani, H. *et al.* (2014). Identification of novel adipokines differential regulated in C57BL/Ks and C57BL/6. *Arch Physiol Biochem*. 120, 208-215.

13. Hollingsworth, M.A., Swanson, B.J. (2004). Mucins in cancer: protection and control of the cell surface. *Nature Reviews Cancer* 4, 45-60.
14. Killen, A.C., Barber, M., Paulin, J.J., Ranscht, B., Parnavelas, J.G., Andrews, W.D. (2017). Protective role of Cadherin 13 in interneuron development. *Brain Struct Funct.* doi: 10.1007/s00429-017-1418-y.
15. Kitamoto, A., Kitamoto, T., Nakamura, T., Matsuo, T., Nakata, Y., Hyogo, H., Ochi, H., Kamohara, S., Miyatake, N., Kotani, K., *et al.*, (2016). CDH13 Polymorphisms are Associated with Adiponectin Levels and Metabolic Syndrome Traits Independently of Visceral Fat Mass. *J Atheroscler Thromb.* 23, 309-319.
16. Knebel, B., Hartwig, S., Haas, J., Lehr, S., Goeddeke, S., Susanto, F., Bohne, L., Jacob, S., Koellmer, C., Nitzgen, U., *et al.*, (2015). Peroxisomes compensate hepatic lipid overflow in mice with fatty liver. *Biochim Biophys Acta.* 1851, 965-976.
17. Kotzka, J., Knebel, B., Avci, H., Jacob, S., Nitzgen, U., Jockenhovel, F., Heeren, J., Haas, J., Muller-Wieland, D. (2010). Phosphorylation of sterol regulatory element-binding protein (SREBP)-1a links growth hormone action to lipid metabolism in hepatocytes. *Atherosclerosis.* 213, 156-165.
18. Lackey, D.E., Burk, D.H., Ali, M.R., Mostaeedi, R., Smith, W.H., Park, J., Scherer, P.E., Seay, S.A., Marie, P.J., Haÿ, E., *et al.*, (2014). Cadherin-mediated cell-cell adhesion and signaling in the skeleton. *Calcif Tissue Int.* 94, 46-54.
19. Matsuda, K., Fujishima, Y., Maeda, N., Mori, T., Hirata, A., Sekimoto, R., Tsushima, Y., Masuda, S., Yamaoka, M., Inoue, K., *et al.*, (2015). Positive feedback regulation between adiponectin and t-cadherin impacts adiponectin levels in tissue and plasma of male mice. *Endocrinol.* 156, 934-946.
20. Matsushita, K., Dzau, V.J. (2017). Mesenchymal stem cells in obesity: insights for translational applications. *Lab Invest.* doi: 10.1038/labinvest.2017.42
21. Muir, L.A., Baker, N.A., Washabaugh, A.R., Neeley, C.K., Flesher, C.G., DelProposto, J.B., Geletka, L.M., Ghafari, A.A., Finks, J.F., Singer, K., *et al.*, (2017). Adipocyte hypertrophy-hyperplasia balance contributes to weight loss after bariatric surgery. *Adipocyte.* doi: 10.1080/21623945.2017.1287639.
22. Parker-Duffen, J.L., Nakamura, K., Silver, M., Kikuchi, R., Tigges, U., Yoshida, S., Denzel, M.S., Ranscht, B., and Walsh, K. (2013). T-cadherin is essential for adiponectin-mediated revascularization. *J Biol Chem* 288, 24886-24897.
23. Ruige, J.B., Bekaert, M., Lapauw, B., Fiers, T., Lehr, S., Hartwig, S., Herzfeld de Wiza, D., Schiller, M., Passlack, W., Van Nieuwenhove, Y., *et al.*, (2012). Sex steroid-induced changes in circulating monocyte chemoattractant protein-1 levels may contribute to metabolic dysfunction in obese men. *J Clin Endocrinol Metab.* 97, E1187-E1191.
24. Siersbæk, R., Nielsen, R., Mandrup, S. (2012). Transcriptional networks and chromatin remodeling controlling adipogenesis. *Trends Endocrinol Metab.* 23, 56-64.
25. Tang, Q.Q., Lane, M.D. (2012) Adipogenesis: from stem cell to adipocyte *Annu. Rev. Biochem.* 81, 715-736.
26. Unger, R.H., Clark, G.O., Scherer, P.E., Orci, L. (2010). Lipid homeostasis, lipotoxicity and the metabolic syndrome. *Biochim Biophys Acta.* 1801 209-214.
27. Zhuang, H., Zhang, X., Zhu, C., Tang, X., Yu, F., Shang, G.W., Cai, X. (2016). Molecular Mechanisms of PPAR-γ Governing MSC Osteogenic and Adipogenic Differentiation *Curr Stem Cell Res Ther.* 11, 255-264.

## Figure legends

### Figure 1 Role of CDH13 in adipocyte differentiation

A CDH13 is reduced in obese compared to lean mouse models Adipocytes were isolated from C57, BKS, dbdb and obob mice and secretomes were harvested (n=5 replicates, each genotype). CDH13 was identified by mass spectrometry. Data are given as Log2 label free quantification based intensities (LFQ) as Whisker Plots. **B** CDH13 mRNA is differentially expressed in visceral adipose tissue Gene expression levels of CDH13 in visceral adipose tissue isolated from C57, BKS, dbdb and obob mice were determined by qPCR (n=5 replicates, each genotype). **C** CDH13 protein administration during differentiation does not interfere with *wnt* pathway. 3T3-L1 preadipocytes were

incubated with CDH13 recombinant protein (5  $\mu$ g = 70 nmol, 24 h). *Axin-2* (d0) was determined by qPCR. The relative RNA amounts (n=6 replicates) are shown in arbitrary units. **D** CDH13 protein administration during differentiation does not interfere with PPAR $\gamma$  expression. 3T3-L1 preadipocytes were incubated with CDH13 recombinant protein (5  $\mu$ g = 70 nmol, 24 h). PPAR $\gamma$  expression (d0, d4) was determined by qPCR. The relative RNA amounts (n=6 replicates) are shown in arbitrary units. **E** CDH13 mRNA declined during adipocyte differentiation CDH13 mRNA was determined by qPCR during adipocyte differentiation in 3T3-L1 fibroblasts (d0), 3T3-L1 small adipocyte (d4) and mature adipocytes (d9) (n=9 replicates). **F** CDH13 mRNA expression in preadipocytes is reduced by differentiation active agents. 3T3-L1 fibroblasts were serum starved (24 h) (5.5 mM glucose, 0 % FCS) and incubated with 800  $\mu$ M PA, 1  $\mu$ g/ml troglitazone, 100  $\mu$ M hydrocortisone, or 300 nM insulin for 24 h, prior to harvesting (d0, n=7 replicates). **G** CDH13 mRNA expression in mature adipocytes is reduced by differentiation active agents. 3T3-L1 mature adipocytes were serum starved (24 h) (5.5 mM glucose, 0 % FCS) and incubated with 800  $\mu$ M PA, 1  $\mu$ g/ml troglitazone, 100  $\mu$ M hydrocortisone, or 300 nM insulin for 24 h, prior to harvesting (d7, n=7 replicates). Data are given  $\pm$ SD with \*\*\* p<0.001, \*\*p<0.01. \*p<0.05 by Student's t test. Abbreviation: CDH13, cadherin 13, PPAR $\gamma$ , peroxisome proliferator-activated receptor  $\gamma$

### Figure 2 Physiological impact of CDH13 mRNA depletion during adipocyte differentiation

3T3-L1 cells were either transfected with NT or CDH13 to various stages (d0, d4, d7) of differentiation. Experiments were performed 24 h following transfection. **A** Insulin induced glucose uptake is not affected by CDH13. **B** Lipid Uptake in early stages of differentiation is reduced by CDH13 depletion, **C** Cellular lipid content is reduced in early stages of differentiation by CDH13 depletion **D** 3T3-L1 were transfected 24 h prior to differentiation with NT or CDH13. Expression levels of PPAR $\gamma$  were determined by qPCR (n=9 replicates)

at d0 and d4 of differentiation. **E** 3T3-L1 were transfected 24 h prior to differentiation with NT or CDH13. Lipolysis was determined in mature adipocytes (d9) (n=5 replicates). Data are given as mean  $\pm$ SD. NT transfected vs CDH13 knock down cells: \*\*\* p<0.001, \*\* p<0.01. \* p<0.05 by Student's t test. Abbreviations: FA, fatty acid, O-R-O, oil red O staining, KD: knock down, NT: non-target transfected cells, PPAR $\gamma$ , peroxisome proliferator-activated receptor  $\gamma$ .

### Figure 3 CDH13 mRNA depletion alters gene expression during adipocyte differentiation

Gene expression of key lipid metabolic genes in 3T3-L1 cells with CDH13 knockdown to various stages of differentiation. Gene expression levels were determined by qPCR (n = 9 replicates). The relative RNA amount shown in arbitrary units was calculated and plotted  $\pm$ SD. Data are given as mean  $\pm$ SD. NT transfected vs CDH13 knock down cells: \*\* p<0.01. \* p<0.05 by Student's t test. Abbreviations: CDH13, cadherin 13; C/EBP $\alpha$ , CCAAT/enhancer-binding protein  $\alpha$ ; NT, non-target transfected cells, PPAR $\gamma$ , peroxisome proliferator-activated receptor  $\gamma$ ; SREBP, sterol-regulatory element binding protein

### Figure 4 CDH13 in human obesity

**A** CDH13 mRNA is differentially expressed in human visceral adipose tissue of obese compared to lean humans (n=37 lean, n=58 obese, n=53 obese and T2D). The relative RNA amount shown in arbitrary units was calculated and plotted  $\pm$  SD. Obese vs lean participants: \*\* p<0.01. \* p<0.05 by Student's t test. **B** Circulating CDH13 is reduced in obese compared to lean humans. CDH13 concentrations were determined in serum of lean and obese participants (n=37 lean, n=58 obese, n=53 obese and T2D). Data were given as mean  $\pm$ SD. Obese vs lean participants: \*\*\* p<0.001, \*\* p<0.01, \* p<0.05 by Student's t test. **C** Expression of CDH13mRNA correlates to PPAR $\gamma$  but not C/EBP $\alpha$  mRNA. The relative RNA expression was used for correlation analyses. NT transfected vs CDH13 knock down cells: \*\*p < 0.01. \*p < 0.05 by

Student's t test. **C** Association of CDH13 mRNA expression in VAT with adipocyte differentiation relevant PPAR $\gamma$  and C/EBP $\alpha$  mRNA expression. Correlation coefficients (rs) were calculated using Spearman analysis. p-values < 0.05 were considered as statistically significant. Linear regression and 95 % confidence bands (dotted lines) are indicated. Normal-weight controls (white dots), obese individuals (gray dots), obese with T2DM (black dots). **D** Circulating CDH13 is restored after bariatric surgery in morbid obese humans (n=14). Data were analyzed by paired Student's t test. (overall p-value < 0.0014).

Graphical abstract

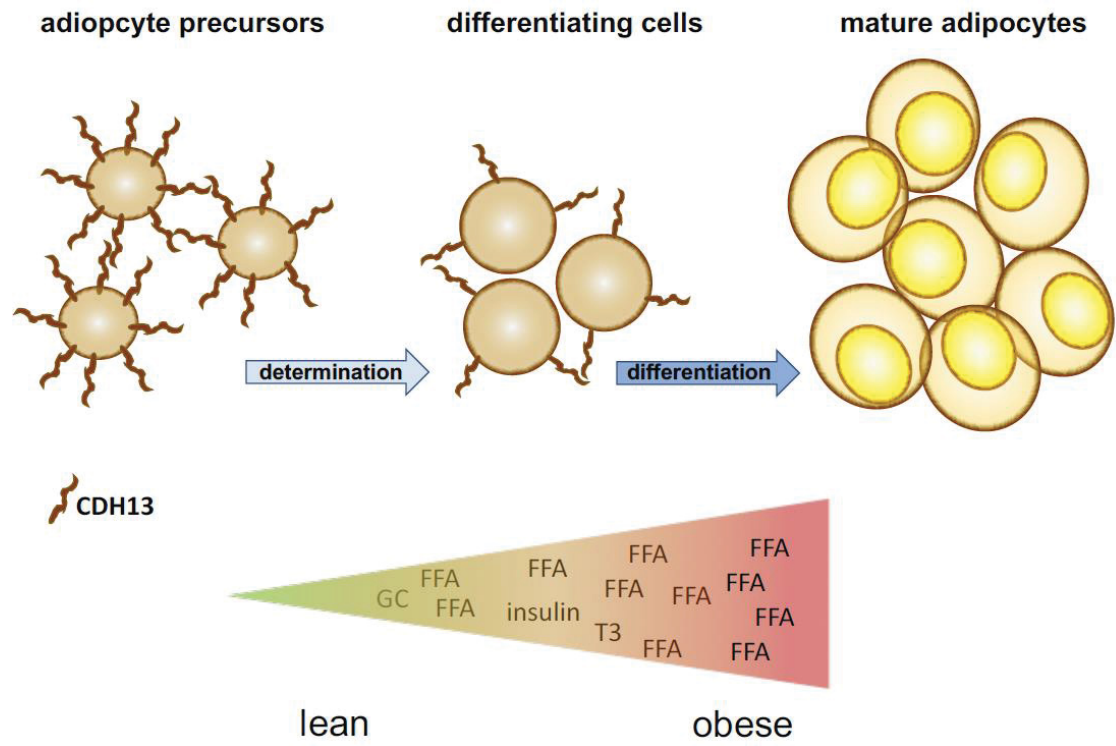


figure 1

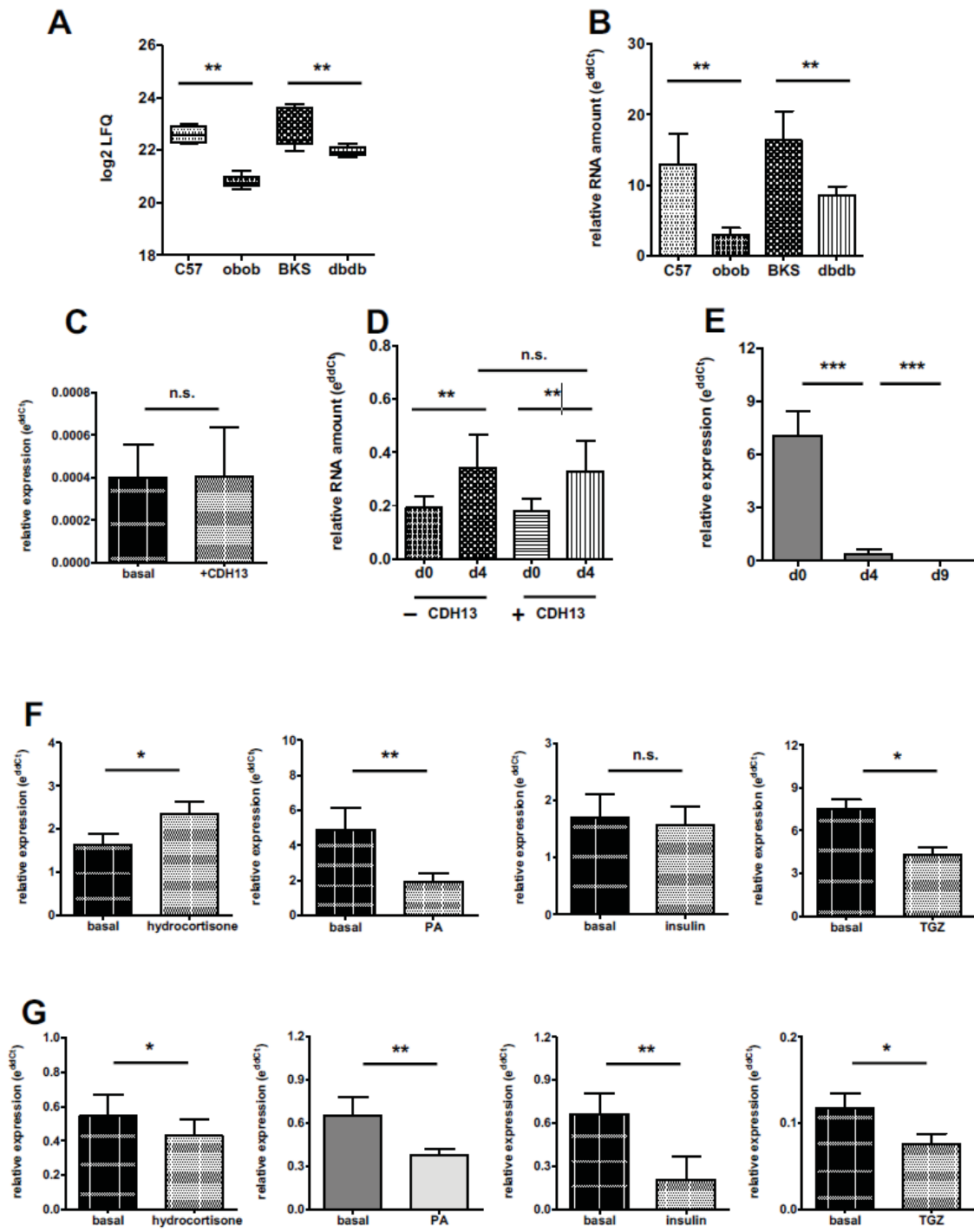


Figure 2 d0

d4

d7

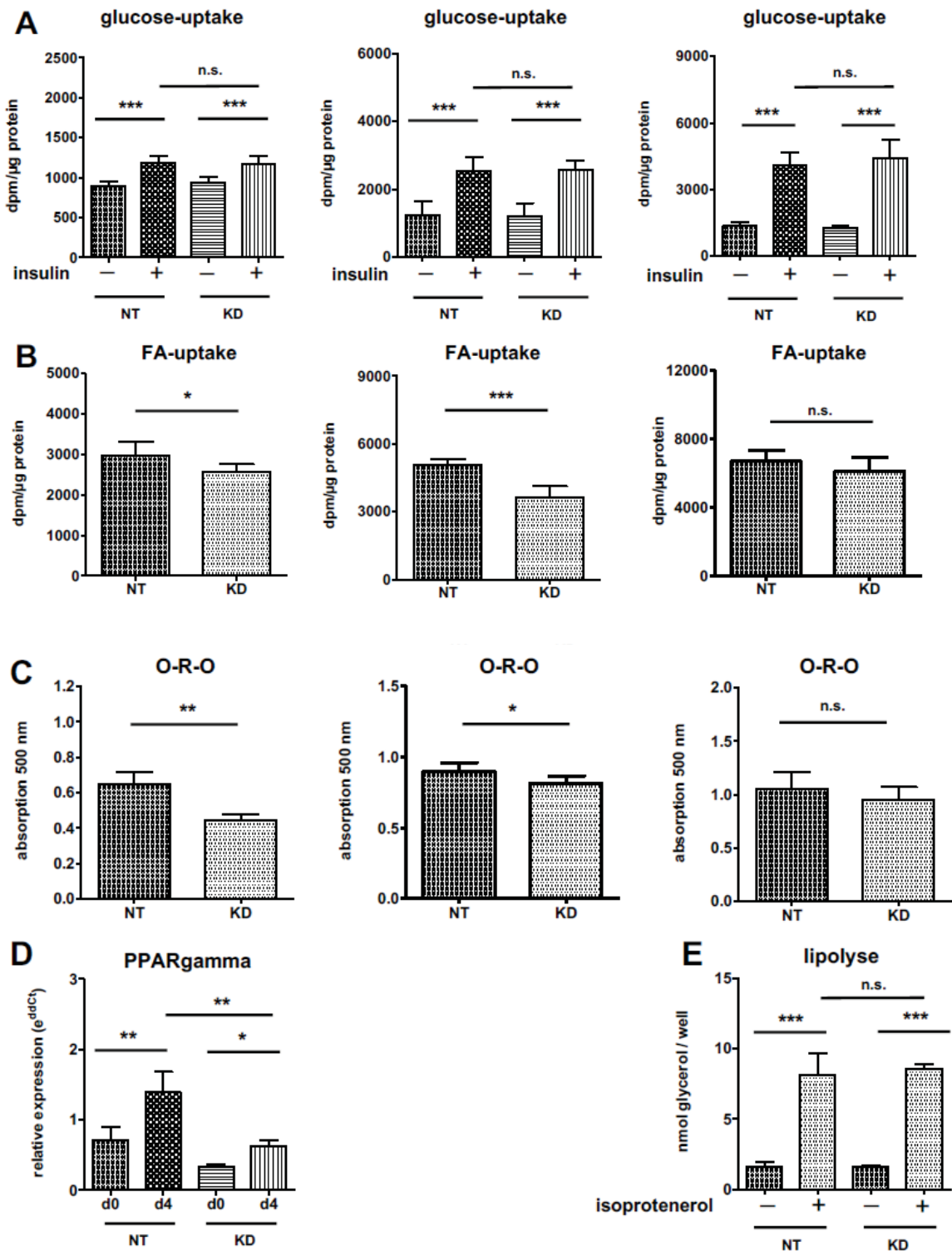


Figure 3

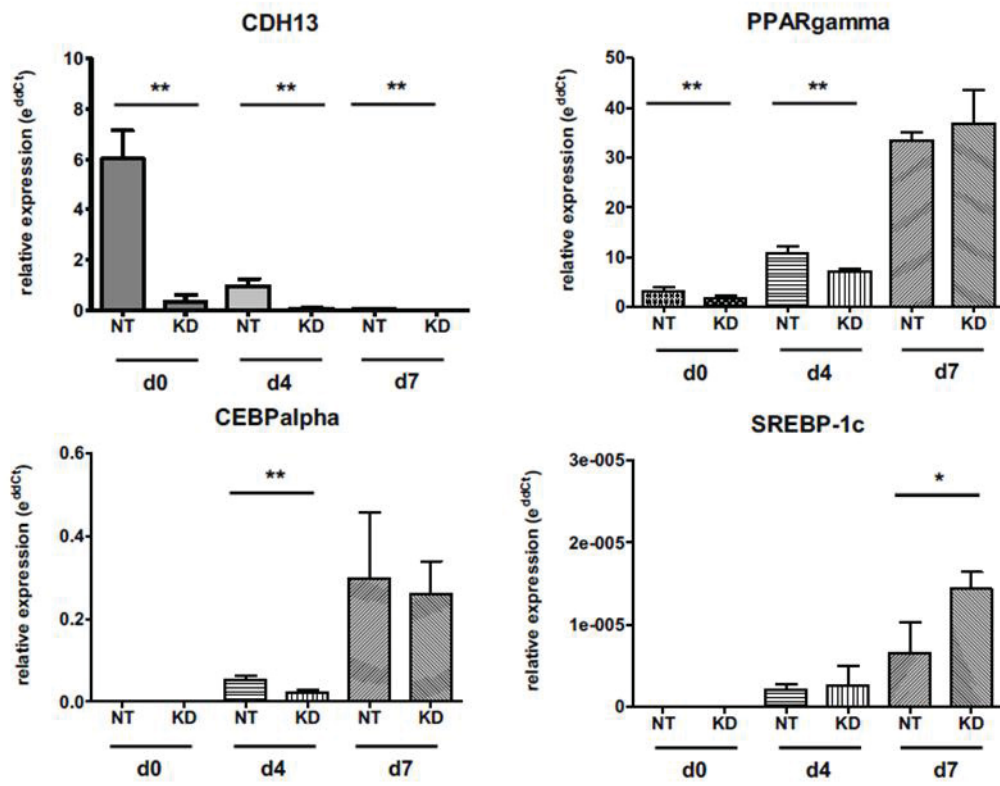
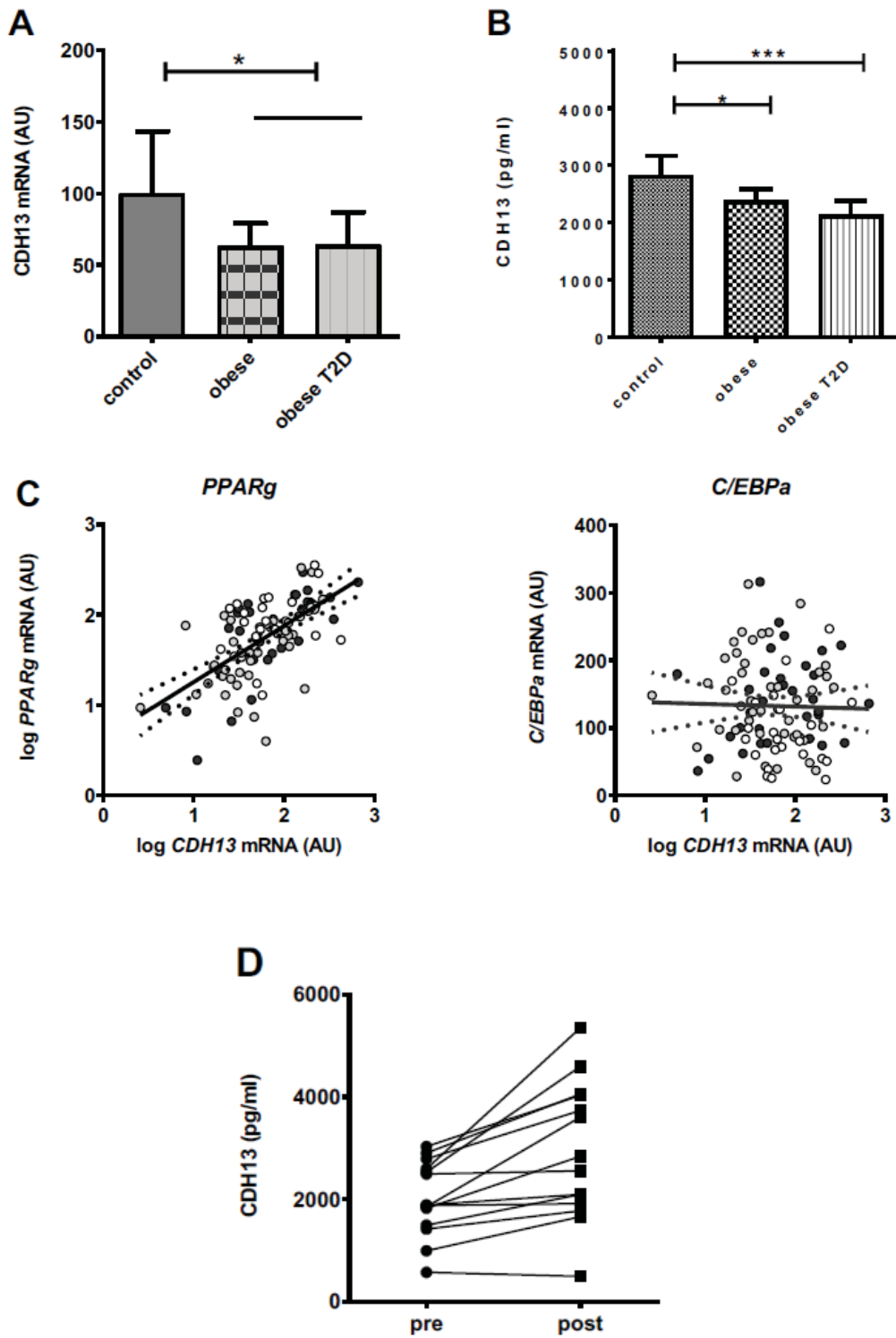


Figure 4



## Patient characteristics:

Variable	Normal weight	Obese wo T2D	Obese + T2D	<i>P</i> <sub>ANOVA</sub>
n	37	58	51	
Age, years	48.2 ± 13.6	42.1 ± 11.1 *	52.2 ± 9.87 ###	<0.001
BMI, kg/m <sup>2</sup>	24.0 ± 2.76	41.2 ± 5.46 ***	43.1 ± 6.88 ***	<0.001
<sup>a</sup> Fat, % body weight	24.1 ± 3.54	37.5 ± 5.80 ***	44.1 ± 6.27 ***, ##	<0.001
<sup>a</sup> SAT cell size, μm <sup>2</sup>	3262 ± 1475	6370 ± 1009 ***	5765 ± 1192 ***	<0.001
<sup>a</sup> VAT cell size, μm <sup>2</sup>	3227 ± 1534	6394 ± 1934 ***	5576 ± 1527 ***	<0.001
Glucose, mmol/l	5.03 ± 1.09	5.67 ± 1.69	8.06 ± 3.16 ***, ###	<0.001
Insulin, pmol/l	35.9 ± 20.7	136 ± 171 ***	170 ± 118 ***	<0.001
HOMA-IR	1.15 ± 0.74	5.78 ± 10.6 *	8.82 ± 6.71 ***	<0.001
HOMA2-%B	79.7 ± 48.9	139 ± 77.4 ***	106 ± 61.7 #	<0.001
Adiponectin, μg/ml	8.70 ± 4.72	5.04 ± 2.88 ***	4.30 ± 2.36 ***	<0.001
ALT, IU/l	28.3 ± 21.7	53.4 ± 30.1 ***	52.3 ± 36.7 ***	<0.001
AST, IU/l	24.6 ± 11.0	32.9 ± 15.9	38.4 ± 25.8 **	0.005
γGT, IU/l	28.1 ± 20.9	44.8 ± 21.5 *	50.2 ± 40.1 **	0.003
Cholesterol, mg/dl	186 ± 39.5	185 ± 46.2	164 ± 38.0 #	0.017
HDL, mg/dl	47.8 ± 14.0	37.4 ± 12.6 ***	36.5 ± 10.7 ***	<0.001
LDL, mg/dl	108 ± 36.8	100 ± 27.9	85.2 ± 29.1 **, #	0.003
NEFA, mEq/l	0.69 ± 0.28	0.63 ± 0.20	0.58 ± 0.18	0.269
TG, mg/dl	140 ± 69.7	217 ± 187	197 ± 154	0.037
CEBP $\alpha$ , mRNA, AU	100 ± 54	142 ± 67.8 *	142 ± 63.0 *	0.011
PPAR $\gamma$ , mRNA, AU	100 ± 75	64.7 ± 66.2	90.3 ± 67.0	0.076

<sup>a</sup>n=46 (16 normal weight, 11 obese without T2D, 19 obese +T2D)

The data are presented as mean ± SD. Differences between the participant groups were calculated using ANOVA followed by Bonferroni analysis for multiple comparisons. BMI, body mass index; SAT, subcutaneous adipose tissue; VAT, visceral adipose tissue; \*\*\*, \*\*, and \* indicate *P*<0.001, *P*<0.01, and *P*<0.05 versus normal weight control men, respectively, whereas ###, ##, and # indicate *P*<0.001, *P*<0.01, and *P*<0.05 for differences between obese men with and without type 2 diabetes

## Pearson analysis – CIRCULATING CDH13

Variable	Entire cohort	Normal weight	Obese – T2D	Obese + T2D	All obese
n	143	37	56	50	106
Age, years	-0.245 (0.003)	-0.359 (0.029)	-0.238 (0.078)	-0.069 (0.634)	<b>-0.229 (0.018)</b>
BMI, kg/m <sup>2</sup>	-0.263 (0.002)	-0.192 (0.263)	0.007 (0.962)	-0.087 (0.548)	-0.081 (0.409)
Fat, % body weight	<b>-0.528 (&lt;0.001)</b>	<b>-0.529 (0.035)</b>	0.227 (0.502)	<b>-0.612 (0.002)</b>	<b>-0.509 (0.002)</b>
SAT cell size, μm <sup>2</sup>	-0.293 (0.041)	0.288 (0.280)	-0.081 (0.813)	<b>-0.571 (0.005)</b>	0.313 (0.076)
VAT cell size, μm <sup>2</sup>	<b>-0.344 (0.015)</b>	-0.115 (0.672)	0.076 (0.824)	<b>-0.427 (0.047)</b>	-0.242 (0.175)
<sup>§</sup> Glucose, mmol/l	-0.153 (0.070)	0.210 (0.212)	<b>-0.386 (0.004)</b>	0.203 (0.162)	-0.135 (0.171)
<sup>§</sup> Insulin, pmol/l	<b>-0.181 (0.031)</b>	<b>0.408 (0.014)</b>	-0.220 (0.103)	-0.040 (0.784)	-0.171 (0.080)
<sup>§</sup> HOMA-IR	<b>-0.197 (0.020)</b>	<b>0.456 (0.005)</b>	<b>-0.295 (0.029)</b>	0.039 (0.794)	<b>-0.199 (0.044)</b>
<sup>§</sup> HOMA2-%B	-0.038 (0.656)	0.156 (0.363)	0.069 (0.615)	-0.174 (0.238)	-0.019 (0.853)
<sup>§</sup> Adiponectin, μg/ml	<b>0.403 (&lt;0.001)</b>	<b>0.439 (0.008)</b>	<b>0.433 (0.002)</b>	0.166 (0.258)	<b>0.307 (0.002)</b>
<sup>§</sup> ALT, IU/l	-0.062 (0.467)	-0.053 (0.757)	0.088 (0.524)	0.047 (0.747)	0.081 (0.414)
<sup>§</sup> AST, IU/l	-0.078 (0.355)	-0.068 (0.692)	0.070 (0.613)	0.014 (0.924)	0.014 (0.887)
<sup>§</sup> γGT, IU/l	-0.085 (0.316)	0.047 (0.788)	-0.059 (0.666)	-0.014 (0.925)	-0.023 (0.813)
<sup>§</sup> Cholesterol, mg/dl	0.163 (0.053)	0.019 (0.910)	<b>0.387 (0.003)</b>	-0.101 (0.486)	0.177 (0.070)
<sup>§</sup> HDL, mg/dl	<b>0.236 (0.005)</b>	0.219 (0.199)	<b>0.327 (0.014)</b>	-0.033 (0.821)	0.152 (0.123)
<sup>§</sup> LDL, mg/dl	<b>0.183 (0.035)</b>	0.154 (0.376)	<b>0.373 (0.006)</b>	-0.120 (0.439)	0.141 (0.169)
<sup>§</sup> NEFA, mEq/l	-0.117 (0.273)	-0.249 (0.290)	-0.042 (0.789)	-0.160 (0.445)	-0.061 (0.618)
<sup>§</sup> TG, mg/dl	-0.128 (0.130)	<b>-0.530 (0.001)</b>	0.073 (0.591)	0.120 (0.406)	0.096 (0.329)

The data are Pearson's  $r$  ( $p$ ). Variables with a skewed distribution (<sup>§</sup>) were log-transformed prior to the analysis.

## Linear regression analysis – CIRCULATING CDH13 - ENTIRE COHORT

Variable	unadjusted	Age	Age + BMI
BMI, kg/m <sup>2</sup>	-0.263 (0.002)	-0.284 (<0.001)	n.a.
Fat, % body weight	-0.528 (<0.001)	-0.537 (<0.001)	-0.902 (0.019)
SAT cell size, μm <sup>2</sup>	-0.293 (0.041)	-0.429 (0.003)	-0.092 (0.640)
VAT cell size, μm <sup>2</sup>	-0.344 (0.015)	-0.410 (0.003)	-0.193 (0.196)
<sup>§</sup> Glucose, mmol/l	-0.153 (0.070)	-0.203 (0.019)	0.028 (0.759)
<sup>§</sup> Insulin, pmol/l	-0.183 (0.030)	-0.181 (0.028)	-0.029 (0.771)
<sup>§</sup> HOMA-IR	-0.199 (0.019)	-0.182 (0.030)	-0.009 (0.934)
<sup>§</sup> Adiponectin, μg/ml	0.403 (<0.001)	0.416 (<0.001)	0.363 (<0.001)
<sup>§</sup> Cholesterol, mg/dl	0.166 (0.049)	0.148 (0.072)	0.125 (0.118)
<sup>§</sup> HDL, mg/dl	0.241 (0.004)	0.270 (0.001)	0.205 (0.014)
<sup>§</sup> LDL, mg/dl	0.186 (0.033)	0.153 (0.077)	0.123 (0.143)
<sup>§</sup> NEFA, mEq/l	-0.117 (0.277)	-0.088 (0.407)	-0.085 (0.418)
<sup>§</sup> TG, mg/dl	-0.127 (0.132)	-0.120 (0.144)	-0.059 (0.475)

Variable	unadjusted	Age	Age + BMI
<sup>§</sup> HDL, mg/dl (entire cohort)	0.241 (0.004)	0.270 (0.001)	0.205 (0.014)
<sup>§</sup> HDL, mg/dl (controls)	0.251 (0.147)	0.345 (0.036)	0.345 (0.059)
<sup>§</sup> HDL, mg/dl (obese without T2D)	0.327 (0.014)	0.300 (0.023)	0.298 (0.026)
<sup>§</sup> HDL, mg/dl (obese with T2D)	-0.033 (0.821)	-0.014 (0.929)	-0.013 (0.934)
<sup>§</sup> HDL, mg/dl (all obese)	0.152 (0.123)	0.164 (0.088)	0.160 (0.096)

The data are β (p). Variables with a skewed distribution (<sup>§</sup>) were log-transformed prior to the analysis.

Pearson analysis – mRNA levels <sup>5</sup>CDH13

Variable	Entire cohort	Normal weight	Obese – T2D	Obese + T2D	All obese
n	93	17	50	26	76
Age, years	0.049 (0.643)	0.229 (0.376)	0.090 (0.535)	-0.189 (0.355)	0.004 (0.970)
BMI, kg/m <sup>2</sup>	-0.180 (0.084)	0.070 (0.789)	0.048 (0.738)	-0.121 (0.557)	-0.018 (0.877)
Fat, % body weight	-0.329 (0.323)	-0.729 (0.480)	0.593 (0.121)	n.a.	0.593 (0.121)
SAT cell size, μm <sup>2</sup>	-0.355 (0.257)	-0.248 (0.840)	0.557 (0.120)	n.a.	0.557 (0.120)
VAT cell size, μm <sup>2</sup>	-0.474 (0.120)	-0.421 (0.723)	0.014 (0.971)	n.a.	0.014 (0.971)
<sup>5</sup> Glucose, mmol/l	-0.122 (0.244)	0.196 (0.451)	0.118 (0.415)	-0.497 (0.010)	-0.126 (0.279)
<sup>5</sup> Insulin, pmol/l	-0.031 (0.768)	-0.191 (0.463)	0.082 (0.577)	0.200 (0.327)	0.121 (0.301)
<sup>5</sup> HOMA-IR	-0.068 (0.521)	-0.085 (0.747)	0.102 (0.485)	-0.047 (0.819)	0.059 (0.617)
<sup>5</sup> HOMA2-%B	0.081 (0.442)	-0.268 (0.298)	-0.005 (0.972)	<b>0.489 (0.011)</b>	0.198 (0.088)
<sup>5</sup> Adiponectin, μg/ml	0.192 (0.083)	0.069 (0.808)	0.065 (0.674)	0.036 (0.867)	0.054 (0.664)
<sup>5</sup> ALT, IU/l	-0.103 (0.330)	0.323 (0.223)	-0.094 (0.519)	-0.015 (0.940)	-0.061 (0.601)
<sup>5</sup> AST, IU/l	0.109 (0.306)	<b>0.510 (0.044)</b>	0.228 (0.115)	-0.033 (0.872)	0.113 (0.336)
<sup>5</sup> γGT, IU/l	-0.002 (0.984)	<b>0.501 (0.048)</b>	0.037 (0.801)	-0.015 (0.940)	0.013 (0.914)
<sup>5</sup> Cholesterol, mg/dl	-0.044 (0.675)	-0.058 (0.826)	0.047 (0.745)	-0.159 (0.439)	-0.035 (0.763)
<sup>5</sup> HDL, mg/dl	-0.032 (0.757)	0.332 (0.192)	<b>-0.370 (0.008)</b>	0.079 (0.702)	-0.212 (0.066)
<sup>5</sup> LDL, mg/dl	-0.050 (0.641)	-0.131 (0.617)	0.051 (0.728)	-0.130 (0.553)	-0.045 (0.707)
<sup>5</sup> NEFA, mEq/l	0.005 (0.963)	-0.155 (0.597)	0.037 (0.817)	0.138 (0.520)	0.080 (0.529)
<sup>5</sup> TG, mg/dl	-0.013 (0.903)	-0.347 (0.173)	0.189 (0.189)	0.109 (0.596)	0.166 (0.153)

The data are Pearson's  $r$  ( $p$ ). Variables with a skewed distribution (<sup>5</sup>) were log-transformed prior to the analysis.

Linear regression analysis – mRNA levels <sup>†</sup>CDH13

Variable	unadjusted	Age	Age + BMI
BMI, kg/m <sup>2</sup>	-0.180 (0.084)	-0.178 (0.089)	n.a.
Fat, % body weight	-0.329 (0.323)	-0.126 (0.693)	0.817 (0.492)
SAT cell size, μm <sup>2</sup>	-0.355 (0.257)	-0.229 (0.417)	-0.211 (0.653)
VAT cell size, μm <sup>2</sup>	-0.474 (0.120)	-0.375 (0.163)	-0.373 (0.247)
<sup>‡</sup> Glucose, mmol/l	-0.122 (0.244)	-0.151 (0.171)	-0.105 (0.357)
<sup>‡</sup> Insulin, pmol/l	-0.031 (0.768)	-0.032 (0.761)	0.060 (0.608)
<sup>‡</sup> HOMA-IR	-0.068 (0.521)	-0.075 (0.483)	0.016 (0.896)
<sup>‡</sup> Adiponectin, μg/ml	0.192 (0.083)	0.193 (0.082)	0.107 (0.371)
<sup>‡</sup> Cholesterol, mg/dl	-0.044 (0.675)	-0.045 (0.670)	-0.042 (0.686)
<sup>‡</sup> HDL, mg/dl	-0.032 (0.757)	-0.036 (0.736)	-0.104 (0.344)
<sup>‡</sup> LDL, mg/dl	-0.050 (0.641)	-0.047 (0.665)	-0.053 (0.622)
<sup>‡</sup> NEFA, mEq/l	0.005 (0.963)	0.015 (0.900)	0.019 (0.873)
<sup>‡</sup> TG, mg/dl	-0.013 (0.903)	-0.018 (0.866)	0.038 (0.727)

Linear regression analysis – mRNA levels <sup>†</sup>CDH13

Variable	unadjusted	Age	Age + BMI
<sup>‡</sup> HDL, mg/dl (entire cohort)	-0.032 (0.757)	-0.036 (0.736)	-0.104 (0.344)
<sup>‡</sup> HDL, mg/dl (controls)	0.332 (0.192)	0.287 (0.302)	0.307 (0.312)
<sup>‡</sup> HDL, mg/dl (obese without T2D)	<b>-0.370 (0.008)</b>	<b>-0.367 (0.009)</b>	<b>-0.365 (0.011)</b>
<sup>‡</sup> HDL, mg/dl (obese with T2D)	0.079 (0.702)	0.147 (0.496)	0.112 (0.615)
<sup>‡</sup> HDL, mg/dl (all obese)	-0.212 (0.066)	-0.212 (0.068)	-0.220 (0.063)

The data are  $\beta$  (p). Variables with a skewed distribution (<sup>‡</sup>) were log-transformed prior to the analysis.

Linear regression analysis – mRNA levels <sup>5</sup>CDH13 - ENTIRE COHORT

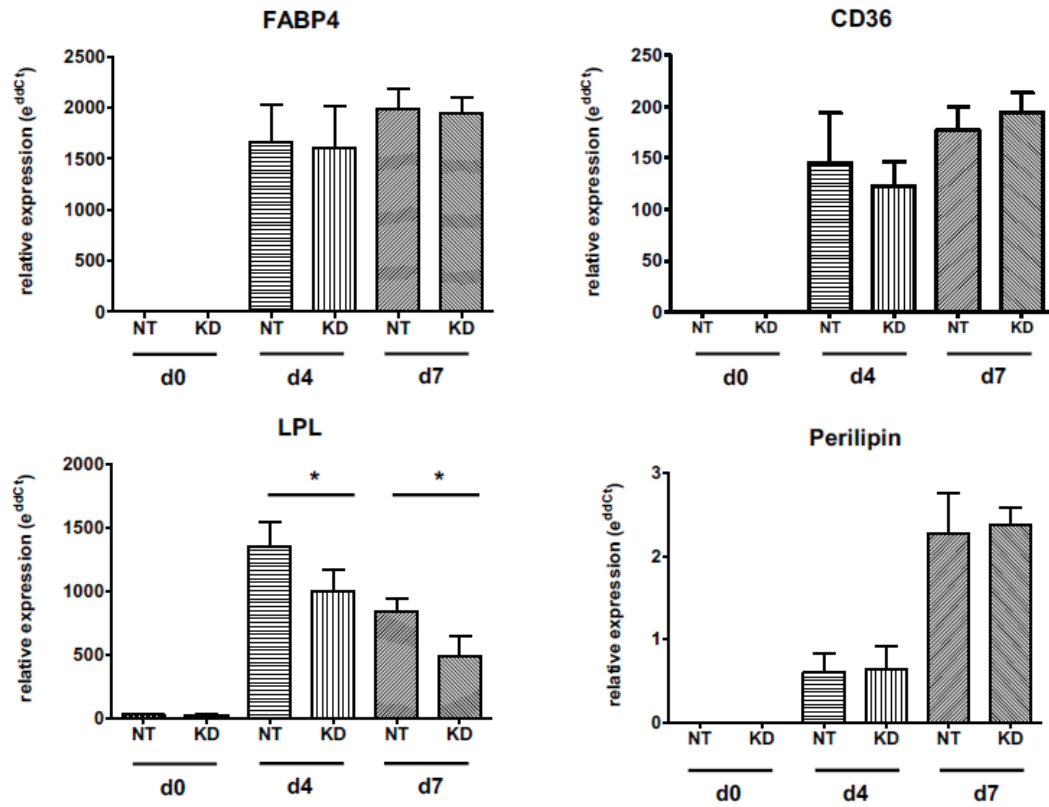
Variable	unadjusted	Age	Age + BMI
<sup>5</sup> PPAR $\gamma$ , mRNA, AU	0.632 (<0.001)	0.634 (<0.001)	0.610 (<0.001)

## Patient characteristics Bariatrix

Variable	baseline	Follow-up	P
n	14	14	
Age, years	50.9 $\pm$ 12.2	53.1 $\pm$ 12.0	<0.001
Weight, kg	145 $\pm$ 26.3	109 $\pm$ 26.7	0.005
BMI, kg/m <sup>2</sup>	44.9 $\pm$ 7.67	34.3 $\pm$ 8.24	0.005
<sup>5</sup> Fat, % body weight	45.0 $\pm$ 9.1	36.8 $\pm$ 11.9	0.011
Glucose, mmol/l	6.52 $\pm$ 1.67	5.34 $\pm$ 0.77	0.963
Insulin, pmol/l	165 $\pm$ 90.1	89.6 $\pm$ 72.7	0.005
HOMA-IR	7.28 $\pm$ 4.51	3.36 $\pm$ 2.82	0.035
Adiponectin, $\mu$ g/ml	6.20 $\pm$ 4.03	11.2 $\pm$ 5.55	0.236
Cholesterol, mg/dl	164 $\pm$ 31.1	167 $\pm$ 37.0	0.036
HDL, mg/dl	43.2 $\pm$ 9.48	61.3 $\pm$ 13.1	0.136
LDL, mg/dl	92.6 $\pm$ 26.8	86.1 $\pm$ 30.8	0.302
TG, mg/dl	138 $\pm$ 70.3	96.0 $\pm$ 41.1	0.735

The data are presented as mean  $\pm$  SD. Differences between the participant groups were calculated using a paired t-test. BMI, body mass index; SAT, subcutaneous adipose tissue; VAT, visceral adipose tissue; \*\*\*, \*\*, and \* indicate  $P < 0.001$ ,  $P < 0.01$ , and  $P < 0.05$  versus baseline, respectively.

## Figure Supplement



## Supplement inventory

### Table S1:

Patient characteristics:

Pearson analysis – CIRCULATING CDH13

Linear regression analysis –  
CIRCULATING CDH13 - ENTIRE  
COHORT

Pearson analysis – mRNA levels CDH13

Linear regression analysis – mRNA levels  
sCDH13

Linear regression analysis – mRNA levels  
CDH13

Linear regression analysis – mRNA levels  
CDH13 : PPAR $\alpha$ , - ENTIRE COHORT

Patient characteristics Bariatrics

### Figure S1:

#### **Supplement Figure 1 CDH13 mRNA depletion alters gene expression during adipocyte differentiation.**

Gene expression of key lipid metabolic genes in 3T3-L1 cells with CDH13 knockdown to various stages of differentiation. Gene expression levels were determined by qPCR (n = 9 replicates). The relative RNA amount shown in arbitrary units was calculated and plotted  $\pm$ SD. NT transfected vs CDH13 knock down cells: \*\* p<0.01. \* p<0.05 by Student's t test.

Abbreviations: CD36, cluster of differentiation 36; FABP4, fatty acid binding protein 4; FAS, fatty acid synthase; KD, knock down, LPL, lipoprotein lipase; NT, non-target transfected cells

Journal: International Journal of Obesity

Impact factor: 5.487

Contribution: Conceived / designed experiments: 33 %

Performed experiments: 55 %

Analysed data: 40 %

Wrote the manuscript: 30 %

Contributed to discussion: ø

Author: 1st author (shared)

## Study 4: Novel insights into the adipokinome of obese and obese/diabetic mouse models.

Accepted 09/2017; IJMS

Birgit Knebel<sup>1,2</sup>, Simon Goeddeke<sup>1,2</sup>, Gereon Poschmann<sup>3</sup>, Daniel F. Markgraf<sup>2,4</sup>, Sylvia Jacob<sup>1,2</sup>, Ulrike Nitzgen<sup>1,2</sup>, Waltraud Passlack<sup>1,2</sup>, Christina Preuss<sup>2,4</sup>, Hans-Dieter Dicken<sup>5</sup>, Kai Stühler<sup>3,6</sup>, Sonja Hartwig<sup>1,2</sup>, Stefan Lehr<sup>1,2,§</sup>, Jorg Kotzka<sup>1,2</sup>

**Running title:** Murine Adipokinome

<sup>1</sup>Institute of Clinical Biochemistry and Pathobiochemistry, German Diabetes Center at the Heinrich-Heine-University Duesseldorf, Leibniz Center for Diabetes Research; Duesseldorf, Germany

<sup>2</sup>German Center for Diabetes Research (DZD), Partner Duesseldorf, Germany

<sup>3</sup>Heinrich-Heine-University Duesseldorf, Molecular Proteomics Laboratory, Biomedizinisches Forschungszentrum (BMFZ), Duesseldorf, Germany

<sup>4</sup>Institute of Clinical Diabetology, German Diabetes Center at the Heinrich-Heine-University Duesseldorf, Leibniz Center for Diabetes Research; Duesseldorf, Germany

<sup>5</sup>Multimedia Center, Heinrich-Heine-University Duesseldorf, Duesseldorf, Germany

<sup>6</sup>Institute for Molecular Medicine, University Hospital Duesseldorf, Heinrich Heine University Duesseldorf, 40225 Duesseldorf, Germany

### Abstract

The group of adipokines comprises hundreds of biological active proteins and peptides released from adipose tissue. Alterations of those complex protein signatures are suggested to play a crucial role in the pathophysiology of multifactorial, metabolic diseases. We hypothesized that also the pathophysiology of type-2-diabetes is linked to the dysregulation of the adipocyte secretome. To test this, we investigated mouse models with monogenic defects in leptin signaling which are susceptible to adipositas (C57BL/6 Cg-Lep<sup>ob</sup> (obob)) or adipositas with diabetes (C57BL/KS Cg-Lepr<sup>db</sup>

(dbdb)) according to their genetic background. At the age of 17 weeks, visceral fat was obtained and primary murine adipocytes were isolated to harvest secretomes. Quantitative proteome analyses (LC-ESI-MS/MS) identified more than 800 potential secreted proteins. The secretome patterns revealed significant differences connected to the pathophysiology of obese mice. Pathway analyses indicated that these differences focus on exosome modelling, but failed to provide more precise specifications. To investigate the relationship of secretome data to insulin sensitivity, we examined the content of diabetogenic lipids, i.e. diacylglycerols (DAGs), identified as key players in lipid-

**induced insulin resistance. In contrast to obob mice, fat tissue of dbdb mice showed elevated DAG content, especially of DAG species with saturated fatty acid C16:0 and C18:0, while unsaturated fatty acid C16:1 were only changed in obob. Furthermore, DAG signatures of the models specifically correlate to secreted regulated adipokines indicating specific pathways. In conclusion, our data further support the concept that the fat tissue is an endocrine organ that releases bioactive factors corresponding to adipose tissue health status.**

### Keywords

Primary adipocyte; mass spectrometry; healthy adipose tissue; diacylglycerol; diabetes and obesity

### Introduction

Obesity is a worldwide health burden caused by increased energy intake and sedentary lifestyle. It increases the overall risk for life threatening comorbidities including cardiovascular risk, hypertension, pulmonary obstructive syndrome, dyslipidemia, metabolic syndrome or diabetes, and cancer (1-3). Adipose tissue comprises mature adipocytes, preadipocytes and various invasive immune cells which, in sum, act as secretory organ of bioactive proteins, designated as adipokines. The secreted adipokine patterns in a certain metabolic conditions or stage of obesity are thought to reflect the state of the adipose tissue condition and “health” or its “metabolic flexibility” (4).

A recent investigation described the secretome of visceral adipose tissue from two closely related, well-characterized and metabolically healthy mouse strains, i.e. C57BL/Ks (BKS) and C57BL/6 (C57) by combining state-of-the-art protein identification and quantification tools (5). A reference map comprising about 600 adipokines was generated (<http://www.diabetesityprot.org>). Both commonly used experimental “wild-type” mouse strains differ in their response to

metabolic stress. In contrast to animals with C57 genetic background, mice with a BKS genetic background are prone to develop diabetes under such conditions (6,7). Therefore, mouse models with genetic defects in leptin signaling are obese (obob) or obese and diabetic (dbdb), depending on genetic background.

Obesity is accompanied by disturbed lipid metabolism, elevated levels of free fatty acids (FFA) and triglycerides (TG), either due to over-nutrition or increased hepatic *de novo* lipid synthesis (8). Besides adipose tissue, multiple organs, e.g. liver, skeletal muscle, pancreas, or kidneys, are affected. These organs can be the target of ectopic lipid accumulation and obesity-associated insulin resistance. The systemic overflow with increased fluxes of plasma FFA and TGs towards these tissues leads to the ectopic accumulation of lipids and obesity associated insulin resistance, ultimately altering tissue glucose metabolism and affecting blood glucose clearance. Ectopic lipid accumulation is accompanied by the accumulation of bioactive metabolites, e.g. diacylglycerol (DAG), in the various tissues (9). DAGs are a result of several metabolic fluxes, including triglyceride hydrolysis, triglyceride synthesis, or phosphoinositide hydrolysis. In liver, it has been shown that DAG content is significantly increased in lipid-induced hepatic insulin resistance. DAGs act as second messengers activating members of novel protein kinase C (nPKC) family (10). This raised our hypothesis that an excess of these bioactive metabolites alters the intracellular signaling also in adipose tissue and in consequence the inter-organ communication in form of the adipocyte secreted protein patterns.

We intended to investigate the specific differences in the secretome of adipocytes in states of obesity and obesity with diabetes. For this, we utilized obese and obese/diabetic mouse models to compare the adipocyte-derived, not fat tissue, secretion pattern of adipokines and return the information to the adipocyte-derived DAG patterns. Our results suggest that DAG-

signaling in adipose tissue acts as intermediary between healthy or diabetic state.

## Results and Discussion

C57BL/KS.Cg-Lepr<sup>db</sup> (dbdb) mice on C57BL/KS (BKS) genetic background, a well-accepted mouse model of hyperphagia induced obesity with overt diabetes, and C57BL/6.Cg-Lep<sup>ob</sup> (obob) mice on C57BL/6 (C57) background which are protected from diabetes (6, 7, 11-15) were selected for this study. The clinical characteristics of the investigated mouse models are summarized in Fig. 1. The obese mouse model and the obese/diabetic mouse model showed increased body weight with more than 50 % fat mass compared to the lean models. Overall the models also showed specific differences in direct comparison to the genetic background model. Fasting glucose, triglycerides, insulin, and HOMA-IR were each significantly higher in dbdb compared to BKS mice, while HOMA-B was lower, indicating the definitions of overt diabetes in the dbdb model compared to obob mice. In contrast, in obob mice, insulin and HOMA-IR were significantly higher compared to C57. HOMA-B were strongly elevated while glucose was normal indicating that the beta cells are still capable to compensate required insulin levels. Leptin was significantly elevated only in dbdb, as expected from the genetic defect of this model. Similarly, glucagon and glucagon like peptide (GLP)-1 were significantly increased only in dbdb mice. This can be attributed to the diabetic state of these mice which was confirmed by high HOMA-IR index and thus peripheral insulin resistance. Ghrelin was 4-fold reduced in the obese and 2-fold reduced in obese/diabetic mice, whereas glucose-dependent insulinotropic peptide (GIP), adiponectin or resistin levels did not differ significantly between models.

To further analyze differences between adipose tissue of these mouse models, we determined the content of secreted proteins by mass spectrometry. The overall comparison is given in *Supplement table 1*.

According to our experimental design, identified proteins were located outside of intact primary adipocytes. Proteins traffic through the secretory pathway according to their N-terminal signaling sequence to reach their intracellular destination, e.g. an organelle, or to ultimately be secreted. Transport throughout the endomembrane system occurs via the endoplasmic reticulum and the golgi apparatus towards the plasma membrane. Here, the release can occur passive, active channel-mediated, or driven by formation of secretory granules and exosomes. Proteins are targeted according to classical (SP(+)) or non-classical (SP(-)) signal sequences. Proteins without any known signal sequence [201] are thought to follow e.g. pore-mediated translocation across the plasma membrane, ABC transporter-based secretion or autophagosome/endosome-based secretion (16). This classification can also help to determine transmembrane proteins (17). Nevertheless, we cannot completely exclude that some of the proteins might be identified due to apoptosis or autophagy.

The comparisons identified 873 non-redundant proteins. Of these, 216 were assigned to contain a SP(+) signal peptide, 290 were SP(-), thus not carrying a classical signaling peptide and 367 were NP without a signaling domain. The pairwise comparison of the four animal models showed significant alteration (*Supplement Table 2*). The comparisons of BKS and dbdb models identified 198 upregulated and 153 downregulated proteins in dbdb (94 SP(+), 118 SP(-), 139 NP). The comparisons of C57 and obob indicated 182 upregulated and 118 downregulated proteins in obob (88 SP(+), 98 SP(-), 114 NP). The individual comparisons indicated in the lean models 108 upregulated and 136 downregulated proteins in BKS (59 SP(+), 87 SP(-), 98 NP), and in the obese and obese/diabetic models 88 upregulated and 112 downregulated proteins in dbdb (61 SP(+), 75 SP(-), 64 NP). Table 1 (see *Supplement Table 2* for complete analyses) summarizes the top 10 up- and down- regulated putative secreted (SP(+), SP(-)) proteins of the comparisons.

Furthermore, there were proteins specific for either genotype in the comparisons (Table 2). Additionally, there were 38 solitaire proteins in BKS vs C57 (8 SP(+), 13 SP(-), 17 NP), 22 in C57 vs obob (10 SP(+), 6 SP(-), 6 NP), 60 in BKS vs dbdb (17 SP(+), 17 SP(-), 26 NP) or 10 in dbdb vs obob (5 SP(+), 2 SP(-), 3 NP).

With regard to function, top regulated proteins or solitaire proteins were comprehensively, among them proteins involved in lipid transport (e.g. ApoE, ApoA4), enzymes (e.g. Lpl, Aad9, Acadvl, Fbp1, Acyl, Ca4, Khk, Pgp), and signaling proteins (e.g. Il6, Sdpr, Gc, Esp15, Rbp-1, Cxcl-5, -3, -9) proteins. Overall, the total adipocyte secreted proteins were able to differentiate lean, obese and the obese/diabetic mouse models (Figure 2). Nevertheless, patterns do not only show overlap according to the lean or obese and obese/diabetic phenotype, but also according to genotype. So, we compared all differentially abundant proteins in the various groups (Figure 3, *Supplement table 3*). With these analyses, we were able to account on any different abundance in conditions depending on genetic background. So, we identified 36 proteins that were solely differential abundant within lean and obese mice (C57 vs obob), 67 proteins that differed in the comparison of lean to obese/diabetic mice (BKS vs dbdb), and 42 proteins that differed in the lean background strains. These candidates might be of interest in regard to the phenotype, but still contain the genotype bias.

Consistent with the experimental design of adipocyte secretome analyses, all comparisons in databases such as GO, KEGG or IPA annotated to keywords like “extracellular exosome” (FDR= 1.03e-10 - 7.13e-27), or “membrane-bounded vesicle” (FDR= 1.03e-10 - 7.08e-24) with the highest significance. Other keywords were rather unspecific e.g. “amide metabolism” (n=7, FDR= 2.02e-3), or “regulation of protein metabolic process” (n=13, FDR= 2.02e-3) for C57 based comparisons. BKS based comparisons also identified general

metabolic pathways like “metabolic process” (n=46, FDR= 2.86e-05), “regulation of protein transport” (n=10, FDR= 7.3e-4), or “protein metabolic process” (n=23, FDR= 8.94e-4).

The analyses further identified proteins, that differed in both obese and obese/diabetic models compared to the lean mice (n=106, “obesity pattern”). These proteins were related to the obese phenotype independent of genotypes investigated. Another 19 proteins differed between obese and obese/diabetic regardless of genotype, and 36 proteins were specific for diabetes despite obesity as they differ among obese and obese/diabetic (Figure 3, *Supplement table 3*). In pathway analyses of these protein sets, functional annotation only indicated direct secretion or vesicle secretion, as expected from experimental design (*Supplement Table 3*). Functional annotation identified key words like “extracellular exosome” (n=70, FDR= 3.26e-41) or “membrane-bounded vesicle” (n=75, FDR= 3.36e-41) for the obesity pattern, “extracellular region” (n=13, FDR= 3.34e-05) for the diabetes pattern or “extracellular exosome” (n=24, FDR= 5.89e-13), and “membrane-bounded vesicle” (n=25, FDR= 3.96e-12) for the diabetes despite obesity pattern as best hits. Other key terms of potential interest to metabolic energy balance showed lower significance and limited numbers of assigned proteins e.g. mitochondria (BKS vs dbdb, n=17, FDR= 1.76e-3; diabetes despite obesity, n=15, FRD= 6.44e-07), lipid metabolism (BKS genotype based differences, n=11, FDR= 1.12e-3), lipid catabolic process, lipid- or phospholipid binding (obesity pattern, n=5, FDR= 3.17e-3; n=12, FDR= 4.68e-4; n=9, FDR= 4.68e-4), or fatty acid degradation (diabetic despite obesity pattern, n=3, FDR= 1.42e-4) (*Supplement Table 3*).

In general, enrichment analyses were used to facilitate the interpretation of numerous genes or proteins which are the usual outcome of hypothesis generating experimental designs. Thus, the accumulation of candidates with known

biological function or interaction, either directly experiment proven or deduced from literature, were monitored in a dataset. Knowledge based pathway annotation or gene enrichment analyses can help to classify “Omics” data, but also bares some restrictions. Next to bioinformatics, the main issue being intrinsic to the experimental setting (18). We use secreted proteins, so enrichment of secreted proteins or related pathways with highest significance confirmed our experimental approach. The other bias, for sure is the limited number of differential proteins in the specific regulations we focus on, that hampers annotations in a general way.

So, we decided to focus on our initial working hypothesis, i.e. to identify alterations in the adipocyte “communication” with regard to specific physiological states. Adipose tissue controls systemic energy storage and needs to expand in regard to metabolic needs. In healthy conditions this can be due to hyperplasia, but in metabolically affected adipose tissue as in obesity or diabetes, increased *ad libitum* storage of fatty acids occurs, even in non-adipose tissues. Increased lipid load in these cells favors accumulation of fatty acids (FA)-derived metabolites such as fatty acyl-CoA or DAG which initiated cellular processes *via* PKC signaling (19). As chronic process the cells get insulin resistance with dysfunctional mitochondria resulting in the development of obesity and diabetes. With regard to adipocyte function, the combination of both should alter the DAG patterns in adipocytes, like observed in other insulin-sensitive tissues as liver, skeletal muscle or even pancreas (9, 20-22).

Adipose tissue DAGs were determined by mass spectrometry (Figure 4). In contrary to the obese obob, there was an increase in total DAG content in obese/diabetic dbdb mice compared to their backgrounds. Nevertheless, the comparison of the distinct DAGs revealed that in both obese models the DAG species with the fatty acid C18:1 were equally regulated (C18:0\_18:1; C18:1\_18:1). DAG species with saturated

fatty acid C16:0 and C18:0 were only changed in dbdb (C16:0\_C18:0; C16:0\_C18:1, C18:0\_C20:4), whereas the DAG species with unsaturated fatty acid C16:1 were only changed in obob (C16:1\_C16:1).

According to our hypothesis, intensities of a vast amount of adipose secreted proteins correlated to the total adipose derived DAGs (n=152; 23 SP(+), 53 SP(-), 76 NP). Of these 105 proteins (20 SP(+), 36 SP(-), 49 NP) also showed differential abundance in either comparison of mouse phenotypes. In addition, specific DAG species correlate to adipocyte-secreted proteins (Figure 5, *Supplement table 4*). Here, all secreted correlated proteins can be assigned to metabolic active proteins with the highest prevalence. Of note, DAG species specific for obob shows poly(A) RNA binding proteins as highest annotation (poly(A)RNA binding, n=30, FDR= 6.71e-09, RNA binding, n=31, FDR= 4.1e-07). This is also observed, if not in highest position with DAG species specific for dbdb (n=20, FDR= 5.96e-4) (Figure 5). This is of interest as it focused the differences in obesity and obesity/diabetes to the concept of moonlighting enzymes in metabolic control. Moonlighting proteins or gene sharing defines various functions of a certain gene and are independent to alternative splicing, posttranslational modification or multifunctionality. Especially ancestral and conserved proteins in central metabolic processes show moonlighting functions, e.g. glycolysis or tricarboxylic acid cycle enzymes (23). This process of metabolic regulation can account for expression levels, differential localization, protein interactions and is mediated by binding of RNA species to a distinct, but not necessary active domain of an enzyme. Best known examples of metabolic enzymes regulated by binding of RNA species are GOT2, FASN, or GAPDH (24). We identified Adk, Alfh6A1, Aldoa, Eno, Lta4h and Hsd17B10 to be secreted from adipocytes and to correlate to DAG species C16:1\_C16:1 or DAG species C18:1\_C20:4. All of these proteins were previously identified in RNA interaction

studies and implicated to have moonlighting functions (24). For example, the metabolic enzyme fructose-1,6-bisphosphate aldolase (Aldoa) which catalyzes the reversible cleavage of fructose-1,6-bisphosphate to glyceraldehyde 3-phosphate and dihydroxyacetone phosphate in glycolysis and gluconeogenesis pathways, has been shown to regulate insulin-dependent glucose transporter GLUT4 in mouse adipocyte cell lines 3T3-L1 (25). Furthermore, enolase (Eno) catalyzes the dehydrolyzation of 2-phospho-D-glycerate to phosphoenolpyruvate in glycolysis, but has also been shown to bind plasminogen and to mediate its cell surface peptidase activity (26, 27). So, one could speculate that alterations in such regulatory processes might interfere with the subcellular localization and trafficking of proteins, depending on which functions is favored, and are also an essential target in the overall picture of metabolic regulation.

## Conclusion

We showed that genetic mouse models, which are susceptible to obesity or obesity/diabetes according to their genetic background genotype show phenotype-specific differences in primary adipocyte adipokinome in quantitative proteome analyses. Knowledge based annotation of identified differentially regulated adipokinome did not add much further information. According to the predictive value of DAG-species for lipid metabolism and insulin resistance in liver and skeletal muscle (9), we determined DAG levels also as classifying parameter for lipid metabolism and insulin resistance in adipose tissue. Adipose tissue DAG patterns differ in obesity and obesity/diabetes especially of DAG species with saturated fatty acid C16:0 and C18:0 in diabetes and unsaturated fatty acid C16:1 in obesity or unsaturated fatty acid C20:4 in obesity/diabetes. Our study provides evidence that the analyses of one “Omics”-like secretome might not be sufficient to get insight in a complex phenotypical problem.

Here, the combination of specific DAG species and the holistic pattern of primary adipocyte-secreted proteins helped to get hints to an interacting mechanism and to unravel RNA-binding proteins involved in metabolic control differing in obesity and obesity/diabetes.

## Materials and Methods

### Mouse models

C57BL/6 (C57), C57BL/KS (BKS), C57BL/KS.Cg<sup>-Lep<sup>rd</sup>b</sup> (dbdb) and C57BL/KS.Cg<sup>-Lep<sup>ob</sup></sup> (obob) mice were bred and maintained in a regular 12 h light/dark cycle under constant temperature, humidity ( $22 \pm 1$  °C,  $50 \pm 5\%$  humidity) with free access to water and standard laboratory food (Ssniff, Soest, Germany). Mice were sacrificed by CO<sub>2</sub> asphyxiation at 17 weeks of age. Mice (n=5 each genotype) were sacrificed after 6h food restriction and visceral adipose tissue was removed (5, 28). Serum was collected by left ventricular punctation. The Animal Care Committee of the University Duesseldorf approved all animal care and procedures (Approval#50.05-240-35/06).

### Metabolic characterization of the mouse models

Blood parameters were measured at 17 weeks of age (n=8). Blood glucose was measured with Freestyle™ and leptin, insulin as well as glucagon levels were determined using quantitative Bio-Plex Pro Mouse Diabetes 8-Plex Assay (Bio-Rad) according to the manufacturer's instructions. Data were collected and analyzed using a BioPlex 200 instrument equipped with BioManager analysis software (Bio-Rad). To determine insulin resistance and pancreatic beta cell function the surrogate parameters HOMA-IR (homeostatic model assessment of insulin resistance) and HOMA-β (homeostatic model assessment of beta cell function) were used. Body composition was measured using nuclear magnetic resonance (n=9-23/per genotype, Whole Body Composition Analyzer; Echo MRI, Texas, USA)

### **Secretome profiling by liquid chromatography (LC)-electrospray ionization (ESI)-MS/MS and data analyses**

Murine mature adipocytes from visceral fat isolated by collagenase digestion were cultured for 24 h and secretomes were harvested as described (29). Data of all mouse models were acquired in parallel as described in detail (5). In brief, secretome samples were tryptically digested and analyzed using LC-ESI mass spectrometry using an Ultimate 3000 Rapid Separation liquid chromatography system (Dionex/Thermo Scientific, Idstein, Germany). Afterwards, mass spectrometry was carried out (Orbitrap Elite high resolution instrument, Thermo Scientific, Bremen, Germany). For the comparison of mouse strains, log<sub>2</sub> PSM values were used. MaxQuant (version 1.4.1.2, Max Planck Institute for Biochemistry, Munich, Germany) was used for protein and peptide identification and quantification with default parameters if not otherwise stated. Searches were carried out using 16,671 mouse sequences from the Swiss-Prot part of UniProtKB (release 9.7.2014) applying the following parameters: mass tolerance precursor (Orbitrap): mass tolerance precursor: 20 ppm first search and 4.5 ppm after recalibration (Orbitrap), mass tolerance fragment spectra: 0.4 Da (linear ion trap), trypsin specific cleavage (maximum of one missed cleavage site), fixed modification: carbamidomethyl, variable modifications: methionine oxidation and N-terminal acetylation. For peptide and protein acceptance, the false discovery rate (FDR) was set to 1%, only proteins with at least two identified peptides were used for protein assembly. Quantification was carried out using the label-free quantification algorithm implemented in MaxQuant using a minimal ratio count of 2 and the “match between runs” option enabled.

### **Lipid analysis of adipose tissue**

Extraction, purification and analysis of DAGs from frozen adipose tissue samples was conducted using an LC-MS/MS approach (21). In brief, 20 mg of adipose tissue was homogenized in 20 mM Tris/HCL, 1 mM EDTA 0.25 mM EGTA, pH 7.4, using a tight-fitting glass douncer (Wheaton, UK). Internal standard (d517:0-DAG; Avanti Polar Lipids, Ala, USA) was added and lipids were extracted according to Folch *et al.*, (30). Diacylglycerols were separated from triglycerides using solid phase extraction (Sep Pak Diol Cartridges; Waters, MA, USA). The resulting lipid phase was dried under a gentle flow of nitrogen and re-suspended in methanol. Diacylglycerols were separated using a Phenomenex Luna Omega column (1,6 µm 100 Å; Phenomenex, CA, USA) on an Infinity 1290 HPLC system (Agilent Technologies, CA, USA) and analyzed by multiple reaction monitoring on a triple quadrupole mass spectrometer (Agilent 6495; Agilent Technologies, CA, USA), operated in positive ion mode.

### **Prediction and annotation of secretory proteins**

Secretory protein prediction and functional annotation was done using different independent methods. First, protein information of all identified proteins was extracted from the Swiss-Prot database (<http://www.uniprot.org/>). To assess secretory properties, protein sequences were analysed by SignalP 4.1 (17); <http://www.cbs.dtu.dk/services/SignalP/>) and SecretomeP 2.0. (31); <http://www.cbs.dtu.dk/services/SecretomeP/>). Literature screening was performed with NCBI/Pubmed (<http://www.ncbi.nlm.nih.gov/pubmed>).

### **Web-Based Functional Annotation**

The identification types were uniprot\_swissprot\_accession or gene\_ID, respectively. Information driven analyses including functional annotation was performed with String v10.5 (<https://string->

db.org/) (32), David Bioinformatics Resources 6.8 (<https://david.ncifcrf.gov/>) [33, 34], and IPA (Ingenuity™, Qiagen). For differential protein sets expression analyses, expression fold change (1.5x) and expression differences (p-value < 0.05) were analyzed following the core analyses modules. Differential abundant proteins (1.5x fold difference, p-value < 0.05 (one-way ANOVA, posthoc) were analyzed separately for C57 vs BKS, C57 vs obob, BKS vs dbdb and dbdb vs obob.

### **Statistical Methods**

Statistical analyses were performed in GraphPad Prism 5.0 and SPSS 22 (IBM). Data are given as mean ± standard deviation [102] and data were directly compared with an unpaired Student's t test. Figure legends indicate the statistical tests applied for each experiment in detail.

### **Author Contributions**

S.G., G.P., D.F.M., C.P. W.P., U.N., S.J., S.H., researched the data. B.K., and J.K. designed experiments, analyzed data and wrote the manuscript. H.-D.D. curates the database (<http://www.diabetesprot.org>). K.S. and S.L., contributed to design of the secretome analyses and supervised the adipokine identification. All authors have confirmed the final version of the manuscript. J.K. is the guarantor of the work.

### **Conflict of Interest**

The authors state no conflict of interests.

### **Acknowledgement**

The work was supported by the German Diabetes Center (DDZ), which is funded by the German Federal Ministry of Health and the Ministry of Innovation, Science, Research and Technology of the state North Rhine-Westphalia. This study was supported in part by a grant from the German Federal Ministry of Education and Research (BMBF) to the German Center for Diabetes Research (DZD e. V.).

## Figure Legends

### Figure 1. Metabolic characterization of C57, BKS, obob and dbdb mice used in the study

Data are expressed as mean  $\pm$  SD (n = 8 of each phenotype). \* p<0.05, \*\* p<0.01 \*\*\* p<0.001 by Student's t test.

### Figure 2. Heatmap of all identified adipokines

### Figure 3. Venn analyses of differential abundant proteins.

Proteins with differential abundance in the comparisons C57 vs BKS, C57 vs obob, BKS vs dbdb and dbdb vs obob (>1.5 fold, one-way ANOVA posthoc p-value < 0.05) were analyzed for overlap to determine genotype specific and genotype independent alterations. Genotype independent differential abundant proteins for "obesity" (n=106, turquoise), diabetes (n=36, red) and diabetes despite obesity (n=19, yellow) are highlighted. Further information of proteins of all groups are detailed in Supplement Table 3.

### Figure 4 Diacylglycerol pattern in adipose tissue of C57, BKS, obob and dbdb mice

Data are given in ( $\mu$ mol or nmol/g tissue) and expressed as mean  $\pm$  SD (n = 5 of each phenotype). \* p <0.05, \*\*p <0.01, \*\*\*p <0.001 by Student's t test.

### Figure 5. Functional network of adipokines correlated to DAG species.

Adipokines with significant correlation to total DAG content or indicated DAG species were used for over representation analyses. **A.** Adipokines correlated to total DAGs, DAG C16:0\_C18:0 DAG C16:0\_C18:1 species are enriched in metabolic pathways (highlighted in red).

**B.** Adipokines correlating to DAG C16:1\_C16:1 and DAG C18:0\_C20:4 are enriched in metabolic pathways or poly(A)

RNA binding (highlighted in red). Enrichment FDR is given.

### Online Supplement Data

Supplemental Table 1 Raw Data sheet of identified adipokines

Supplemental Table 2 Determination of differential abundant adipokines

Supplemental Table 3 Accompanying data to Figure 3: Enrichment analyses of phenotype predictive differential abundant adipokines

Supplemental Table 4 Overall correlation of DAG to the adipokinome

Supplemental Table 5 Accompanying data to Figure 5, Strings Enrichment analyses of phenotype predictive DAG-correlated adipokines.

## References

1. Meldrum, D.R.; Morris, M.A.; Gambone, J.C. Obesity pandemic: causes, consequences, and solutions-but do we have the will? *Fertil Steril.* **2017**, *107*, 833-839, doi:10.1016/j.fertnstert.2017.02.104.
2. Hall, J.E.; do Carmo, J.M.; da Silva, A.A.; Wang, Z.; Hall, M.E. Obesity-induced hypertension: interaction of neurohumoral and renal mechanisms *Circ Res*, **116**, **2015**, 991-1006, doi: 10.1161/CIRCRESAHA.116.305697
3. Lohmann, A.E.; Goodwin, P.J.; Chlebowski, R.T.; Pan, K.; Stambolic, V.; Dowling, R.J. Association of obesity-related metabolic disruptions with cancer risk and Outcome. *J Clin Oncol.* **2016**, *34*, 4249-4255. doi:10.1200/JCO.2016.69.6187
4. Ouchi, N.; Parker, J.L.; Lugus, J.J.; Walsh, K. Adipokines in inflammation and metabolic disease *Nat. Rev. Immunol.*, *11*, **2011**, 85–97, doi: 10.1038/nri2921.
5. Hartwig, S.; Goeddeke, S.; Poschmann, G.; Dicken, H.D.; Jacob, S.; Nitzgen, U.; Passlack, W.; Stühler, K.; Ouwens, D.M.; Al-Hasani, H.; Knebel, B.; Kotzka, J.; Lehr, S. Identification of novel adipokines differentially regulated in C57BL/Ks and C57BL/6. *Arch Physiol Biochem.* **2014**, *120*, 208-215. doi:10.3109/13813455.2014.970197.
6. Coleman, D.L.; Hummel, K.P. Symposium IV: Diabetic syndrome in animals. Influence of genetic background on the expression of mutations at the diabetes locus in the mouse. II. Studies on background modifiers. *Isr J Med Sci.* **1975**, *11*, 708-713,
7. Hummel, K.P.; Coleman, D.L.; Lane, P.W. The influence of genetic background on expression of mutations at the diabetes locus in the mouse. I. C57BL-KsJ and C57BL-6J strains. *Biochem Genet.* **1972**, *7*, 1-13.
8. Unger, R.H.; Clark, G.O.; Scherer, P.E.; Orci, L. Lipid homeostasis, lipotoxicity and the metabolic syndrome. *Biochim Biophys Acta.* **2010**, *1801*, 209-214. doi:10.1016/j.bbaliip.2009.10.006.
9. Petersen, M.C.; Shulmann G.I. Roles of Diacylglycerols and Ceramides in Hepatic Insulin Resistance. *Trends Pharmacol Sci.* **2017**, *38*, 649-665, doi:10.1016/j.tips.2017.04.004.
10. Sampson, S.R., Cooper, D.R. Specific protein kinase C isoforms as transducers and modulators of insulin signaling. *Molecular Genetics and Metabolism* **2006**, *89*, 32-47, doi\_10.1016/j.ymgme.2006.04.017
11. Leiter, E.H.; Chapman, H.D.; Coleman, D.L. The influence of genetic background on the expression of mutations at the diabetes locus in the mouse. V. Interaction between the db gene and hepatic sex steroid sulfotransferases correlates with gender-dependent susceptibility to hyperglycemia. *Endocrinology* **1989**, *124*: 912–922, doi:10.1210/endo-124-2-912
12. Leiter, E.H.; Reifsnnyder, P.C.; Flurkey, K.; Partke, H.-J.; Junger, E.; Herberg, L. NIDDM genes in mice. Deleterious synergism by both parental genomes contributes to diabetic thresholds. *Diabetes.* **1998**, *47*, 1287–1295, doi:10.2337/diab.47.8.1287
13. Schattenberg, P.; Gallem, R. Steatohepatitis: Of Mice and Man Animal Models of Non-Alcoholic Liver and Metabolic Syndrome. *Dig Dis* **2010**, *28*, 247–254, doi:10.1159/000282097
14. Friedman, J.M.; Leibel, R.L.; Siegel, D.S.; Walsh, J.; Bahary, N.

- Molecular mapping of the mouse obesity mutation. *Genomics*. **1991**, 11, 1054-1062.
15. Wang, B.; Chandrasekera, P.C.; Pippin, J.J. Leptin- and leptin receptor-deficient rodent models: relevance for human type 2 diabetes. *Curr Diabetes Rev*. **2014**, 10, 131-145, doi:10.2174/1573399810666140508121012.
  16. Rabouille, C. Pathways of Unconventional Protein Secretion. *Trends Cell Biol*. **2017**, 27, 230-240, doi:10.1016/j.tcb.2016.11.007.
  17. Petersen, T.N.; Brunak, S.; von Heijne, G.; Nielsen, H. SignalP 4.0: discriminating signal peptides from transmembrane regions. *Nat Methods*. **2011**, 8, 785-786, doi:10.1038/nmeth.1701.
  18. Sung, J.; Wang, Y.; Chandrasekaran, S.; Witten, D.M.; Price, N.D. Molecular signatures from omics data: from chaos to consensus. *Biotechnol J*. **2012**, 8, 946-957, doi:10.1002/biot.201100305.
  19. Jornayvaz, F.R.; Shulman G.I. Diacylglycerol activation of protein kinase C $\epsilon$  and hepatic insulin resistance *Cell Metab.*, **2012**, 15, 574-584 doi:10.1016/j.cmet.2012.03.005.
  20. Itani, S.I.; Ruderman, N.B.; Schmieder, F.; Boden, G. Lipid-induced insulin resistance in human muscle is associated with changes in diacylglycerol, protein kinase C, and I $\kappa$ B- $\alpha$ . *Diabetes*. **2002**, 51, 2005-2011, doi.org/10.2337/diabetes.51.7.2005
  21. Kumashiro, N.; Erion, D.M.; Zhang, D.; Kahn, M.; Beddow, S.A.; Chu, X.; Still, C.D.; Gerhard, G.S.; Han, X.; Dziura, J.; Petersen, K.F.; Samuel, V.T.; Shulman, G.I. Cellular mechanism of insulin resistance in nonalcoholic fatty liver disease. *Proc Natl Acad Sci U S A*. **2011**, 108, 16381-16385, doi:10.1073/pnas.1113359108.
  22. Magkos, F.; Su, X.; Bradley, D.; Fabbrini, E.; Conte, C.; Eagon, J.C.; Varela, J.E.; Brunt, E.M.; Patterson, B.W.; Klein, S. Intrahepatic diacylglycerol content is associated with hepatic insulin resistance in obese subjects. *Gastroenterology*. **2012**, 142, 1444-1446, doi:10.1053/j.gastro.2012.03.003.
  23. Sriram G., Martinez J.A., McCabe E.R., Liao J.C., Dipple K.M. Single-gene disorders: what role could moonlighting enzymes play? *American Journal of Human Genetics* **2005** 76, 911-924. doi:10.1086/430799
  24. Castello, A.; Hentze, M.W.; Preiss, T. Metabolic Enzymes Enjoying New Partnerships as RNA-Binding Proteins. *Trends Endocrinol Metab*. **2015**, 12, 746-757, doi:10.1016/j.tem.2015.09.012.
  25. Kao A.W.; Noda Y.; Johnson J.H.; Pessin J.E.; Saltiel A.R. Aldolase mediates the association of F-actin with the insulin-responsive glucose transporter GLUT4. *J Biol Chem* **1999** 274, 17742-17747, doi:10.1074/jbc.274.25.17742
  26. Miles, L.A.; Dahlberg, C.M.; Plescia, J.; Felez, J.; Kato, K.; Plow, E.F. Role of cell-surface lysines in plasmin(ogen)-binding to cells: identification of alpha-enolase as a candidate plasminogen receptor. *Biochemistry* **1991** 30, 1682-16891.
  27. Redlitz A.; Fowler B.J.; Plow E.F.; Miles L.A. The role of an enolase-related molecule in plasminogen binding to cells. *Eur J Biochem*. **1995**, 227, 407-415. doi:10.1111/j.1432-1033.1995.tb20403.x
  28. Knebel, B.; Hartwig, S.; Haas, J.; Lehr, S.; Goeddeke, S.; Susanto, F.; Bohne, L.; Jacob, S.; Koellmer, C.; Nitzgen, U.; Müller-Wieland, D.; Kotzka, J. Peroxisomes compensate hepatic lipid overflow in mice with fatty liver. *Biochim Biophys Acta*.

- 2015**, 1851, 965-976, doi:10.1016/j.bbaliip.2015.03.003.
29. Göddeke, S.; Kotzka, J.; Lehr, S. Investigating the adipose tissue secretome: a protocol to generate high-quality samples appropriate for comprehensive proteomic profiling. *Methods Mol Biol.* **2015**, 1295, 43-53. doi:10.1007/978-1-4939-2550-6\_4.
30. Folch, J.; Lees, M.; Sloane Stanley, G.H. A simple method for the isolation and purification of total lipids from animal tissues. *J Biol Chem* **1957** 226, 497-509.
31. Bendtsen, J.D.; Jensen, L.J.; Blom, N.; von Heijne, G.; Brunak, S. Feature-based prediction of non-classical and leaderless protein secretion. *Protein Eng Des Sel.* **2004** 17: 349-356, doi:10.1093/protein/gzh037.
32. Szklarczyk, D.; Morris, J.H.; Cook, H.; Kuhn, M.; Wyder, S.; Simonovic, M.; Santos, A.; Doncheva, N.T.; Roth, A.; Bork, P.; Jensen, L.J.; von Mering, C. The STRING database in 2017: quality-controlled protein-protein association networks, made broadly accessible *Nucleic Acids Res.* **2017**, D362–D368, doi:10.1093/nar/gkw937.
33. Huang, D.W.; Sherman, B.T.; Lempicki, R.A. Systematic and integrative analysis of large gene lists using DAVID Bioinformatics Resources. *Nature Protoc.* **2009**; 4, 44-57, doi:10.1038/nprot.2008.211.
34. Huang, D.W.; Sherman, B.T.; Lempicki, R.A. Bioinformatics enrichment tools: paths toward the comprehensive functional analysis of large gene lists. *Nucleic Acids Res.* **2009**, 37, 1-13, doi:10.1093/nar/gkn923.

## Figures

Figure 1

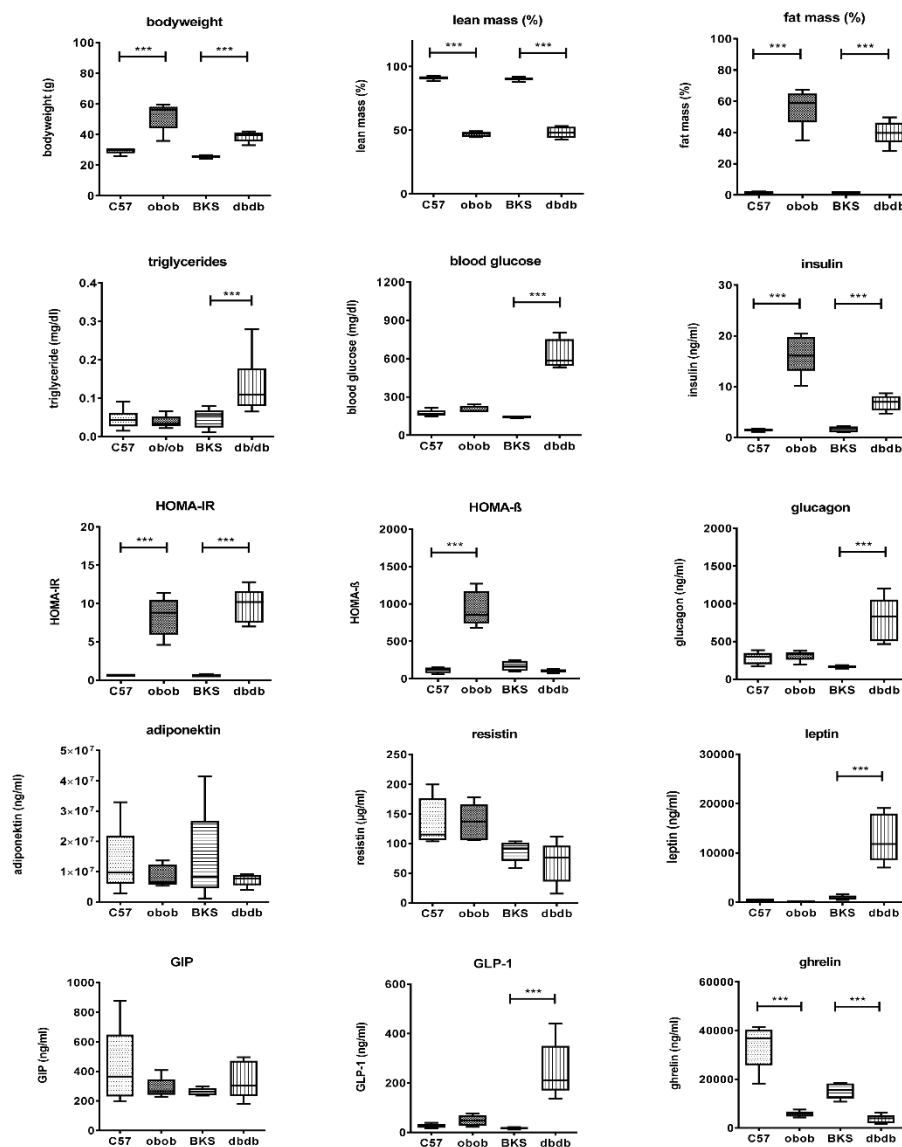


Figure 1. Metabolic characterization of C57, BKS, obob and dbdb mice used in the study

Data are expressed as mean  $\pm$  SD (n=8 of each phenotype). \*  $p < 0.05$ , \*\*  $p < 0.01$  \*\*\*  $p < 0.001$  by Student's t test.

Figure 2

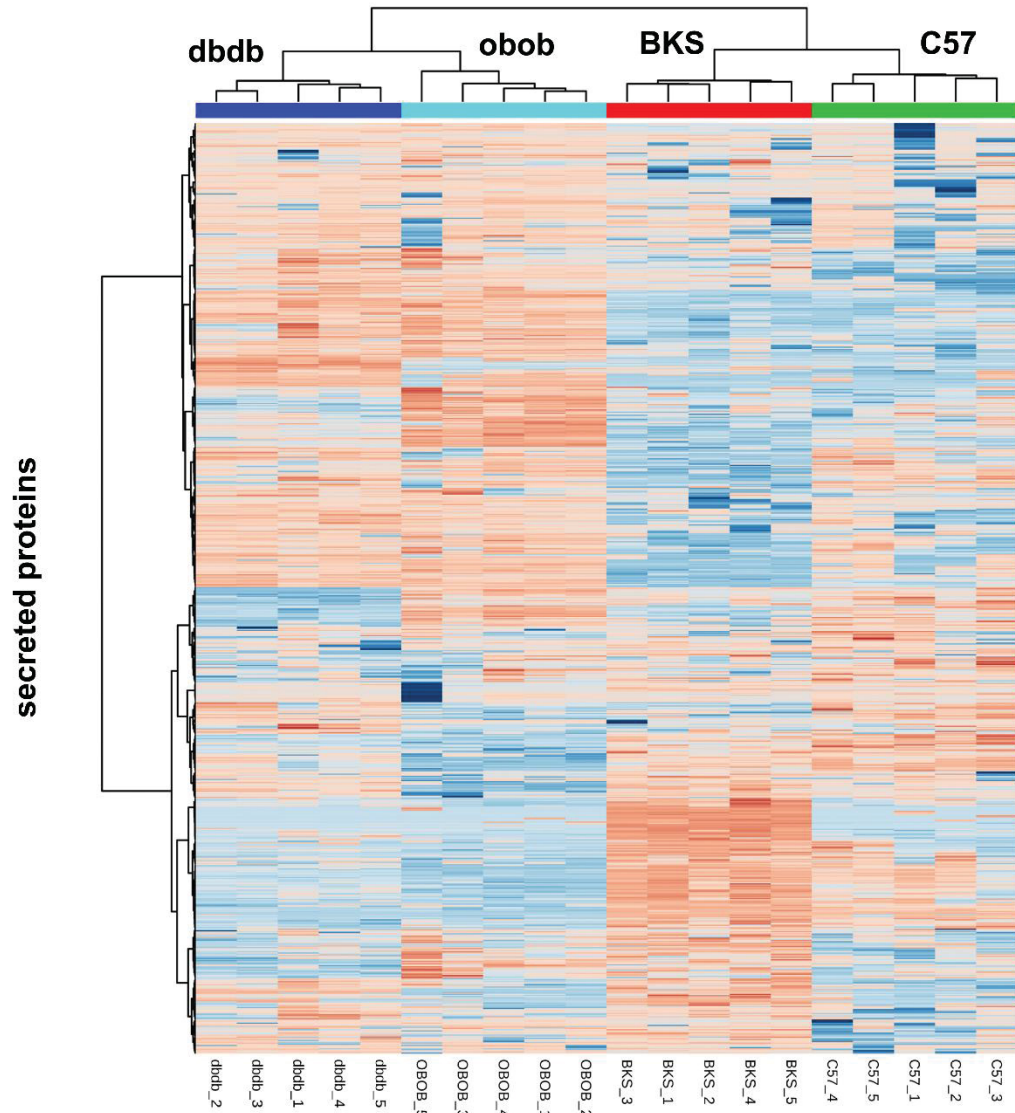
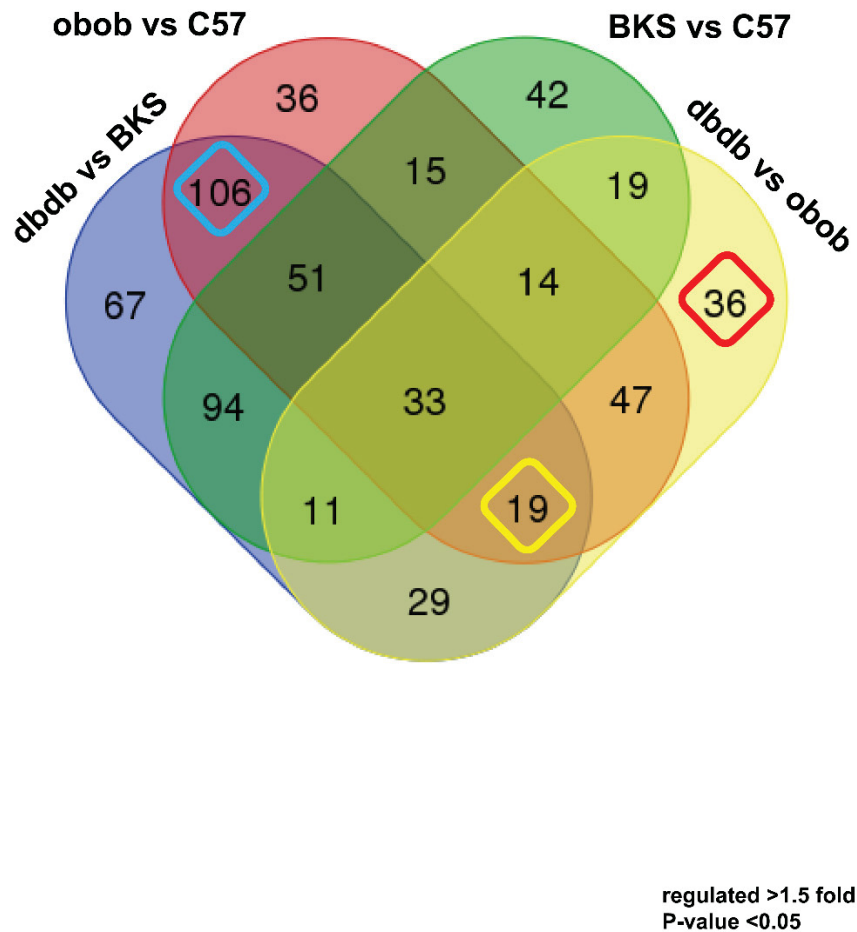


Figure 2. Heatmap of all identified adipokines

Figure 3



**Figure 3. Venn analyses of differential abundant proteins.**

Proteins with differential abundance in the comparisons C57 vs BKS, C57 vs obob, BKS vs dbdb and dbdb vs obob (>1.5 fold, one-way ANOVA posthoc p-value < 0.05) were analyzed for overlap to determine genotype specific and genotype independent alterations. Genotype independent differential abundant proteins for “obesity” (n=106, turquoise), diabetes (n=36, red) and diabetes despite obesity (n=19, yellow) are highlighted. Further information of proteins of all groups are detailed in Supplement Table 3.

Figure 4

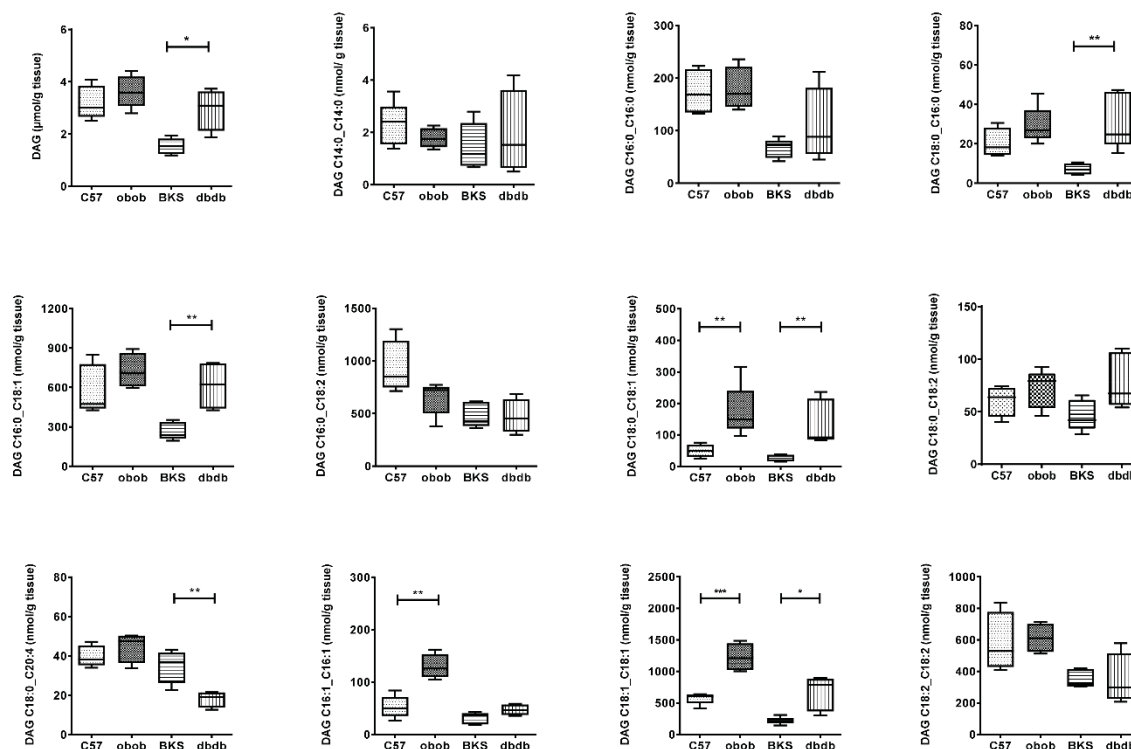
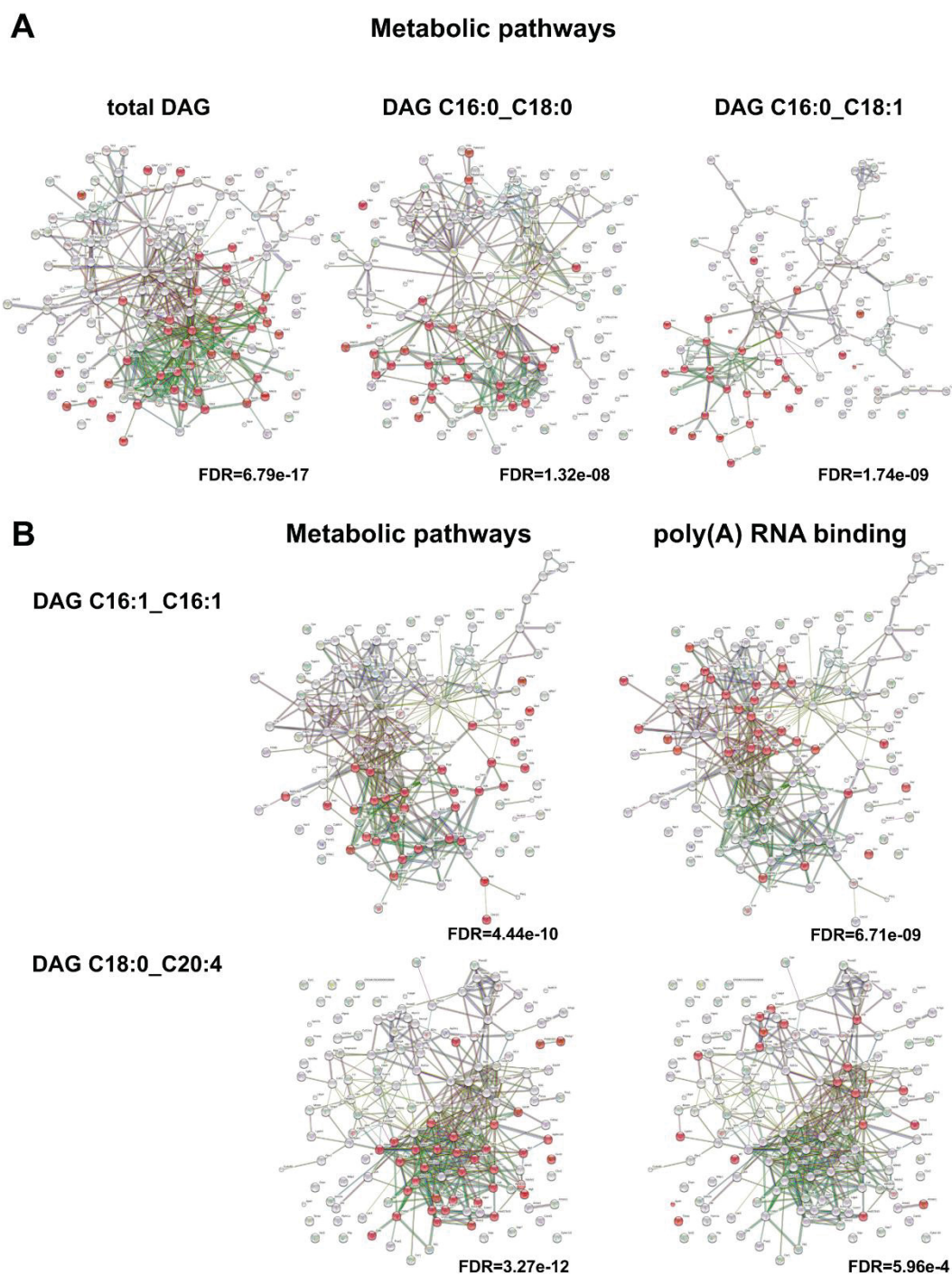


Figure 4 Diacylglycerol pattern in adipose tissue of C57, BKS, obob and dbdb mice

Data are given in (μmol or nmol/g tissue) and expressed as mean ± SD (n = 5 of each phenotype).  
 \* p < 0.05, \*\* p < 0.01, \*\*\* p < 0.001 by Student's t test.

Figure 5



**Figure 5. Functional network of adipokines correlated to DAG species.**

Adipokines with significant correlation to total DAG content or indicated DAG species were used for over representation analyses.

**A.** Adipokines correlated to total DAGs, DAG C16:0\_C18:0 DAG C16:0\_C18:1 species are enriched in metabolic pathways (highlighted in red).

**B.** Adipokines correlating to DAG C16:1\_C16:1 and DAG C18:0\_C20:4 are enriched in metabolic pathways or poly(A) RNA binding (highlighted in red). Enrichment FDR is given.

## Tables

**Table 1 Top putatively regulated proteins (SP(+), SP(-)) in the comparisons**

Protein names	Protein ID	Gene names	log2 fold change	p-value
			BKS C57	BKS C57
Complement factor D	P03953	Cfd	-5.42	1.49E-06
cAMP-dependent protein kinase type II-beta	P31324	Prkar2b	-2.47	2.73E-06
Apolipoprotein E	P08226	ApoE	-2.17	7.51E-04
Receptor expression-enhancing protein 6	Q9JM62	Reep6	-2.14	9.00E-04
Lipoprotein lipase	P11152	Lpl	-2.03	8.64E-03
Prolargin	Q9JK53	Prelp	-1.90	8.59E-04
26S protease regulatory subunit 10B	P62334	Psmc6	-1.89	6.65E-05
Coiled-coil domain-containing protein 80	Q8R2G6	Ccdc80	-1.89	2.33E-04
Pentraxin-related protein PTX3	P48759	Ptx3	-1.87	3.35E-02
Tenascin	Q80YX1	Tnc	-1.86	6.09E-05
Inositol polyphosphate 1-phosphatase	P49442	Inpp1	1.52	1.24E-05
Carbonic anhydrase 2	P00920	Ca2	1.57	1.29E-04
Dolichyl-diphosphooligosaccharide-protein glycosyltransferase 48 kDa subunit	O54734	Ddost	1.71	9.47E-05
Dolichyl-diphosphooligosaccharide-protein glycosyltransferase subunit 2	Q9DBG6	Rpn2	1.72	4.48E-04
Nodal modulator 1	Q6GQT9	Nomo1	1.78	1.74E-05
60S ribosomal protein L12	P35979	Rpl12	1.86	9.57E-05
Ketohexokinase	P97328	Khk	1.94	9.40E-05
Carbonyl reductase 3	Q8K354	Cbr3	1.98	1.06E-04
Carbonic anhydrase 1	P13634	Ca1	2.38	3.45E-07
Glutathione S-transferase theta-2	Q61133	Gstt2	3.25	4.80E-09
Protein names	Protein IDs	Gene names	obob_C57	obob_C57
Complement factor D	P03953	Cfd	-9.46	5.52E-10
Collagen alpha-1(XII) chain	Q60847	Col12a1	-6.39	1.12E-09
Collagen alpha-5(VI) chain	A6H584	Col6a5	-6.20	1.22E-09
Angiotensinogen	P11859	Agt	-4.43	2.77E-07
Fructose-1,6-bisphosphatase 1	Q9QXD6	Fbp1	-3.94	1.45E-07
Carboxypeptidase Q	Q9WVJ3	Cpq	-3.64	1.15E-06
Alpha-amylase 1	P00687	Amy1	-3.64	1.84E-05
Coiled-coil domain-containing protein 80	Q8R2G6	Ccdc80	-3.47	2.67E-07
Tissue alpha-L-fucosidase	Q99LJ1	Fuca1	-3.28	9.84E-07
Ganglioside GM2 activator	Q60648	Gm2a	-3.26	2.29E-06
Actin-related protein 2/3 complex subunit 3	Q9JM76	Arpc3	1.94	4.89E-05
NADH-cytochrome b5 reductase 3	Q9DCN2	Cyb5r3	2.07	5.69E-05
Epoxide hydrolase 1	Q9D379	Ephx1	2.12	3.21E-08
Acyl-CoA dehydrogenase 9, mitochondrial	Q8JZN5	Acad9	2.18	5.98E-08
Serum deprivation-response protein	Q63918	Sdpr	2.22	2.03E-06
Serpin H1	P19324	Serpinh1	2.25	3.14E-05
Galectin-3	P16110	Lgals3	2.25	6.50E-07
GTP:AMP phosphotransferase AK3, mitochondrial	Q9WTP7	Ak3	2.28	2.06E-07
Apolipoprotein A-IV	P06728	Apoa4	2.42	6.29E-07
Interleukin-6	P08505	Il6	3.19	6.96E-07
Protein names	Protein IDs	Gene names	dbdb_BKS	dbdb_BKS
Collagen alpha-5(VI) chain	A6H584	Col6a5	-7.87	3.53E-11
Fructose-1,6-bisphosphatase 1	Q9QXD6	Fbp1	-4.10	1.64E-07
Tissue alpha-L-fucosidase	Q99LJ1	Fuca1	-3.92	4.32E-08
Carboxypeptidase Q	Q9WVJ3	Cpq	-3.34	1.63E-06
Complement factor D	P03953	Cfd	-3.33	2.71E-04

Ganglioside GM2 activator	Q60648	Gm2a	-3.28	1.18E-06
Carboxylesterase 1D	Q8VCT4	Ces1d	-2.97	1.49E-11
Dolichyl-diphosphooligosaccharide-protein glycosyltransferase subunit 2	Q9DBG6	Rpn2	-2.87	2.22E-04
Fructose-1,6-bisphosphatase isozyme 2	P70695	Fbp2	-2.80	5.61E-05
Angiotensinogen	P11859	Agt	-2.44	2.67E-04
Phospholipid transfer protein	P55065	Pltp	2.77	1.62E-02
Serum deprivation-response protein	Q63918	Sdpr	2.86	5.17E-07
Polymerase I and transcript release factor	O54724	Ptrf	2.93	1.87E-08
Platelet-activating factor acetylhydrolase	Q60963	Pla2g7	2.97	4.03E-03
Vimentin	P20152	Vim	3.12	8.70E-11
C-C motif chemokine 2	P10148	Ccl2	3.37	1.23E-02
Prolargin	Q9JK53	Prelp	3.39	1.65E-06
cAMP-dependent protein kinase type II-beta	P31324	Prkar2b	3.70	4.52E-09
Growth-regulated alpha protein	P12850	Cxcl1	4.36	1.13E-06
Interleukin-6	P08505	Il6	5.35	2.09E-10

Protein names	Protein IDs	Gene names	dbdb_obob	dbdb_obob
Transthyretin	P07309	Ttr	-3.06	9.14E-08
ATP-citrate synthase	Q91V92	Acly	-2.98	4.13E-11
Sarcosine dehydrogenase, mitochondrial	Q99LB7	Sardh	-2.34	3.51E-06
GTP:AMP phosphotransferase AK3, mitochondrial	Q9WTP7	Ak3	-2.15	1.91E-07
Serpin H1	P19324	Serpinh1	-2.01	2.23E-04
Acyl-CoA dehydrogenase 9, mitochondrial	Q8JZN5	Acad9	-1.99	2.95E-07
Vitamin D-binding protein	P21614	Gc	-1.90	9.29E-07
3-hydroxyisobutyrate dehydrogenase, mitochondrial	Q99L13	Hibadh	-1.86	3.24E-04
Pyruvate dehydrogenase E1 mitochondrial	P35486	Pdha1	-1.81	1.05E-03
Citrate synthase, mitochondrial	Q9CZU6	Cs	-1.70	1.07E-05
Calmodulin	P62204	Calm1	1.51	3.03E-05
Laminin subunit beta-2	Q61292	Lamb2	1.55	7.46E-07
C-X-C motif chemokine 5;GCP-2(1-78);GCP-2(9-78)	P50228	Cxcl5	1.77	4.79E-04
Prolargin	Q9JK53	Prelp	1.82	3.83E-03
Pentraxin-related protein PTX3	P48759	Ptx3	1.84	9.82E-03
Desmin	P31001	Des	2.09	5.46E-07
Lactotransferrin	P08071	Ltf	2.15	9.64E-04
Collagen alpha-1(XII) chain	Q60847	Col12a1	4.45	1.31E-07

p-value: post hoc test (ANOVA)

**Table 2 Proteins detected in only one genotype in comparisons**

Protein names	Protein ID	Gene names	SP(+)	SP(-)	NP
<b>BKS_C57</b>					
Tyrosine-protein phosphatase non-receptor type 6	P29351	Ptpn6			+
NADPH--cytochrome P450 reductase	P37040	Por		+	
Vacuolar protein sorting-associated protein 13C	Q8BX70	Vps13c			+
Annexin A11	P97384	Anxa11		+	
Epidermal growth factor receptor substrate 15	P42567	Eps15			+
Adenosine deaminase	P03958	Ada			+
Pyruvate dehydrogenase E1 subunit alpha, mitochondrial	P35486	Pdha1		+	
Carnitine O-acetyltransferase	P47934	Crat		+	
Histidine triad nucleotide-binding protein 1	P70349	Hint1		+	
Heat shock protein 75 kDa, mitochondrial	Q9CQN1	Trap1		+	
COP9 signalosome complex subunit 8	Q8VVBV7	Cops8			+
Endothelial cell-selective adhesion molecule	Q925F2	Esam	+		

Carbonic anhydrase 4	Q64444	Ca4	+	
Arsenite methyltransferase	Q91WU5	As3mt		+
Deoxyguanosine kinase, mitochondrial	Q9QX60	Dguok		+
H-2 class I histocompatibility antigen, D-B alpha chain	P01899	H2-D1	+	
Phosphoserine phosphatase	Q99LS3	Psph		+
Mannosyl-oligosaccharide 1,2-alpha-mannosidase IA	P45700	Man1a1		+
Band 4.1-like protein 2	O70318	Epb4112		+
Glucosamine-6-phosphate isomerase 1	O88958	Gnpda1		+
Beta-galactosidase	P23780	Glb1	+	
Semaphorin-7A	Q9QUR8	Sema7a	+	
Very long-chain acyl-CoA dehydrogenase, mitochondrial	P50544	Acadvl		+
Inter-alpha-trypsin inhibitor heavy chain H1	Q61702	Itih1	+	
Glutathione S-transferase theta-1	Q64471	Gstt1		+
Catenin beta-1	Q02248	Ctnnb1		+
BTB/POZ domain-containing protein KCTD12	Q6WVG3	Kctd12		+
Retinol-binding protein 2	Q08652	Rbp2		+
Small nuclear ribonucleoprotein Sm D3	P62320	Snrpd3		+
Coronin-7	Q9D2V7	Coro7		+
DNA topoisomerase 2-beta	Q64511	Top2b		+
Mast cell protease 2	P15119	Mcpt2	+	
Retinol-binding protein 1	Q00915	Rbp1		+
Phosphoglycolate phosphatase	Q8CHP8	Pgp		+
Beta-hexosaminidase subunit beta	P20060	Hexb	+	
Putative hydroxypyruvate isomerase	Q8R1F5	Hyi		+
S-adenosylmethionine synthase isoform type-2	Q3THS6	Mat2a		+
Bisphosphoglycerate mutase	P15327	Bpgm		+
<b>obob C57</b>				
Semaphorin-7A	Q9QUR8	Sema7a	+	
Alpha-methylacyl-CoA racemase	O09174	Amacr		+
Leukemia inhibitory factor	P09056	Lif	+	
Fructose-1,6-bisphosphatase isozyme 2	P70695	Fbp2		+
Thiosulfate sulfurtransferase	P52196	Tst		+
Eukaryotic translation initiation factor 3 subunit C	Q8R1B4	Eif3c		+
Tyrosine-protein phosphatase non-receptor type 6	P29351	Ptpn6		+
Signal transducer and activator of transcription 1	P42225	Stat1		+
Fibromodulin	P50608	Fmod	+	
Growth-regulated alpha protein	P12850	Cxcl1	+	
Plasminogen activator inhibitor 2, macrophage	P12388	Serpnb2		+
1-acyl-sn-glycerol-3-phosphate acyltransferase beta	Q8K3K7	Agpat2	+	
BTB/POZ domain-containing protein KCTD12	Q6WVG3	Kctd12		+
C-X-C motif chemokine 3	Q6W5C0	Cxcl3	+	
Epidermal growth factor receptor substrate 15	P42567	Eps15		+
26S proteasome non-ATPase regulatory subunit 13	Q9WVJ2	Psm13		+
Glutathione S-transferase Mu 7	Q80W21	Gstm7		+
Hereditary hemochromatosis protein homolog	P70387	Hfe	+	
Very long-chain specific acyl-CoA dehydrogenase, mitochondrial	P50544	Acadvl		+
Cadherin-16	O88338	Cdh16	+	
C-X-C motif chemokine 5	P50228	Cxcl5	+	
Alpha-1-antitrypsin 1-5	Q00898	Serpina1e	+	
<b>dbdb BKS</b>				
Tyrosine-protein phosphatase non-receptor type 6	P29351	Ptpn6		+
Hereditary hemochromatosis protein homolog	P70387	Hfe	+	
Proteasome activator complex subunit 3	P61290	Psme3		+
C-C motif chemokine 9	P51670	Ccl9	+	
Tripeptidyl-peptidase 2	Q64514	Tpp2		+
Vacuolar protein sorting-associated protein 13C	Q8BX70	Vps13c		+
Fibromodulin	P50608	Fmod	+	
Eukaryotic translation initiation factor 2 subunit 1	Q6ZWX6	Eif2s1		+
Metalloproteinase inhibitor 2	P25785	Timp2	+	
Mannosyl-oligosaccharide 1,2-alpha-mannosidase IA	P45700	Man1a1		+

Importin-9	Q91YE6	Ipo9		+
Carnitine O-acetyltransferase	P47934	Crat		+
Small glutamine-rich tetratricopeptide repeat-containing protein alpha	Q8BJU0	Sgta		+
T-complex protein 1 subunit zeta	P80317	Cct6a		+
Epidermal growth factor receptor substrate 15	P42567	Eps15		+
Arginase-1	Q61176	Arg1		+
Granulocyte colony-stimulating factor	P09920	Csf3		+
AP-2 complex subunit mu	P84091	Ap2m1		+
Phosphoserine phosphatase	Q99LS3	Psph		+
Histidine triad nucleotide-binding protein 1	P70349	Hint1		+
Plasminogen activator inhibitor 2, macrophage	P12388	Serpinb2		+
Basigin	P18572	Bsg	+	
Dynactin subunit 2	Q99KJ8	Dctn2		+
COP9 signalosome complex subunit 8	Q8V BV7	Cops8		+
Coatomer subunit zeta-1	P61924	Copz1		+
6-pyruvoyl tetrahydrobiopterin synthase	Q9R1Z7	Pts		+
Inter-alpha-trypsin inhibitor heavy chain H1	Q61702	Itih1	+	
Annexin A11	P97384	Anxa11		+
Plastin-1	Q3V0K9	Pls1		+
Eosinophil cationic protein 1	P97426	Ear1	+	
Isopentenyl-diphosphate Delta-isomerase 1	P58044	Idi1		+
Cadherin-1	P09803	Cdh1	+	
4-hydroxy-2-oxoglutarate aldolase, mitochondrial	Q9DCU9	Hoga1		+
Nucleoside diphosphate-linked moiety X motif 19, mitochondrial	P11930	Nudt19		+
Dolichyl-diphosphooligosaccharide-protein glycosyltransferase 48 kDa subunit	O54734	Ddost	+	
Thiosulfate sulfurtransferase	P52196	Tst		+
Cysteine and glycine-rich protein 1	P97315	Csrp1		+
N(G),N(G)-dimethylarginine dimethylaminohydrolase 1	Q9CWS0	Ddah1		+
Small nuclear ribonucleoprotein Sm D3	P62320	Snrpd3		+
SUMO-conjugating enzyme UBC9	P63280	Ube2i		+
Band 4.1-like protein 2	O70318	Epb4112		+
Semaphorin-7A	Q9QUR8	Sema7a	+	
Adenosine deaminase	P03958	Ada		+
Coronin-7	Q9D2V7	Coro7		+
Nodal modulator 1	Q6GQT9	Nomo1	+	
Phosphoglycolate phosphatase	Q8CHP8	Pgp		+
C-X-C motif chemokine 3	Q6W5C0	Cxcl3	+	
Beta-hexosaminidase subunit beta	P20060	Hexb	+	
Putative hydrolase RBBP9	O88851	Rbbp9		+
Ketohexokinase	P97328	Khk		+
Interleukin-1 receptor antagonist protein	P25085	Il1rn	+	
Alpha-methylacyl-CoA racemase	O09174	Amacr		+
Protein kinase C delta-binding protein	Q91VJ2	Prkcdpb		+
Retinol-binding protein 1	Q00915	Rbp1		+
S-adenosylmethionine synthase isoform type-2	Q3THS6	Mat2a		+
Glutathione S-transferase theta-2	Q61133	Gstt2		+
Cadherin-16	O88338	Cdh16	+	
Bisphosphoglycerate mutase	P15327	Bpgm		+
C-X-C motif chemokine 5	P50228	Cxcl5	+	
Alpha-1-antitrypsin 1-5	Q00898	Serpina1e	+	
<b>dbdb_obob</b>				
Deoxyguanosine kinase, mitochondrial	Q9QX60	Dguok		+
Semaphorin-7A	Q9QUR8	Sema7a	+	
Glutathione S-transferase Mu 7	Q80W21	Gstm7		+
Phosphoglucomutase-like protein 5	Q8BZF8	Pgm5		+
1-acyl-sn-glycerol-3-phosphate acyltransferase beta	Q8K3K7	Agpat2	+	
Regulator of microtubule dynamics protein 3	Q3UJU9	Rmdn3		+
Eosinophil cationic protein 1	P97426	Ear1	+	

H-2 class I histocompatibility antigen, D-B alpha chain	P01899	H2-D1	+	
Interleukin-1 receptor antagonist protein	P25085	Il1rn	+	
Putative hydroxypyruvate isomerase	Q8R1F5	Hyi		+

Journal: International Journal of Molecular Sciences

Impact factor: 3.226

Contribution: Conceived / designed experiments: 10 %

Performed experiments: 12 %

Analysed data: 10 %

Wrote the manuscript: 10 %

Contributed to discussion: ø

Author: Co-author

## 2 General discussion

### 2.1 Analysis of high quality secretome

We designed a protocol that is essential to generate high quality secretome from primary adipocytes as well as from differentiated preadipocytes. The aim was to minimize contamination of cytosolic proteins deriving from other cell types or apoptotic cells. In order to generate samples that enable proper MS/MS analysis, concentration via microcolumns and parallel depletion of high abundant proteins was performed. For all following investigations, the conditioned medium of the primary mature adipocytes was used which comprises the entity of all secreted factors peptides and proteins and corresponds to the vWAT secretome. One of the advantages using mature adipocytes is that the secretome is gained roughly 30 hours after dissection and better reflects the *in vivo* situation than secretome deriving from differentiated preadipocytes that were cultivated *ex vivo* for about two weeks. Furthermore, the isolation of preadipocytes always involves possible mixing with other cell types like endothelial cells, fibroblasts and various immune cells. Due to similar sizes of these cells a separation is difficult and a cultivation could falsify the secretome.

When using preadipocytes, an important task is to maintain cell viability. Therefore, differentiation medium containing fetal calf serum (FCS) was used. FCS contains high amounts of albumin, which can impede the detection of low abundant adipokines. Hence, fresh medium without FCS was used for subsequent incubation to generate conditioned medium. Additionally, a modified washing procedure was applied (PBS supplemented with CaCl<sub>2</sub>; [198]) which leads to enhancement of albumin clearance by maintaining cell viability (Fig. 3). Other protocols typically use washing buffers containing magnesium which was omitted in our protocol because an improvement in separation of adipocytes was visible ([202]; data not shown).

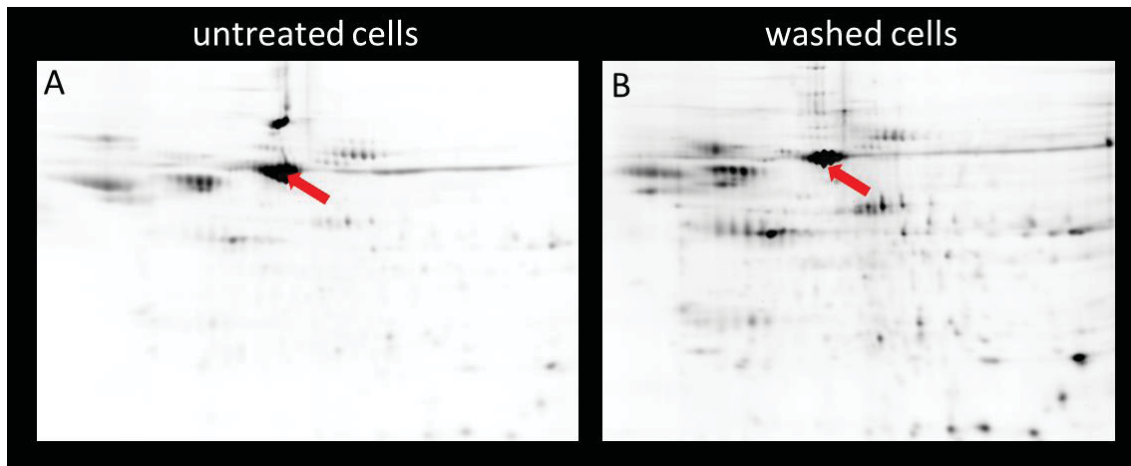


**Figure 3: 2-D gels (stainfree image) of conditioned medium from primary WAT adipocytes.** (A) untreated adipocytes; (B) adipocytes washed with PBS + 3 mM CaCl<sub>2</sub>. Red arrow indicates position of albumin spots.

Cell viability for both cell types was also monitored for different incubation times resulting in using 2 hours for the final protocol. The conditioned medium was further processed by ultracentrifugation (20'; 80,000 g; 4 °C) to remove remaining cell debris. Subsequently, the supernatants were transferred to a filter concentrator with a pore size of 3 kDa that enables concentration up to 100 X of the starting concentration (Study 1). This step is obligatory for the further use in proteomic approaches, because otherwise the volume would exceed technical application feasibility.

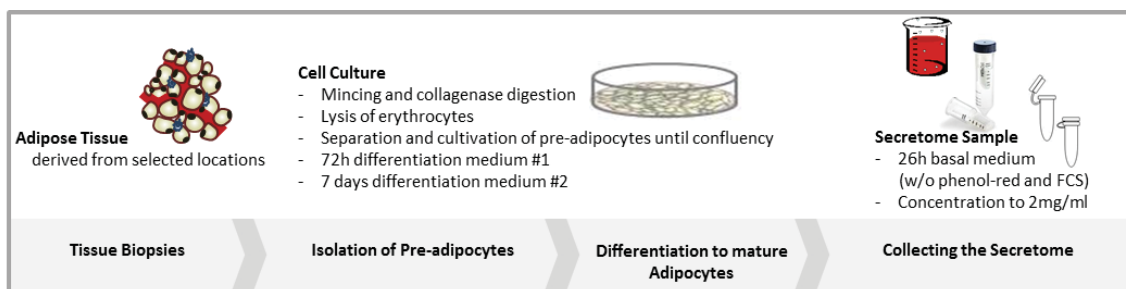


**Figure 4: Workflow scheme to generate secretome sample from differentiated mouse adipocytes.**

## 2.2 Proteomic analyses identify T-cadherin as a novel adipokine

The protocol established in study 1 was used in study 2, 3 and 4 to investigate the vWAT secretome. In study 2, vWAT secretome samples from two different mouse models (BL6 and BKS) was generated. The samples were focused on polyacrylamide (PAA) stacking gels. This step serves to remove low molecular impurities, detergents or buffer components. A defined amount of 500 ng peptides was subjected to liquid chromatography afterwards. The subsequent MS/MS analysis and combined protein and peptide identification with a specific software (Proteome Discoverer; version 1.4.1.14, Thermo Fisher Scientific, Dreieich, Germany) yielded in the final secretome protein list (Study 2). The secretome protein list of the vWAT was analyzed using MaxQuant software to evaluate regulations between the two mouse strains [203]. The data were generated using a label-free quantification approach [204]. Here, 520 unique proteins were identified describing the secretome of visceral adipose tissue of BKS mice. According to the SignalP and SecretomeP databases, 208 proteins were potentially secreted due to classical (signal peptide; SP+) or non-classical (e.g. hydrophobic sequence segments, SP-) secretory properties. In the vWAT secretome of BL6 mice, 494 adipokines were identified comprising 293 potentially secreted proteins. In the comparison of the secretomes 35 adipokines were differentially regulated between the mouse strains including six proteins that had not been described as adipokines before. One of these proteins was the bifunctional purine biosynthesis protein PURH. It was significantly higher abundant in the secretome of BKS compared to BL6 and identified to be non-classically secreted (SP-). This protein was described to be involved in insulin receptor autophosphorylation and internalization in hepatocytes suggesting putative importance in T2DM susceptibility [205]. However, the only protein that exhibited a signal peptide (SP+) was T-cadherin. T-cadherin abundance was higher in BL6 compared to BKS (Table 1, Study 2). Several studies showed associations of T-cadherin with insulin resistance, obesity and cardiovascular diseases [206]; [207]. Hence, T-cadherin was chosen as the target for follow-up-research.

## 2.3 T-cadherin function in cell growth and metabolism

T-cadherin, with CDH13 as the human homolog, is a member of the cadherin superfamily residing in the plasma membrane. It is the only cadherin protein that does not possess a cytosolic domain and that is anchored to the membrane via a GPI-anchor but exhibits the typical extracellular type I cadherin structure [208]. It was identified first in neural crest cells of the chick embryo brain in 1991 and lately described to be highly expressed in the nervous system, endothelial cells and muscle cells [209], [210]. Because of these features, the protein is either called T-cadherin (T = truncated) or H-cadherin (H = heart). According to the protein structure, it is proposed that T-cadherin is not able to interact with the intracellular filaments for cell-cell interaction. In line with that, T-cadherin did not accumulate at sites for cell-cell contact in monolayer cultures in contrast to other cadherins [211]. In polarized epithelial cells T-cadherin was localized apically whereas classical cadherins were found at the basolateral pole [212]. Furthermore, T-cadherin is localized to caveolin-rich domains like lipid-rafts and is proposed to interact with other resident signaling proteins [213].

T-cadherin has been extensively studied in relation to human cancers. According to being involved in cell proliferation and motility in smooth muscle and endothelial cells, T-cadherin expression also correlates with increased adhesion and reduced proliferation in cancer cell lines [214]. Methylation of T-cadherin in cancer cells leads to increased tumor cell aggressiveness and proliferation, identifying T-cadherin as a tumor suppressor or at least a biomarker of certain cancer types [215]; [216]. The regulations of T-cadherin seem to be controversial in cancer development, because T-cadherin promotes neovascularization, but acts tumor suppressive in cancerous cells. This regulation was investigated within cell cycle in vascular cells [217]. T-cadherin protein level was higher in cells residing in the S- and G[218]/M-phase than in the G(1)/G(0)-phase. Moreover, overexpression of T-cadherin in HUVECs and hSMCs resulted in entering the S-phase earlier. The simulation of homophilic interaction of T-cadherin *in vitro* results in increased cellular expression of the CDK inhibitor p21<sup>CIP1/WAF1</sup> [219]. Because T-cadherin is located in lipid rafts it was proposed that ligands like Platelet-derived growth factor (PDGF), epidermal growth factor (EGF) and insulin-like growth factor (IGF), whose receptors are also lipid raft associated, downregulate the expression of T-cadherin [220]. Moreover, T-cadherin silencing was shown to activate EGFR signaling and overexpression of T-cadherin deteriorated EGFR activation [221].

Ultimately, these findings support the hypothesis, that T-cadherin is highly expressed in proliferating and expanding cells until confluency. This proliferation is inhibited by induction of p21 by contact inhibition via increasing proximity of T-cadherin molecules.

Recently, T-cadherin was identified to bind adiponectin [222]. In addition to the typical receptors AdipoR1 and AdipoR2, which predominantly bind globular and full-length adiponectin, T-cadherin serves as a third type of receptor that binds hexameric and high molecular weight (HMW) adiponectin [223]; [224]. Multimeric forms of adiponectin are known to be more biologically active and knockdown of T-cadherin leads to abrogation of adiponectin induced AMPK phosphorylation [225]. Moreover, adiponectin expression and the expression of T-cadherin correlate positively and T-cadherin knockout mice more or less resemble adiponectin knockout mice. It was even shown that plasma adiponectin levels increase in T-cadherin deficient mice due to reduced association of adiponectin to tissues [226].

Plasma T-cadherin is negatively associated with severity of coronary lesions and acute coronary syndrome [227]. Adiponectin was not able to induce AMPK phosphorylation in T-cadherin deficient mice and due to that cardioprotection fails during stress conditions [228]. T-cadherin binds LDL and adiponectin, but it is still unclear how those ligands act via T-cadherin. Although T-cadherin was essential for phosphorylation of AMPK by adiponectin the interaction of T-cadherin with mediators was not shown [225]. Following LDL binding, T-cadherin induces mitogenic signaling by ERK1/2 via PLC, IP<sub>3</sub> and intracellular Ca<sup>2+</sup> mobilization. Here, overexpression of T-cadherin in HEK293 cells resulted in accelerated cell proliferation [229]. Ultimately, T-cadherin homophilic interactions were shown to prevent cell spreading, induce polarization and migration. Philippova *et al.* showed that this was mediated by RhoA-ROCK- and Rac- dependent mechanisms, however not revealing the concrete circuitry [230]

To the best knowledge, T-cadherin has not been described in the adipose tissue so far. However, it was mentioned to play a role in tethering adiponectin to M2 macrophages in scWAT thereby inducing beige and anti-inflammatory processes [231]. Similar, our findings demonstrate that T-cadherin vWAT expression as well as plasma levels negatively correlate with the obese and inflamed state (Study 3). Despite the suggestion that T-cadherin does not act as a signaling receptor itself, because of the missing intracellular moiety, there is evidence that it is involved in signaling processes. As pointed out for adiponectin, crosstalk with other receptors and mediators is likely to exert such effects but these links are not unraveled completely. The only adaptor protein that has been identified so far to be directly linked with T-cadherin signaling is the Integrin-linked kinase (ILK). Nuclear translocation of  $\beta$ -catenin was observable after overexpression of T-cadherin in endothelial cells (ECs), postulating GSK-3 $\beta$  activation. The crucial link is supposed to be ILK, which knockdown results in absence of Akt and GSK-3 $\beta$  phosphorylation [232].

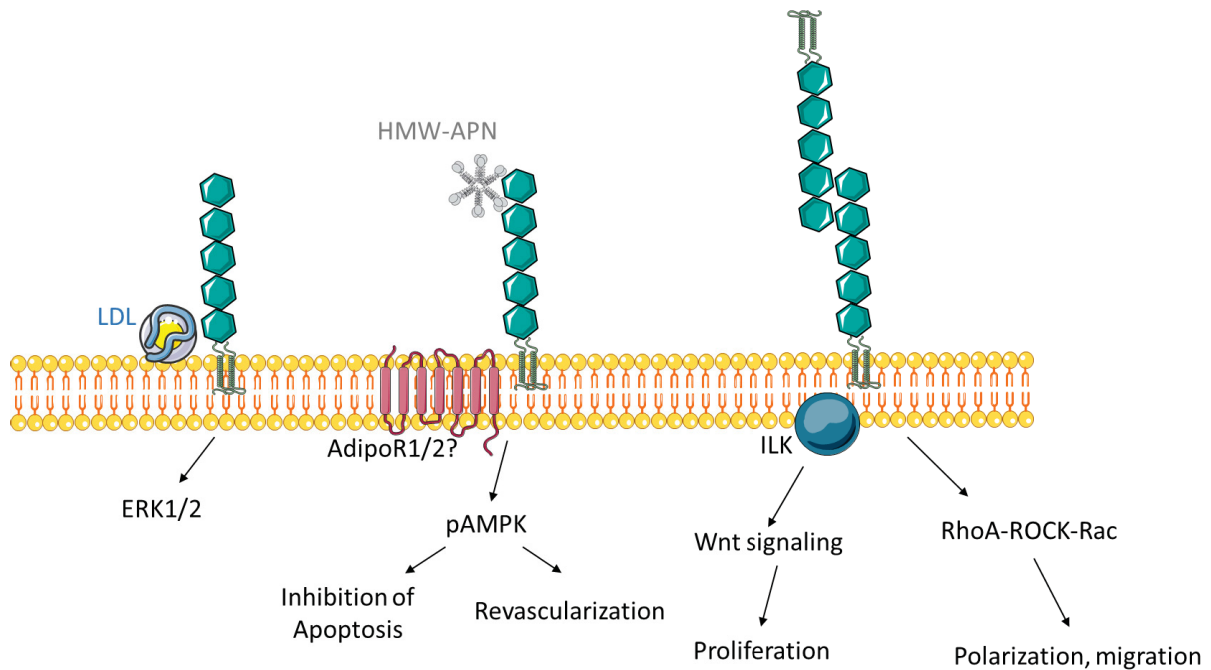


**Figure 5: Interactions of T-cadherin.** The different binding partners of T-cadherin. T-cadherin is described to bind LDL and induce activation of ERK1/2. Binding of HMW or hexameric APN induces phosphorylation of AMPK and inhibits apoptosis but triggers revascularization depending on cell type. The possible interaction with T-cadherin as a co-receptor for AdipoR1/2 is not elucidated. Homophilic interaction of T-cadherin molecules leads to proliferation via interaction of ILK and activation of the Wnt-signaling pathway. On the other hand it can impact polarization or migration via RhoA-ROCK-Rac signaling.

## 2.4. T-cadherin regulation in the WAT and lipid metabolism

Because T-cadherin abundance was detected in vWAT secretomes for the first time, the aim of study 3 was to elucidate the function of the protein within the adipose tissue. In addition to the analysis of the BL6 and BKS mice, the secretome of vWAT from ob and db mice was generated and the secretomes of all four genotypes were differentially analyzed. In order to investigate the mouse strains in a reproducible way we applied stringent criteria in the MS/MS analysis. For protein identification at least two peptide spectrum matches were necessary. For valid protein detection, only proteins that had been “identified in 3 of 5 biological replicates” or “no identification vs identification in all biological replicates (0-5)” were used for further analysis (Study 4).

T-cadherin was detected to be upregulated in proliferative states [217]. Further,  $\beta$ -catenin, that is upregulated similarly, is also described to be stabilized by T-cadherin. This interconnection seems to be a positive feedback-loop that keeps the proliferation ongoing. As reported, we hypothesize that T-cadherin is a marker for a not fully differentiated state of a cell, thus reflects the plasticity of the tissue (Study 3). T-cadherin knockout was demonstrated to induce reduction of phosphorylation of Akt which in turn leads to increased apoptosis [233]; [234-236]. Although

insulin action upon T-cadherin knockdown was not investigated in this thesis, these studies support our hypothesis that T-cadherin expression may preserve cell viability (Study 3).

In the comparison of BL6 and BKS vWAT secretomes, different T-cadherin levels suggest a positive role for T-cadherin in the disease susceptibility. It was hypothesized in study 3 that higher levels in BL6 might maintain adiponectin function and protect the ob mice to become diabetic. However, the regulation that was observed between the background strains was not confirmed between the diseased mouse models which rebutted the hypothesis. Ob/ob mice exhibit the lowest T-cadherin levels of all genotypes involved (Study 3, Fig. 1A, B). Conversely, silencing of T-cadherin did not lead to an increase in lipid accumulation but to a decrease of lipid content of 3T3-L1 (Study 3, Fig. 2B). Thus, it was speculated that T-cadherin expression is not causative for the grade of obesity but rather a secondary factor. Overexpression of adiponectin increases proliferation and differentiation in 3T3-L1 cells [237]. Hence, knockdown of T-cadherin might lead to a decrease in lipid content because adiponectin signaling is disturbed. This hypothesis would be in line with our findings showing that T-cadherin knockdown decreases central factors for adipogenesis, PPAR $\gamma$  and C/EBP $\alpha$  which leads to a deceleration of differentiation and results in reduced cellular lipid content (Study 3, Fig. 3).

It was demonstrated that T-cadherin is downregulated with progression of differentiation *in vitro* (Study 3, Figure 1E) and that knockdown of T-cadherin reduces expression of LPL in the early and late adipocyte state (Study 3, Figure S1). Therefore, it was reasoned that T-cadherin expression might reflect the differentiation status of the cell and thereby the need for cellular fuel like FFAs. Thus, the artificial depletion of T-cadherin by knockdown might mimic a differentiated and fueled cell status resulting in downregulation of LPL expression.

Downregulation of T-cadherin had an influence on several players in lipid metabolism, but fatty acid transporters like FABP4 or CD36 were not affected (Study 3, Figure S1). In contrast to this, knockdown of T-cadherin reduces FFA uptake in the fibroblast (d0) and early adipocyte state (d4) suggesting that other factors like FABP(pm) or FATP1 might be involved. Because fatty acid transport proteins are sequestered in vesicles, knockdown of T-cadherin might have influenced fatty acid transporter vesicular regulation or membranal presentation which was not determined in our experiments. Based on the protein structure it has been suggested that T-cadherin may even act as a co-receptor for fatty acid transport proteins [225]. The reduced lipid accumulation after T-cadherin knockdown can also be evoked by alterations in lipolysis although the expression of key enzyme HSL was not changed (data not shown). Additionally, we demonstrated in differentiated 3T3-L1 cells that the glycerol release was not changed upon T-cadherin knockdown. Since glycerol release is an indicator for lipolysis, these results ultimately point to the hypothesis that T-cadherin does not directly affect lipid uptake or lipolysis but differentiation and thereby indirectly influences players of lipid metabolism.

Certain T-cadherin polymorphisms or systemic loss of T-cadherin correlate with higher adiponectin plasma levels [226]. In this line, recent studies identified 3 further genetic variations (rs3865188, rs4783244 and rs12051272) that are associated with higher plasma adiponectin and parameters like higher fasting insulin, HOMA-IR and plasma triglycerides. However, the polymorphisms could not be associated with visceral fat accumulation [238]. We showed that treatment of cells with palmitate or insulin decreased T-cadherin expression suggesting affluent lipids and insulin might restrain T-cadherin (Study 3, Figure 1G). This undermines a possible interrelation of T-cadherin and plasma insulin and triglyceride levels.

Although T-cadherin is described to bind LDL particles [229], correlations of LDL plasma concentration and T-cadherin plasma levels were not observed (Study 3, table S1). On the contrary, interactions of T-cadherin and HDL are not known so far. In the human probands, however, HDL plasma levels highly correlated with T-cadherin expression in the WAT as well as T-cadherin plasma levels. This correlation was even present after adjustment for age and BMI. Intra-abdominal fat is a strong negative correlate of HDL and weight loss can elevate HDL levels [239]. In our paradigm, T-cadherin was regulated in a comparable way suggesting possible interconnections within the lipid metabolism of HDL and T-cadherin.

T-cadherin was described to play a role in insulin secretion via its function as an adiponectin receptor. In beta cells of TCAD knockout mice, the second phase insulin secretion was reduced while first phase insulin secretion was not affected [240]. Because adiponectin affects insulin signaling and glucose metabolism, it was postulated that T-cadherin might influence glucose uptake [241], [140]. However, in our analysis T-cadherin knockdown did not influence glucose uptake in the early (d4) or late (d7) adipocytes (Study 3, Figure 2A).

Ultimately, T-cadherin was identified in the vWAT from different mouse models and human patients upon mRNA level. Additionally, the regulation was confirmed upon protein level in the adipose tissue secretome and furthermore in the circulation of the human probands. Strikingly, human plasma concentration was restored to the levels of normal-weight controls after bariatric surgery and subsequent caloric uptake restriction (Study 3, Figure 4D).

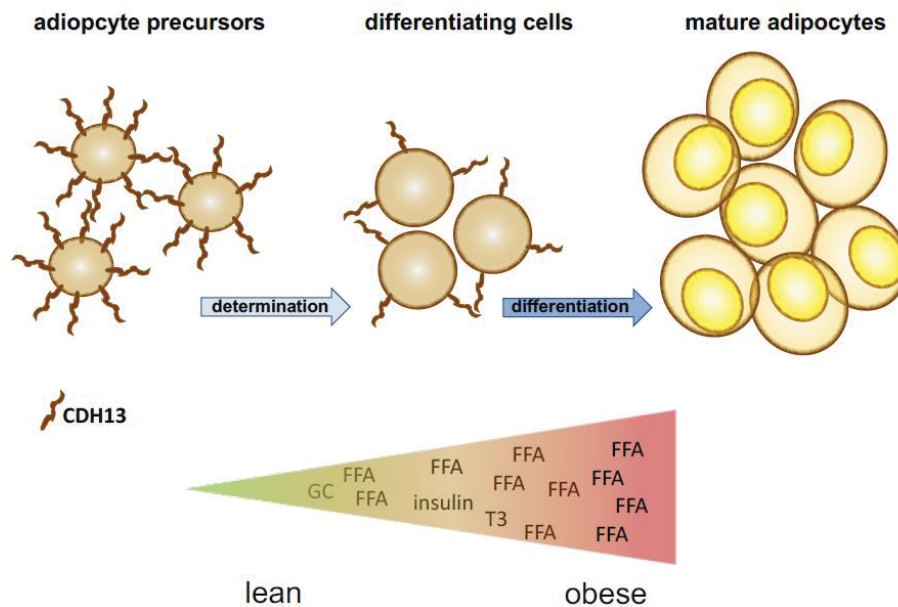


**Figure 6: Scheme of T-cadherin abundance during vWAT differentiation.** T-cadherin abundance is high in undifferentiated adipocyte precursor cells. Increasing levels of insulin and circulating FFAs reduce T-cadherin protein. In the mature adipocyte T-cadherin is severely downregulated. FFA= free fatty acids; GC= glucocorticoid; CDH13=T-cadherin. From Study 3

Studies with specific mouse models intended to examine the mechanisms of healthy and unhealthy obesity, showed that an essential factor is the preservation of adipose tissue function with adiponectin signaling as a central modulator. A newly established mouse model, the PLO (PPAR $\gamma$  P465L  $\times$  ob/ob) mouse that carries a dominant negative mutation in the pro-adipogenic transcription factor PPAR $\gamma$  on an ob genetic background is 14% less obese than ob mice but more insulin resistant [242]. On the other hand, the AdTG-ob/ob mouse model exhibits a transgenic overexpression of adiponectin in the adipose tissue. These mice show increased body weight by 50% but are protected from ectopic lipid accumulation. The AdTG-ob/ob mice are proposed as a model for healthy obesity, because insulin sensitivity is preserved [243]. Moreover, it was demonstrated that T-cadherin expression guides mesenchymal stromal cells and upregulates extracellular matrix components [244]. Concluding, T-cadherin might represent a link of adiponectin function according to adipose tissue remodeling and expansion.

In conclusion, T-cadherin was described the first time as an adipokine although its functional role is not fully elucidated yet. This thesis strengthens the hypothesis of T-cadherin as a potent modulator of proliferation and cellular phenotype [245]. Mice lacking T-cadherin do not show a pathological phenotype but exhibit increased adiponectin plasma levels and disrupted adiponectin signaling on tissues [228]. The functional correlations which have been observed due to knockdown of T-cadherin in this thesis are presumably indirect effects. Moreover, translational investigations of T-cadherin plasma levels show that it represents a biomarker for healthy adipose tissue that is negatively correlated with BMI.

## 2.5 Comprehensive analysis of vWAT secretome

In study 3, adipose tissue-derived secretomes of four different genetic backgrounds were analyzed. Pathway analyses of the secreted proteins yielded secretion annotations like “extracellular region” or “membrane-bounded vesicle”. Moreover, the secretome data were associated with clinical parameters in study 4 to receive possible functional correlations. Some metabolites like DAGs can alter intracellular signaling via members of the novel protein kinase C (nPKC) family and have diabetogenic effects [246], [247]. Therefore, the lipid profiles of adipocytes from all four genotypes were investigated. In terms of obesity and insulin resistance, deteriorations of insulin signaling by lipid metabolites is part of the concept of glucolipotoxicity [248]. We accomplished a combination of both proteomic and lipidomic analyses to possibly draw-back the secretome information to differences in DAG patterns.

Total DAG levels were upregulated in the obese/diabetic controls compared to the BKS mice. According to the diabetogenic effect there is still no clear evidence which DAG species act beneficial or worsening. We found 16:0 DAGs differentially abundant in obese and diabetic animals. 16:1 DAGs were significantly upregulated in the obese mice whereas 20:4 DAGs were measured to be less abundant in the obese/diabetic animals compared with their respective controls (Study 4). DAG species specific for obese and obese/diabetic mice showed highest annotation to poly(A) RNA binding proteins. These proteins have been described to have moonlighting functions which can alter their cellular location or trafficking and thereby influence metabolic regulation [249]; [250]; [251].

In this study we demonstrate that the correlation of different analyses via lipid profiling and secretome analysis might be reasonable to get insights into possible new targets of metabolic control e.g. RNA-binding proteins that are differentially regulated in obesity and T2DM.

## 2.6 Perspectives

In this thesis, a protocol for preparation and analysis of adipocyte-secreted proteins was developed. The secretome of diabetes-resistant and diabetes-prone background mouse strains was analyzed and 6 novel, differentially regulated adipokines were identified. T-cadherin was chosen for further studies due to known interactions with adiponectin. Subsequent analyses investigated the regulation of T-cadherin in mouse models for obesity and T2DM. Studies with human biopsies demonstrated that it negatively correlates with BMI and might be a biomarker for healthy adipose tissue.

- It was demonstrated that gender is a crucial factor for T-cadherin and HMW adiponectin levels [252]. In this line it might be of interest to investigate female mice and women to complete the translational approach.
- Because T-cadherin is hypothesized to be a marker for healthy adipose tissue it would be reasonable to investigate T-cadherin levels in the adipose tissue of obese and healthy obese patients.
- For the assessment of the result that T-cadherin knockdown decreases lipid accumulation in 3T3-L1 cells we accomplished fatty acid uptake, glucose uptake and lipolysis assays. Adiponectin is described to increase fatty acid oxidation in the adipose tissue [253]. Therefore, fatty acid oxidation measurements after knockdown of T-cadherin would be a reasonable add-on to complete the investigation of its function in lipid metabolism.
- In our paradigm T-cadherin expression was downregulated by palmitate as well as by insulin treatment. Both palmitate and insulin can reduce the expression of PGC-1 $\alpha$  or even negatively phosphorylate PGC-1 $\alpha$  [254]; [255]; [256]. Thus, PGC-1 $\alpha$  might be an interesting target to examine the mechanism of T-cadherin regulation.
- T-cadherin was analyzed in the white adipose tissue extensively with a focus on downregulation of expression. In the hypothesis that was based on our results it would be of interest to investigate T-cadherin's function by overexpression. In spite of the fact that downregulation of T-cadherin is not causative for obesity, the overexpression in the adipose tissue in combination with a HFD could clarify its role in obesity.

The holistic proteomic and lipidomic investigation of the WAT revealed certain DAG species exclusively regulated in specific mouse models for obesity or obesity/diabetes (C16:1\_16:1 and C18:0\_20:4) which also showed high annotation with RNA-binding proteins.

- The combined analysis of secretome and lipid profile of the adipose tissue revealed RNA-binding proteins that might play a role in metabolic disorders like obesity or T2DM. Therefore, these candidates could be investigated upon their moonlighting function in the adipose tissue by interactome and protein-ribosome interaction analyses.

### 3. Further contributions

**Article Z1: So close and yet so far: mitochondria and peroxisomes are one but with specific talents.**

Biochim Biophys Acta (2015) Jul; 1851(7):965-976.

Hartwig S<sup>1</sup>, Knebel B, Goeddeke S, Koellmer C, Jacob S, Nitzgen U, Passlack W, Schiller M, Dicken HD, Haas J, Muller-Wieland D, Lehr S, Kotzka J.

<sup>1</sup> Institute of Clinical Biochemistry and Pathobiochemistry, German Diabetes Center at the Heinrich-Heine-University Duesseldorf, Leibniz Center for Diabetes Research, 40225 Düsseldorf, Germany.

Abstract: Cellular compartmentalization of central metabolic pathways as lipid metabolism to mitochondria and peroxisomes enables high efficient control processes. The basis to understand mitochondrial or peroxisomal function is exactly to determine proteins physically present. For proteomic investigations of mouse liver organelles, we developed 2-DE reference maps covering the range pH 4-9, available under ([www.diabetesityprot.org](http://www.diabetesityprot.org)). MALDI-TOF-MS/MS analyses identified a total of 799 (mitochondria) and 681 (peroxisome) protein spots resembling 323 and 293 unique proteins, respectively. Direct comparison of mitochondrial and peroxisomal proteins indicated an approximate overlap of 2/3 of identified proteins. Gene Ontologies (GO) of the identified proteins in respect to physical presence confirmed functional specifications within the organelles. The 2-DE organelle reference maps will aid to point out functional differences and similarities. Our observations suggest that for functional analyses metabolic alterations focusing on one organelle are not sufficient and parallel comparison of both organelles is to be preferred.

Contribution: Performed experiments (10%)

## **Article Z2: Peroxisomes compensate hepatic lipid overflow in mice with fatty liver.**

Arch Physiol Biochem (2013) Jul; 119(3): 126-35.

Birgit Knebel<sup>a</sup>, Sonja Hartwig<sup>a</sup>, Jutta Haas<sup>b</sup>, Stefan Lehr<sup>a</sup>, Simon Goeddeke<sup>a</sup>, Franciscus Susanto<sup>a</sup>, Lothar<sup>a</sup>, Sylvia Jacob<sup>a</sup>, Cornelia Koellmer<sup>a</sup>, Ulrike Nitzgen<sup>a</sup>, Dirk Müller-Wieland<sup>b</sup>, Jorg Kotzka<sup>a</sup>, □

<sup>a</sup> Institute of Clinical Biochemistry and Pathobiochemistry, German Diabetes Center, Leibniz Center for Diabetes Research, Heinrich-Heine-University Duesseldorf, Aufm Hennekamp 65,

Duesseldorf 40225, Germany

<sup>b</sup> Institute for Diabetes Research, Department of General Internal Medicine, Asklepios Clinic St. Georg, Medical Faculty of Semmelweis University, Asklepios Campus Hamburg, Lohmuehlen Str 5,

Hamburg 20099, Germany

**Abstract:** Major causes of lipid accumulation in liver are increased import or synthesis or decreased catabolism of fatty acids. The latter is caused by dysfunction of cellular organelles controlling energy homeostasis, i.e., mitochondria. Peroxisomes also appear to be an important organelle in lipid metabolism of hepatocytes, but little is known about their role in the development of non-alcoholic fatty liver disease (NAFLD). To investigate the role of peroxisomes alongside mitochondria in excessive hepatic lipid accumulation, we used leptin-resistant db/db mice on C57BL/Ks background, a mouse model that develops hyperphagia-induced diabetes with obesity and NAFLD. Proteome and gene expression analyses along with lipid analyses in the liver revealed differential expression of genes related to lipid metabolism and  $\beta$ -oxidation, whereas genes for peroxisomal proteins were predominantly regulated. Our investigations show that in fatty liver disease in combination with obesity and diabetes, the hepatocyte-protecting organelle peroxisome is altered. Hence, peroxisomes might indicate a stage of pre-NAFLD, play a role in the early development of NAFLD and appear to be a potential target for treatment and prevention of NAFLD.

Contribution: Performed experiments (10%)

## **Article Z3: Alteration of liver peroxisomal and mitochondrial functionality in the NZO mouse model of metabolic syndrome.**

Accepted 10/2017; Proteomics Clinical Applications

Birgit Knebel,<sup>1,2</sup> Simon Göddeke,<sup>1,2</sup> Sonja Hartwig,<sup>1,2</sup> Tina Hörbelt,<sup>1,2</sup> Pia Fahlbusch,<sup>1,2</sup> Hadi Al-Hasani,<sup>1,2</sup> Sylvia Jacob,<sup>1,2</sup> Cornelia Koellmer,<sup>1,2</sup> Ulrike Nitzgen,<sup>1,2</sup> Martina Schiller,<sup>1,2</sup> Stefan Lehr,<sup>1,2,\*</sup> and Jorg Kotzka<sup>1,2,§</sup>

<sup>1</sup>Institute of Clinical Biochemistry and Pathobiochemistry, German Diabetes Center at the Heinrich-Heine-University Duesseldorf, Leibniz Center for Diabetes Research, Aufm Hennekamp 65, 40225 Duesseldorf, Germany

<sup>2</sup>German Center of Diabetes Research Partner, Duesseldorf, Germany

**Abstract:** MetS consists of five risk factors: elevated blood pressure and fasting glucose, visceral obesity, dyslipidemia and hypercholesterinemia. The physiological impact of lipid metabolism indicated as visceral obesity and hepatic lipid accumulation on MetS is still under debate. One major cause of disturbed lipid metabolism might be dysfunction of cellular organelles controlling energy homeostasis, i.e. mitochondria and peroxisomes. The New Zealand Obese (NZO) mouse model exhibits a polygenic syndrome of obesity, insulin resistance, triglyceridemia and hypercholesterolemia that resembles human metabolic syndrome. We applied a multi-omics approach combining lipidomics with liver transcriptomics and top-down mass spectroscopy based organelle proteomics (2D-DIGE<sup>TM</sup>) of highly purified mitochondria and peroxisomes in male mice, to investigate molecular mechanisms related to the impact of lipid metabolism in the pathophysiology of the metabolic syndrome. Proteome analyses of liver organelles indicated differences in fatty acid and cholesterol metabolism, mainly influenced by PG-C1 $\alpha$ /PPAR $\alpha$  and other nuclear receptor mediated pathways. These results were in accordance with altered serum lipid profiles and elevated organelle functionality. These data emphasize that metabolic syndrome is accompanied with increased mitochondria and peroxisomal activity to cope with dyslipidemia and hypercholesterinemia driven hepatic lipid overflow in developing a fatty liver.

Contribution: Performed experiments (5%), Data analysis (5%)

**Article Z4 (submitted): Liver - to - adipose tissue *de novo* lipid synthesis ratio associates with adipokinome signatures and serum lipid levels in NAFLD mouse models.**

Birgit Knebel<sup>1,2</sup>, Gereon Poschmann<sup>8</sup>, Simon Goeddeke<sup>1,2</sup>, Cora Weigert<sup>5,6</sup>, Jan Krumsiek<sup>3,4</sup>, Parviz Gomari<sup>3,4</sup>, Kai Stühler<sup>8</sup>, Sonja Hartwig<sup>1,2</sup>, Sylvia Jacob<sup>1,2</sup>, Ulrike Kettel<sup>1,2</sup>, Dirk Müller-Wieland<sup>4</sup>, Stefan Lehr<sup>1,2</sup>, Jorg Kotzka<sup>1,2</sup>:

<sup>1</sup>Institute of Clinical Biochemistry and Pathobiochemistry, German Diabetes Center at the Heinrich-Heine-University Duesseldorf, Leibniz Center for Diabetes Research, Aufm Hennekamp 65, 40225 Duesseldorf, Germany

<sup>2</sup>German Center of Diabetes Research Partner, Duesseldorf, Germany

<sup>3</sup>German Center for Diabetes Research (DZD), Partner 85764 München-Neuherberg, Germany.

<sup>4</sup>Institute of Computational Biology, Helmholtz Zentrum München, Neuherberg, Germany; German Center for Diabetes Research (DZD e.V.), Germany.

<sup>5</sup>Division of Pathobiochemistry and Clinical Chemistry, Department of Internal Medicine IV, University Hospital Tübingen, 72076 Tübingen, Germany.

<sup>6</sup>Institute for Diabetes Research and Metabolic Diseases of the Helmholtz Zentrum München at the University of Tübingen, 72076 Tübingen, Germany.

<sup>7</sup> Institute for Diabetes Research, Department of General Internal Medicine, Asklepios Clinic St. Georg, Medical Faculty of Semmelweis University, Asklepios Campus Hamburg, Lohmuehlen Str 5, Hamburg 20099, Germany

<sup>8</sup>Heinrich-Heine-University Duesseldorf, Molecular Proteomics Laboratory, Biomedizinisches Forschungszentrum (BMFZ), Duesseldorf, Germany

Purpose: Hepatic and adipocyte lipid metabolism govern whole-body metabolic homeostasis. One crucial point is the *de novo lipogenesis* (DNL) in liver and adipose tissue, which might interact. Adipose tissue DNL derived fatty acids cC16:1 and cC18:1 interfere with hepatic metabolism, whereas it is poorly understood if further adipocyte-derived molecular mediators indicate adipose functionality.

Experimental Design: We recruited the NAFLD mouse models alb-SREBP-1c with increased hepatic DNL and “healthy” obesity, and obob with hyperphagia-induced “sick” obesity on C57Bl6 background to analyze the impact of tissue-specific DNL on the secreted proteins of primary adipose cells by lipidomics and label free proteomics.

Results: Starved alb-SREBP-1c and obob mice differ in serum lipids, mainly C16:0, C18:0 and cC18:1, but not cC16:1. Hepatic DNL is down in obob but elevated in alb-SREBP-1c, whereas adipose tissue DNL is down in both. We formulate the liver-to-adipose-tissue DNL-ratios and investigate the relationship to adipokinomes. Pathway analyses revealed adipocyte functionality with proteins involved in tissue remodeling or metabolism in lean (C57Bl6) and alb-SREBP-1c mice and fibrotic pathways in obese obob mice.

Conclusion and Clinical Relevance: The composition of the serum lipids reflect the ratio of liver-to-adipose-tissue DNL. Depending on the degree of the DNL-ratio, adipokinomes show fibrotic pathways as marker for adipose tissue health.

Contribution: Performed experiments (10%)

## Bibliography

1. Winterhalter, P.R., et al., *O-glycosylation of the non-canonical T-cadherin from rabbit skeletal muscle by single mannose residues*. FEBS Lett, 2013. **587**(22): p. 3715-21.
2. Diefenbach, C. and M. Abel, [*Economic control in anesthesia and intensive care medicine--do we need new muscle relaxants? Pro*]. Anesthesiol Intensivmed Notfallmed Schmerzther, 1996. **31**(1): p. 44-5.
3. Mathers, C.D. and D. Loncar, *Projections of global mortality and burden of disease from 2002 to 2030*. PLoS Med, 2006. **3**(11): p. e442.
4. Sandu, M.-M., et al., *Data Regarding the Prevalence and Incidence of Diabetes Mellitus and Prediabetes*, in *Romanian Journal of Diabetes Nutrition and Metabolic Diseases*. 2016. p. 95.
5. Maahs, D.M., et al., *Epidemiology of type 1 diabetes*. Endocrinol Metab Clin North Am, 2010. **39**(3): p. 481-97.
6. Kirkman, M.S., et al., *Diabetes in older adults*. Diabetes Care, 2012. **35**(12): p. 2650-64.
7. Zhang, P., et al., *Global healthcare expenditure on diabetes for 2010 and 2030*. Diabetes Res Clin Pract, 2010. **87**(3): p. 293-301.
8. Ogurtsova, K., et al., *IDF Diabetes Atlas: Global estimates for the prevalence of diabetes for 2015 and 2040*. Diabetes Res Clin Pract, 2017. **128**: p. 40-50.
9. American Diabetes, A., *Diagnosis and classification of diabetes mellitus*. Diabetes Care, 2010. **33 Suppl 1**: p. S62-9.
10. Mandviwala, T., U. Khalid, and A. Deswal, *Obesity and Cardiovascular Disease: a Risk Factor or a Risk Marker?* Curr Atheroscler Rep, 2016. **18**(5): p. 21.
11. Wild, S.H. and C.D. Byrne, *ABC of obesity. Risk factors for diabetes and coronary heart disease*. BMJ, 2006. **333**(7576): p. 1009-11.
12. Wearing, S.C., et al., *Musculoskeletal disorders associated with obesity: a biomechanical perspective*. Obes Rev, 2006. **7**(3): p. 239-50.
13. Hawkes, C., et al., *The Global Nutrition Report 2015: what we need to do to advance progress in addressing malnutrition in all its forms*. Public Health Nutr, 2015. **18**(17): p. 3067-9.
14. Boutayeb, A., *The double burden of communicable and non-communicable diseases in developing countries*. Trans R Soc Trop Med Hyg, 2006. **100**(3): p. 191-9.
15. Kearney, J., *Food consumption trends and drivers*. Philos Trans R Soc Lond B Biol Sci, 2010. **365**(1554): p. 2793-807.
16. Drewnowski, A. and B.M. Popkin, *The nutrition transition: new trends in the global diet*. Nutr Rev, 1997. **55**(2): p. 31-43.
17. Denis, G.V. and M.S. Obin, *'Metabolically healthy obesity': origins and implications*. Mol Aspects Med, 2013. **34**(1): p. 59-70.
18. Munoz-Garach, A., I. Cornejo-Pareja, and F.J. Tinahones, *Does Metabolically Healthy Obesity Exist?* Nutrients, 2016. **8**(6).
19. Badoud, F., et al., *Molecular insights into the role of white adipose tissue in metabolically unhealthy normal weight and metabolically healthy obese individuals*. FASEB J, 2015. **29**(3): p. 748-58.
20. Huypens, P., et al., *Epigenetic germline inheritance of diet-induced obesity and insulin resistance*. Nat Genet, 2016. **48**(5): p. 497-9.
21. Somer, R.A. and C.S. Thummel, *Epigenetic inheritance of metabolic state*. Curr Opin Genet Dev, 2014. **27**: p. 43-7.
22. Gibson, L.Y., et al., *The role of family and maternal factors in childhood obesity*. Med J Aust, 2007. **186**(11): p. 591-5.
23. Maffeis, C., G. Talamini, and L. Tato, *Influence of diet, physical activity and parents' obesity on children's adiposity: a four-year longitudinal study*. Int J Obes Relat Metab Disord, 1998. **22**(8): p. 758-64.
24. Schaefer-Graf, U.M., et al., *Birth weight and parental BMI predict overweight in children from mothers with gestational diabetes*. Diabetes Care, 2005. **28**(7): p. 1745-50.

25. Wang, Z., C.M. Patterson, and A.P. Hills, *Association between overweight or obesity and household income and parental body mass index in Australian youth: analysis of the Australian National Nutrition Survey, 1995*. Asia Pac J Clin Nutr, 2002. **11**(3): p. 200-5.
26. Whitaker, R.C., et al., *Predicting obesity in young adulthood from childhood and parental obesity*. N Engl J Med, 1997. **337**(13): p. 869-73.
27. Lumey, L.H., et al., *Lipid profiles in middle-aged men and women after famine exposure during gestation: the Dutch Hunger Winter Families Study*. Am J Clin Nutr, 2009. **89**(6): p. 1737-43.
28. Chau, Y.Y., et al., *Visceral and subcutaneous fat have different origins and evidence supports a mesothelial source*. Nat Cell Biol, 2014. **16**(4): p. 367-75.
29. Chau, Y.Y., et al., *Acute multiple organ failure in adult mice deleted for the developmental regulator *Wt1**. PLoS Genet, 2011. **7**(12): p. e1002404.
30. Grauer, W.O., et al., *Quantification of body fat distribution in the abdomen using computed tomography*. Am J Clin Nutr, 1984. **39**(4): p. 631-7.
31. Golia, E., et al., *Adipose tissue and vascular inflammation in coronary artery disease*. World J Cardiol, 2014. **6**(7): p. 539-54.
32. Guilherme, A., et al., *Adipocyte dysfunctions linking obesity to insulin resistance and type 2 diabetes*. Nat Rev Mol Cell Biol, 2008. **9**(5): p. 367-77.
33. Zhou, J. and G. Qin, *Adipocyte dysfunction and hypertension*. Am J Cardiovasc Dis, 2012. **2**(2): p. 143-9.
34. Patel, P. and N. Abate, *Role of subcutaneous adipose tissue in the pathogenesis of insulin resistance*. J Obes, 2013. **2013**: p. 489187.
35. Porter, S.A., et al., *Abdominal subcutaneous adipose tissue: a protective fat depot?* Diabetes Care, 2009. **32**(6): p. 1068-75.
36. Carey, D.G., et al., *Effect of rosiglitazone on insulin sensitivity and body composition in type 2 diabetic patients [corrected]*. Obes Res, 2002. **10**(10): p. 1008-15.
37. Klein, S., et al., *Absence of an effect of liposuction on insulin action and risk factors for coronary heart disease*. N Engl J Med, 2004. **350**(25): p. 2549-57.
38. Foster, M.T. and M.J. Pagliassotti, *Metabolic alterations following visceral fat removal and expansion: Beyond anatomic location*. Adipocyte, 2012. **1**(4): p. 192-199.
39. Poirier, P. and J.P. Despres, *Exercise in weight management of obesity*. Cardiol Clin, 2001. **19**(3): p. 459-70.
40. Chaston, T.B. and J.B. Dixon, *Factors associated with percent change in visceral versus subcutaneous abdominal fat during weight loss: findings from a systematic review*. Int J Obes (Lond), 2008. **32**(4): p. 619-28.
41. Wing, R.R., et al., *Benefits of modest weight loss in improving cardiovascular risk factors in overweight and obese individuals with type 2 diabetes*. Diabetes Care, 2011. **34**(7): p. 1481-6.
42. Rossi, A.P., et al., *Effect of moderate weight loss on hepatic, pancreatic and visceral lipids in obese subjects*. Nutr Diabetes, 2012. **2**: p. e32.
43. Gustafson, B., et al., *Restricted adipogenesis in hypertrophic obesity: the role of *WISP2*, *WNT*, and *BMP4**. Diabetes, 2013. **62**(9): p. 2997-3004.
44. Gustafson, B., et al., *Insulin resistance and impaired adipogenesis*. Trends Endocrinol Metab, 2015. **26**(4): p. 193-200.
45. Rosen, E.D. and B.M. Spiegelman, *Adipocytes as regulators of energy balance and glucose homeostasis*. Nature, 2006. **444**(7121): p. 847-53.
46. Chang, B.H., et al., *Protection against fatty liver but normal adipogenesis in mice lacking adipose differentiation-related protein*. Mol Cell Biol, 2006. **26**(3): p. 1063-76.
47. Gulbagci, N.T., et al., *SHARP1/DEC2 inhibits adipogenic differentiation by regulating the activity of *C/EBP**. EMBO Rep, 2009. **10**(1): p. 79-86.
48. Wu, Z., et al., *Cross-regulation of *C/EBP* alpha and *PPAR* gamma controls the transcriptional pathway of adipogenesis and insulin sensitivity*. Mol Cell, 1999. **3**(2): p. 151-8.
49. White, U.A. and J.M. Stephens, *Transcriptional factors that promote formation of white adipose tissue*. Mol Cell Endocrinol, 2010. **318**(1-2): p. 10-4.

50. Tanaka, T., et al., *Defective adipocyte differentiation in mice lacking the C/EBPbeta and/or C/EBPdelta gene*. EMBO J, 1997. **16**(24): p. 7432-43.
51. Ren, D., et al., *PPARgamma knockdown by engineered transcription factors: exogenous PPARgamma2 but not PPARgamma1 reactivates adipogenesis*. Genes Dev, 2002. **16**(1): p. 27-32.
52. Moitra, J., et al., *Life without white fat: a transgenic mouse*. Genes Dev, 1998. **12**(20): p. 3168-81.
53. Shimomura, I., et al., *Insulin resistance and diabetes mellitus in transgenic mice expressing nuclear SREBP-1c in adipose tissue: model for congenital generalized lipodystrophy*. Genes Dev, 1998. **12**(20): p. 3182-94.
54. Horton, J.D., et al., *Overexpression of sterol regulatory element-binding protein-1a in mouse adipose tissue produces adipocyte hypertrophy, increased fatty acid secretion, and fatty liver*. J Biol Chem, 2003. **278**(38): p. 36652-60.
55. Smas, C.M., et al., *Transcriptional control of the pref-1 gene in 3T3-L1 adipocyte differentiation. Sequence requirement for differentiation-dependent suppression*. J Biol Chem, 1998. **273**(48): p. 31751-8.
56. Smas, C.M. and H.S. Sul, *Pref-1, a protein containing EGF-like repeats, inhibits adipocyte differentiation*. Cell, 1993. **73**(4): p. 725-34.
57. Moon, Y.S., et al., *Mice lacking paternally expressed Pref-1/Dlk1 display growth retardation and accelerated adiposity*. Mol Cell Biol, 2002. **22**(15): p. 5585-92.
58. Lee, K., et al., *Inhibition of adipogenesis and development of glucose intolerance by soluble preadipocyte factor-1 (Pref-1)*. J Clin Invest, 2003. **111**(4): p. 453-61.
59. Tchoukalova, Y., C. Koutsari, and M. Jensen, *Committed subcutaneous preadipocytes are reduced in human obesity*. Diabetologia, 2007. **50**(1): p. 151-7.
60. Zechner, R., et al., *Lipolysis: pathway under construction*. Curr Opin Lipidol, 2005. **16**(3): p. 333-40.
61. Simsolo, R.B., J.M. Ong, and P.A. Kern, *The regulation of adipose tissue and muscle lipoprotein lipase in runners by detraining*. J Clin Invest, 1993. **92**(5): p. 2124-30.
62. Eckel, R.H., *Lipoprotein lipase. A multifunctional enzyme relevant to common metabolic diseases*. N Engl J Med, 1989. **320**(16): p. 1060-8.
63. Ong, J.M. and P.A. Kern, *Effect of feeding and obesity on lipoprotein lipase activity, immunoreactive protein, and messenger RNA levels in human adipose tissue*. J Clin Invest, 1989. **84**(1): p. 305-11.
64. Pykalisto, O.J., P.H. Smith, and J.D. Brunzell, *Determinants of human adipose tissue lipoprotein lipase. Effect of diabetes and obesity on basal- and diet-induced activity*. J Clin Invest, 1975. **56**(5): p. 1108-17.
65. Kern, P.A., et al., *The effects of weight loss on the activity and expression of adipose-tissue lipoprotein lipase in very obese humans*. N Engl J Med, 1990. **322**(15): p. 1053-9.
66. Schwartz, R.S. and J.D. Brunzell, *Increase of adipose tissue lipoprotein lipase activity with weight loss*. J Clin Invest, 1981. **67**(5): p. 1425-30.
67. Kennedy, D.J., et al., *A CD36-dependent pathway enhances macrophage and adipose tissue inflammation and impairs insulin signalling*. Cardiovasc Res, 2011. **89**(3): p. 604-13.
68. Ma, X., et al., *A common haplotype at the CD36 locus is associated with high free fatty acid levels and increased cardiovascular risk in Caucasians*. Hum Mol Genet, 2004. **13**(19): p. 2197-205.
69. Morii, T., et al., *CD36 single nucleotide polymorphism is associated with variation in low-density lipoprotein-cholesterol in young Japanese men*. Biomarkers, 2009. **14**(4): p. 207-12.
70. Maeda, K., et al., *Role of the fatty acid binding protein mall in obesity and insulin resistance*. Diabetes, 2003. **52**(2): p. 300-7.
71. Black, P.N., et al., *Targeting the fatty acid transport proteins (FATP) to understand the mechanisms linking fatty acid transport to metabolism*. Immunol Endocr Metab Agents Med Chem, 2009. **9**(1): p. 11-17.

72. Girisuse, A., et al., *Partial inhibition of adipose tissue lipolysis improves glucose metabolism and insulin sensitivity without alteration of fat mass*. PLoS Biol, 2013. **11**(2): p. e1001485.
73. Morigny, P., et al., *Adipocyte lipolysis and insulin resistance*. Biochimie, 2016. **125**: p. 259-66.
74. Arner, P., et al., *The antilipolytic effect of insulin in human adipose tissue in obesity, diabetes mellitus, hyperinsulinemia, and starvation*. Metabolism, 1981. **30**(8): p. 753-60.
75. Campbell, P.J., M.G. Carlson, and N. Nurjhan, *Fat metabolism in human obesity*. Am J Physiol, 1994. **266**(4 Pt 1): p. E600-5.
76. Groop, L.C., et al., *Effect of insulin on oxidative and nonoxidative pathways of free fatty acid metabolism in human obesity*. Am J Physiol, 1992. **263**(1 Pt 1): p. E79-84.
77. Robinson, C., et al., *Effect of insulin on glycerol production in obese adolescents*. Am J Physiol, 1998. **274**(4 Pt 1): p. E737-43.
78. Arner, P., *Human fat cell lipolysis: biochemistry, regulation and clinical role*. Best Pract Res Clin Endocrinol Metab, 2005. **19**(4): p. 471-82.
79. Shepherd, P.R. and B.B. Kahn, *Glucose transporters and insulin action--implications for insulin resistance and diabetes mellitus*. N Engl J Med, 1999. **341**(4): p. 248-57.
80. Shepherd, P.R., et al., *Adipose cell hyperplasia and enhanced glucose disposal in transgenic mice overexpressing GLUT4 selectively in adipose tissue*. J Biol Chem, 1993. **268**(30): p. 22243-6.
81. Thiebaud, D., et al., *The effect of graded doses of insulin on total glucose uptake, glucose oxidation, and glucose storage in man*. Diabetes, 1982. **31**(11): p. 957-63.
82. Kahn, B.B., *Lilly lecture 1995. Glucose transport: pivotal step in insulin action*. Diabetes, 1996. **45**(11): p. 1644-54.
83. Pedersen, O., C.R. Kahn, and B.B. Kahn, *Divergent regulation of the Glut 1 and Glut 4 glucose transporters in isolated adipocytes from Zucker rats*. J Clin Invest, 1992. **89**(6): p. 1964-73.
84. Abel, E.D., et al., *Adipose-selective targeting of the GLUT4 gene impairs insulin action in muscle and liver*. Nature, 2001. **409**(6821): p. 729-33.
85. Carvalho, E., et al., *Adipose-specific overexpression of GLUT4 reverses insulin resistance and diabetes in mice lacking GLUT4 selectively in muscle*. Am J Physiol Endocrinol Metab, 2005. **289**(4): p. E551-61.
86. Unger, R.H. and S. Grundy, *Hyperglycaemia as an inducer as well as a consequence of impaired islet cell function and insulin resistance: implications for the management of diabetes*. Diabetologia, 1985. **28**(3): p. 119-21.
87. Unger, R.H. and L. Orci, *Diseases of liporegulation: new perspective on obesity and related disorders*. FASEB J, 2001. **15**(2): p. 312-21.
88. McGarry, J.D., *Banting lecture 2001: dysregulation of fatty acid metabolism in the etiology of type 2 diabetes*. Diabetes, 2002. **51**(1): p. 7-18.
89. Prentki, M., et al., *Malonyl-CoA signaling, lipid partitioning, and glucolipotoxicity: role in beta-cell adaptation and failure in the etiology of diabetes*. Diabetes, 2002. **51 Suppl 3**: p. S405-13.
90. Marchesini, G., et al., *Nonalcoholic fatty liver disease: a feature of the metabolic syndrome*. Diabetes, 2001. **50**(8): p. 1844-50.
91. Schreuder, T.C., et al., *Nonalcoholic fatty liver disease: an overview of current insights in pathogenesis, diagnosis and treatment*. World J Gastroenterol, 2008. **14**(16): p. 2474-86.
92. Haas, M.E., A.D. Attie, and S.B. Biddinger, *The regulation of ApoB metabolism by insulin*. Trends Endocrinol Metab, 2013. **24**(8): p. 391-7.
93. Zeb, I., et al., *Relation of nonalcoholic fatty liver disease to the metabolic syndrome: the Multi-Ethnic Study of Atherosclerosis*. J Cardiovasc Comput Tomogr, 2013. **7**(5): p. 311-8.
94. Razak, F. and S.S. Anand, *Impaired mitochondrial activity in the insulin-resistant offspring of patients with type 2 diabetes*. Petersen KF, Dufour S, Befroy D, Garcia R, Shulman GI. N Engl J Med 2004; 350: 664-71. Vasc Med, 2004. **9**(3): p. 223-4.

95. Koo, S.H., *Nonalcoholic fatty liver disease: molecular mechanisms for the hepatic steatosis*. Clin Mol Hepatol, 2013. **19**(3): p. 210-5.
96. Scheller, J., et al., *The pro- and anti-inflammatory properties of the cytokine interleukin-6*. Biochim Biophys Acta, 2011. **1813**(5): p. 878-88.
97. O'Neill, H.M., *AMPK and Exercise: Glucose Uptake and Insulin Sensitivity*. Diabetes Metab J, 2013. **37**(1): p. 1-21.
98. Pedersen, B.K., A. Steensberg, and P. Schjerling, *Muscle-derived interleukin-6: possible biological effects*. J Physiol, 2001. **536**(Pt 2): p. 329-37.
99. Pedersen, B.K., et al., *Searching for the exercise factor: is IL-6 a candidate?* J Muscle Res Cell Motil, 2003. **24**(2-3): p. 113-9.
100. Wallenius, V., et al., *Interleukin-6-deficient mice develop mature-onset obesity*. Nat Med, 2002. **8**(1): p. 75-9.
101. Banks, W.A., A.J. Kastin, and E.G. Gutierrez, *Penetration of interleukin-6 across the murine blood-brain barrier*. Neurosci Lett, 1994. **179**(1-2): p. 53-6.
102. Markan, K.R., et al., *Circulating FGF21 is liver derived and enhances glucose uptake during refeeding and overfeeding*. Diabetes, 2014. **63**(12): p. 4057-63.
103. Mashili, F.L., et al., *Direct effects of FGF21 on glucose uptake in human skeletal muscle: implications for type 2 diabetes and obesity*. Diabetes Metab Res Rev, 2011. **27**(3): p. 286-97.
104. Kharitononkov, A., et al., *FGF-21 as a novel metabolic regulator*. J Clin Invest, 2005. **115**(6): p. 1627-35.
105. Kharitononkov, A. and A.B. Shanafelt, *FGF21: a novel prospect for the treatment of metabolic diseases*. Curr Opin Investig Drugs, 2009. **10**(4): p. 359-64.
106. Sarr, O., et al., *Subcutaneous and Visceral Adipose Tissue Secretions from Extremely Obese Men and Women both Acutely Suppress Muscle Insulin Signaling*. Int J Mol Sci, 2017. **18**(5).
107. Coskun, T., et al., *Fibroblast growth factor 21 corrects obesity in mice*. Endocrinology, 2008. **149**(12): p. 6018-27.
108. Itoh, N., *FGF21 as a Hepatokine, Adipokine, and Myokine in Metabolism and Diseases*. Front Endocrinol (Lausanne), 2014. **5**: p. 107.
109. Choe, S.S., et al., *Adipose Tissue Remodeling: Its Role in Energy Metabolism and Metabolic Disorders*. Front Endocrinol (Lausanne), 2016. **7**: p. 30.
110. Frayn, K.N., et al., *Integrative physiology of human adipose tissue*. Int J Obes Relat Metab Disord, 2003. **27**(8): p. 875-88.
111. Lean, M.E. and D. Malkova, *Altered gut and adipose tissue hormones in overweight and obese individuals: cause or consequence?* Int J Obes (Lond), 2016. **40**(4): p. 622-32.
112. Jung, U.J. and M.S. Choi, *Obesity and its metabolic complications: the role of adipokines and the relationship between obesity, inflammation, insulin resistance, dyslipidemia and nonalcoholic fatty liver disease*. Int J Mol Sci, 2014. **15**(4): p. 6184-223.
113. Ahima, R.S. and S.Y. Osei, *Adipokines in obesity*. Front Horm Res, 2008. **36**: p. 182-97.
114. Zhang, Y., et al., *Positional cloning of the mouse obese gene and its human homologue*. Nature, 1994. **372**(6505): p. 425-32.
115. Considine, R.V., et al., *Serum immunoreactive-leptin concentrations in normal-weight and obese humans*. N Engl J Med, 1996. **334**(5): p. 292-5.
116. Clapham, J.C., et al., *Plasma leptin concentrations and OB gene expression in subcutaneous adipose tissue are not regulated acutely by physiological hyperinsulinaemia in lean and obese humans*. Int J Obes Relat Metab Disord, 1997. **21**(3): p. 179-83.
117. Karhunen, L., et al., *Serum leptin and short-term regulation of eating in obese women*. Clin Sci (Lond), 1997. **92**(6): p. 573-8.
118. Guerci, B., et al., *No acute response of leptin to an oral fat load in obese patients and during circadian rhythm in healthy controls*. Eur J Endocrinol, 2000. **143**(5): p. 649-55.
119. Vidal, H., et al., *The expression of ob gene is not acutely regulated by insulin and fasting in human abdominal subcutaneous adipose tissue*. J Clin Invest, 1996. **98**(2): p. 251-5.
120. Korek, E., et al., *Fasting and postprandial levels of ghrelin, leptin and insulin in lean, obese and anorexic subjects*. Prz Gastroenterol, 2013. **8**(6): p. 383-9.

121. Coradini, M., et al., *Fat mass, and not diet, has a large effect on postprandial leptin but not on adiponectin concentrations in cats*. *Domest Anim Endocrinol*, 2013. **45**(2): p. 79-88.
122. Mueller, W.M., et al., *Evidence that glucose metabolism regulates leptin secretion from cultured rat adipocytes*. *Endocrinology*, 1998. **139**(2): p. 551-8.
123. Wellhoener, P., et al., *Glucose metabolism rather than insulin is a main determinant of leptin secretion in humans*. *J Clin Endocrinol Metab*, 2000. **85**(3): p. 1267-71.
124. Duncan, I.J., *Designing environments for animals--not for public perceptions*. *Br Vet J*, 1992. **148**(6): p. 475-7.
125. Curat, C.A., et al., *From blood monocytes to adipose tissue-resident macrophages: induction of diapedesis by human mature adipocytes*. *Diabetes*, 2004. **53**(5): p. 1285-92.
126. Hotamisligil, G.S., N.S. Shargill, and B.M. Spiegelman, *Adipose expression of tumor necrosis factor-alpha: direct role in obesity-linked insulin resistance*. *Science*, 1993. **259**(5091): p. 87-91.
127. Moller, D.E., *Potential role of TNF-alpha in the pathogenesis of insulin resistance and type 2 diabetes*. *Trends Endocrinol Metab*, 2000. **11**(6): p. 212-7.
128. Fain, J.N., et al., *Comparison of the release of adipokines by adipose tissue, adipose tissue matrix, and adipocytes from visceral and subcutaneous abdominal adipose tissues of obese humans*. *Endocrinology*, 2004. **145**(5): p. 2273-82.
129. Sell, H. and J. Eckel, *Chemotactic cytokines, obesity and type 2 diabetes: in vivo and in vitro evidence for a possible causal correlation?* *Proc Nutr Soc*, 2009. **68**(4): p. 378-84.
130. Herder, C., et al., *Chemokines as risk factors for type 2 diabetes: results from the MONICA/KORA Augsburg study, 1984-2002*. *Diabetologia*, 2006. **49**(5): p. 921-9.
131. Schernthaner, G.H., et al., *Effect of massive weight loss induced by bariatric surgery on serum levels of interleukin-18 and monocyte-chemoattractant-protein-1 in morbid obesity*. *Obes Surg*, 2006. **16**(6): p. 709-15.
132. Zhang, H.H., et al., *Tumor necrosis factor-alpha stimulates lipolysis in differentiated human adipocytes through activation of extracellular signal-related kinase and elevation of intracellular cAMP*. *Diabetes*, 2002. **51**(10): p. 2929-35.
133. Wang, Y., et al., *Perilipin expression in human adipose tissues: effects of severe obesity, gender, and depot*. *Obes Res*, 2003. **11**(8): p. 930-6.
134. Ryden, M., et al., *Mapping of early signaling events in tumor necrosis factor-alpha-mediated lipolysis in human fat cells*. *J Biol Chem*, 2002. **277**(2): p. 1085-91.
135. Wang, B., J.R. Jenkins, and P. Trayhurn, *Expression and secretion of inflammation-related adipokines by human adipocytes differentiated in culture: integrated response to TNF-alpha*. *Am J Physiol Endocrinol Metab*, 2005. **288**(4): p. E731-40.
136. Xu, H., et al., *Chronic inflammation in fat plays a crucial role in the development of obesity-related insulin resistance*. *J Clin Invest*, 2003. **112**(12): p. 1821-30.
137. Steppan, C.M., et al., *The hormone resistin links obesity to diabetes*. *Nature*, 2001. **409**(6818): p. 307-12.
138. Qatanani, M., et al., *Macrophage-derived human resistin exacerbates adipose tissue inflammation and insulin resistance in mice*. *J Clin Invest*, 2009. **119**(3): p. 531-9.
139. Lihn, A.S., S.B. Pedersen, and B. Richelsen, *Adiponectin: action, regulation and association to insulin sensitivity*. *Obes Rev*, 2005. **6**(1): p. 13-21.
140. Yamauchi, T., et al., *Adiponectin stimulates glucose utilization and fatty-acid oxidation by activating AMP-activated protein kinase*. *Nat Med*, 2002. **8**(11): p. 1288-95.
141. Marinou, K., et al., *Obesity and cardiovascular disease: from pathophysiology to risk stratification*. *Int J Cardiol*, 2010. **138**(1): p. 3-8.
142. Ouwens, D.M., et al., *The role of epicardial and perivascular adipose tissue in the pathophysiology of cardiovascular disease*. *J Cell Mol Med*, 2010. **14**(9): p. 2223-34.
143. Frankel, D.S., et al., *Resistin, adiponectin, and risk of heart failure the Framingham offspring study*. *J Am Coll Cardiol*, 2009. **53**(9): p. 754-62.
144. Goldstein, B.J., R.G. Scalia, and X.L. Ma, *Protective vascular and myocardial effects of adiponectin*. *Nat Clin Pract Cardiovasc Med*, 2009. **6**(1): p. 27-35.
145. Bluher, M., *The distinction of metabolically 'healthy' from 'unhealthy' obese individuals*. *Curr Opin Lipidol*, 2010. **21**(1): p. 38-43.

146. Kloting, N., et al., *Insulin-sensitive obesity*. Am J Physiol Endocrinol Metab, 2010. **299**(3): p. E506-15.
147. Yki-Jarvinen, H., *Ectopic fat accumulation: an important cause of insulin resistance in humans*. J R Soc Med, 2002. **95 Suppl 42**: p. 39-45.
148. Joffe, B.I., V.R. Panz, and F.J. Raal, *From lipodystrophy syndromes to diabetes mellitus*. The Lancet, 2001. **357**(9266): p. 1379-1381.
149. Lee, H.J., S. Patel, and S.J. Lee, *Intravesicular localization and exocytosis of alpha-synuclein and its aggregates*. J Neurosci, 2005. **25**(25): p. 6016-24.
150. Rohrborn, D., J. Eckel, and H. Sell, *Shedding of dipeptidyl peptidase 4 is mediated by metalloproteases and up-regulated by hypoxia in human adipocytes and smooth muscle cells*. FEBS Lett, 2014. **588**(21): p. 3870-7.
151. Rabouille, C., V. Malhotra, and W. Nickel, *Diversity in unconventional protein secretion*. J Cell Sci, 2012. **125**(Pt 22): p. 5251-5.
152. Petersen, T.N., et al., *SignalP 4.0: discriminating signal peptides from transmembrane regions*. Nat Methods, 2011. **8**(10): p. 785-6.
153. Bendtsen, J.D., et al., *Feature-based prediction of non-classical and leaderless protein secretion*. Protein Eng Des Sel, 2004. **17**(4): p. 349-56.
154. Le Bihan, M.C., et al., *In-depth analysis of the secretome identifies three major independent secretory pathways in differentiating human myoblasts*. J Proteomics, 2012. **77**: p. 344-56.
155. Anderson, N.L. and N.G. Anderson, *The human plasma proteome: history, character, and diagnostic prospects*. Mol Cell Proteomics, 2002. **1**(11): p. 845-67.
156. Frobel, J., et al., *Deep serum discoveries: SDF-1alpha and HSA fragments in myelodysplastic syndromes*. Am J Hematol, 2015. **90**(9): p. E185-7.
157. Gianazza, E., et al., *With or without you - Proteomics with or without major plasma/serum proteins*. J Proteomics, 2016. **140**: p. 62-80.
158. Ong, S.E., et al., *Stable isotope labeling by amino acids in cell culture, SILAC, as a simple and accurate approach to expression proteomics*. Mol Cell Proteomics, 2002. **1**(5): p. 376-86.
159. Vercauteren, F.G., et al., *Proteomic approaches in brain research and neuropharmacology*. Eur J Pharmacol, 2004. **500**(1-3): p. 385-98.
160. Van den Bergh, G. and L. Arckens, *Recent advances in 2D electrophoresis: an array of possibilities*. Expert Rev Proteomics, 2005. **2**(2): p. 243-52.
161. Gygi, S.P., et al., *Quantitative analysis of complex protein mixtures using isotope-coded affinity tags*. Nat Biotechnol, 1999. **17**(10): p. 994-9.
162. Ross, P.L., et al., *Multiplexed protein quantitation in Saccharomyces cerevisiae using amine-reactive isobaric tagging reagents*. Mol Cell Proteomics, 2004. **3**(12): p. 1154-69.
163. Alvarez-Llamas, G., et al., *Characterization of the human visceral adipose tissue secretome*. Mol Cell Proteomics, 2007. **6**(4): p. 589-600.
164. Zdychova, J., et al., *Co-cultivation of human aortic smooth muscle cells with epicardial adipocytes affects their proliferation rate*. Physiol Res, 2014. **63 Suppl 3**: p. S419-27.
165. Joshi, R.L., et al., *Targeted disruption of the insulin receptor gene in the mouse results in neonatal lethality*. EMBO J, 1996. **15**(7): p. 1542-7.
166. Bruning, J.C., et al., *A muscle-specific insulin receptor knockout exhibits features of the metabolic syndrome of NIDDM without altering glucose tolerance*. Mol Cell, 1998. **2**(5): p. 559-69.
167. Kulkarni, R.N., et al., *Tissue-specific knockout of the insulin receptor in pancreatic beta cells creates an insulin secretory defect similar to that in type 2 diabetes*. Cell, 1999. **96**(3): p. 329-39.
168. Bruning, J.C., et al., *Role of brain insulin receptor in control of body weight and reproduction*. Science, 2000. **289**(5487): p. 2122-5.
169. Laybutt, D.R., et al., *Overexpression of c-Myc in beta-cells of transgenic mice causes proliferation and apoptosis, downregulation of insulin gene expression, and diabetes*. Diabetes, 2002. **51**(6): p. 1793-804.
170. Graham, M., et al., *Overexpression of Agrt leads to obesity in transgenic mice*. Nat Genet, 1997. **17**(3): p. 273-4.

171. Patel, R., et al., *Mechanism of exocrine pancreatic insufficiency in streptozotocin-induced type 1 diabetes mellitus*. Ann N Y Acad Sci, 2006. **1084**: p. 71-88.
172. Mythili, M.D., et al., *Effect of streptozotocin on the ultrastructure of rat pancreatic islets*. Microsc Res Tech, 2004. **63**(5): p. 274-81.
173. Srinivasan, K., et al., *Combination of high-fat diet-fed and low-dose streptozotocin-treated rat: a model for type 2 diabetes and pharmacological screening*. Pharmacol Res, 2005. **52**(4): p. 313-20.
174. Gounarides, J.S., et al., *Effect of dexamethasone on glucose tolerance and fat metabolism in a diet-induced obesity mouse model*. Endocrinology, 2008. **149**(2): p. 758-66.
175. Melez, K.A., et al., *Diabetes is associated with autoimmunity in the New Zealand obese (NZO) mouse*. Diabetes, 1980. **29**(10): p. 835-40.
176. Subrahmanyam, K., *Metabolism in the New Zealand strain of obese mice*. Biochem J, 1960. **76**(3): p. 548-56.
177. Ingalls, A.M., M.M. Dickie, and G.D. Snell, *Obese, a new mutation in the house mouse*. J Hered, 1950. **41**(12): p. 317-8.
178. Mayer, J. and R.J. Barnett, *Sensitivity to cold in the hereditary obese-hyperglycemic syndrome of mice*. Yale J Biol Med, 1953. **26**(1): p. 38-45.
179. Coleman, D.L. and K.P. Hummel, *The influence of genetic background on the expression of the obese (Ob) gene in the mouse*. Diabetologia, 1973. **9**(4): p. 287-93.
180. Coleman, D.L., *Effects of parabiosis of obese with diabetes and normal mice*. Diabetologia, 1973. **9**(4): p. 294-8.
181. Tartaglia, L.A., et al., *Identification and expression cloning of a leptin receptor, OB-R*. Cell, 1995. **83**(7): p. 1263-71.
182. Dam, J. and R. Jockers, *Hunting for the functions of short leptin receptor isoforms*. Mol Metab, 2013. **2**(4): p. 327-8.
183. Osborn, O., et al., *Metabolic characterization of a mouse deficient in all known leptin receptor isoforms*. Cell Mol Neurobiol, 2010. **30**(1): p. 23-33.
184. Mao, H.Z., E.T. Roussos, and M. Peterfy, *Genetic analysis of the diabetes-prone C57BLKS/J mouse strain reveals genetic contribution from multiple strains*. Biochim Biophys Acta, 2006. **1762**(4): p. 440-6.
185. Choi, B.C. and F. Shi, *Risk factors for diabetes mellitus by age and sex: results of the National Population Health Survey*. Diabetologia, 2001. **44**(10): p. 1221-31.
186. Spector, T.D. and D.R. Blake, *Effect of cigarette smoking on Langerhans' cells*. Lancet, 1988. **2**(8618): p. 1028.
187. Cho, N.H., et al., *Cigarette smoking is an independent risk factor for type 2 diabetes: a four-year community-based prospective study*. Clin Endocrinol (Oxf), 2009. **71**(5): p. 679-85.
188. Haslam, D.W. and W.P. James, *Obesity*. Lancet, 2005. **366**(9492): p. 1197-209.
189. Wahrenberg, H., et al., *Use of waist circumference to predict insulin resistance: retrospective study*. BMJ, 2005. **330**(7504): p. 1363-4.
190. Wang, Y., et al., *Comparison of abdominal adiposity and overall obesity in predicting risk of type 2 diabetes among men*. Am J Clin Nutr, 2005. **81**(3): p. 555-63.
191. Prasad, R.B. and L. Groop, *Genetics of type 2 diabetes-pitfalls and possibilities*. Genes (Basel), 2015. **6**(1): p. 87-123.
192. Pancoska, P., et al., *Family networks of obesity and type 2 diabetes in rural Appalachia*. Clin Transl Sci, 2009. **2**(6): p. 413-21.
193. Ali, O., *Genetics of type 2 diabetes*. World J Diabetes, 2013. **4**(4): p. 114-23.
194. Candib, L.M., *Obesity and diabetes in vulnerable populations: reflection on proximal and distal causes*. Ann Fam Med, 2007. **5**(6): p. 547-56.
195. Swenne, I. and A. Andersson, *Effect of genetic background on the capacity for islet cell replication in mice*. Diabetologia, 1984. **27**(4): p. 464-7.
196. Leiter, E.H., et al., *Physiologic and endocrinologic characterization of male sex-biased diabetes in C57BLKS/J mice congenic for the fat mutation at the carboxypeptidase E locus*. Endocrine, 1999. **10**(1): p. 57-66.

197. Prochazka, M., et al., *Estrone treatment dissociates primary versus secondary consequences of "diabetes" (db) gene expression in mice*. *Diabetes*, 1986. **35**(6): p. 725-8.
198. Goddeke, S., J. Kotzka, and S. Lehr, *Investigating the adipose tissue secretome: a protocol to generate high-quality samples appropriate for comprehensive proteomic profiling*. *Methods Mol Biol*, 2015. **1295**: p. 43-53.
199. Hartwig, S., et al., *Identification of novel adipokines differential regulated in C57BL/Ks and C57BL/6*. *Arch Physiol Biochem*, 2014. **120**(5): p. 208-15.
200. Lehr, S., et al., *Identification and validation of novel adipokines released from primary human adipocytes*. *Mol Cell Proteomics*, 2012. **11**(1): p. M111 010504.
201. Rademacher, D.J., A.P. Anderson, and R.E. Steinpreis, *Acute effects of amperozide and paroxetine on social cohesion in male conspecifics*. *Brain Res Bull*, 2002. **58**(2): p. 187-91.
202. Pellitteri-Hahn, M.C., et al., *Improved mass spectrometric proteomic profiling of the secretome of rat vascular endothelial cells*. *J Proteome Res*, 2006. **5**(10): p. 2861-4.
203. Cox, J. and M. Mann, *MaxQuant enables high peptide identification rates, individualized p.p.b.-range mass accuracies and proteome-wide protein quantification*. *Nat Biotechnol*, 2008. **26**(12): p. 1367-72.
204. Schaab, C., et al., *Analysis of high accuracy, quantitative proteomics data in the MaxQB database*. *Mol Cell Proteomics*, 2012. **11**(3): p. M111 014068.
205. Boutchueng-Djidjou, M., et al., *The last enzyme of the de novo purine synthesis pathway 5-aminoimidazole-4-carboxamide ribonucleotide formyltransferase/IMP cyclohydrolase (ATIC) plays a central role in insulin signaling and the Golgi/endosomes protein network*. *Mol Cell Proteomics*, 2015. **14**(4): p. 1079-92.
206. Kudrjashova, E., et al., *Expression of adhesion molecule T-cadherin is increased during neointima formation in experimental restenosis*. *Histochem Cell Biol*, 2002. **118**(4): p. 281-90.
207. Seino, Y., et al., *High molecular weight multimer form of adiponectin as a useful marker to evaluate insulin resistance and metabolic syndrome in Japanese men*. *Metabolism*, 2007. **56**(11): p. 1493-9.
208. Berx, G. and F. van Roy, *Involvement of members of the cadherin superfamily in cancer*. *Cold Spring Harb Perspect Biol*, 2009. **1**(6): p. a003129.
209. Ranscht, B. and M.T. Dours-Zimmermann, *T-cadherin, a novel cadherin cell adhesion molecule in the nervous system lacks the conserved cytoplasmic region*. *Neuron*, 1991. **7**(3): p. 391-402.
210. Ivanov, D., et al., *Expression of cell adhesion molecule T-cadherin in the human vasculature*. *Histochem Cell Biol*, 2001. **115**(3): p. 231-42.
211. Vestal, D.J. and B. Ranscht, *Glycosyl phosphatidylinositol--anchored T-cadherin mediates calcium-dependent, homophilic cell adhesion*. *J Cell Biol*, 1992. **119**(2): p. 451-61.
212. Koller, E. and B. Ranscht, *Differential targeting of T- and N-cadherin in polarized epithelial cells*. *J Biol Chem*, 1996. **271**(47): p. 30061-7.
213. Philippova, M.P., et al., *T-cadherin and signal-transducing molecules co-localize in caveolin-rich membrane domains of vascular smooth muscle cells*. *FEBS Lett*, 1998. **429**(2): p. 207-10.
214. Andreeva, A.V. and M.A. Kutuzov, *Cadherin 13 in cancer*. *Genes Chromosomes Cancer*, 2010. **49**(9): p. 775-90.
215. Ye, M., et al., *Role of CDH13 promoter methylation in the carcinogenesis, progression, and prognosis of colorectal cancer: A systematic meta-analysis under PRISMA guidelines*. *Medicine (Baltimore)*, 2017. **96**(4): p. e5956.
216. Yang, M. and J.Y. Park, *DNA methylation in promoter region as biomarkers in prostate cancer*. *Methods Mol Biol*, 2012. **863**: p. 67-109.
217. Ivanov, D., et al., *T-cadherin upregulation correlates with cell-cycle progression and promotes proliferation of vascular cells*. *Cardiovasc Res*, 2004. **64**(1): p. 132-43.

218. Qian, W.J., et al., *Quantitative proteome analysis of human plasma following in vivo lipopolysaccharide administration using 16O/18O labeling and the accurate mass and time tag approach*. Mol Cell Proteomics, 2005. **4**(5): p. 700-9.
219. Zhong, Y., et al., *Exogenous expression of H-cadherin in CHO cells regulates contact inhibition of cell growth by inducing p21 expression*. Int J Oncol, 2004. **24**(6): p. 1573-9.
220. Kuzmenko, Y.S., et al., *Density- and proliferation status-dependent expression of T-cadherin, a novel lipoprotein-binding glycoprotein: a function in negative regulation of smooth muscle cell growth?* FEBS Lett, 1998. **434**(1-2): p. 183-7.
221. Kyriakakis, E., et al., *T-Cadherin is an auxiliary negative regulator of EGFR pathway activity in cutaneous squamous cell carcinoma: impact on cell motility*. J Invest Dermatol, 2012. **132**(9): p. 2275-85.
222. Adachi, Y., et al., *An adiponectin receptor, T-cadherin, was selectively expressed in intratumoral capillary endothelial cells in hepatocellular carcinoma: possible cross talk between T-cadherin and FGF-2 pathways*. Virchows Arch, 2006. **448**(3): p. 311-8.
223. Kadowaki, T., et al., *Adiponectin and adiponectin receptors in insulin resistance, diabetes, and the metabolic syndrome*. J Clin Invest, 2006. **116**(7): p. 1784-92.
224. !!! INVALID CITATION !!! {Hug, 2004 #559; Kadowaki, 2006 #600}.
225. Parker-Duffen, J.L., et al., *T-cadherin is essential for adiponectin-mediated revascularization*. J Biol Chem, 2013. **288**(34): p. 24886-97.
226. Matsuda, K., et al., *Positive feedback regulation between adiponectin and T-cadherin impacts adiponectin levels in tissue and plasma of male mice*. Endocrinology, 2015. **156**(3): p. 934-46.
227. Pfaff, D., et al., *Plasma T-cadherin negatively associates with coronary lesion severity and acute coronary syndrome*. Eur Heart J Acute Cardiovasc Care, 2015. **4**(5): p. 410-8.
228. Denzel, M.S., et al., *T-cadherin is critical for adiponectin-mediated cardioprotection in mice*. J Clin Invest, 2010. **120**(12): p. 4342-52.
229. Kipmen-Korgun, D., et al., *T-cadherin mediates low-density lipoprotein-initiated cell proliferation via the Ca(2+)-tyrosine kinase-Erk1/2 pathway*. J Cardiovasc Pharmacol, 2005. **45**(5): p. 418-30.
230. Philippova, M., et al., *RhoA and Rac mediate endothelial cell polarization and detachment induced by T-cadherin*. FASEB J, 2005. **19**(6): p. 588-90.
231. Mandal, P., et al., *Molecular mechanism for adiponectin-dependent M2 macrophage polarization: link between the metabolic and innate immune activity of full-length adiponectin*. J Biol Chem, 2011. **286**(15): p. 13460-9.
232. Joshi, M.B., et al., *Integrin-linked kinase is an essential mediator for T-cadherin-dependent signaling via Akt and GSK3beta in endothelial cells*. FASEB J, 2007. **21**(12): p. 3083-95.
233. Chung, C.M., et al., *A genome-wide association study reveals a quantitative trait locus of adiponectin on CDH13 that predicts cardiometabolic outcomes*. Diabetes, 2011. **60**(9): p. 2417-23.
234. Hug, C., et al., *T-cadherin is a receptor for hexameric and high-molecular-weight forms of Acrp30/adiponectin*. Proc Natl Acad Sci U S A, 2004. **101**(28): p. 10308-13.
235. Zhang, X., et al., *Akt, FoxO and regulation of apoptosis*. Biochim Biophys Acta, 2011. **1813**(11): p. 1978-86.
236. Wang, H., et al., *T-cadherin deficiency increases vascular vulnerability in T2DM through impaired NO bioactivity*. Cardiovasc Diabetol, 2017. **16**(1): p. 12.
237. Fu, Y., et al., *Adiponectin promotes adipocyte differentiation, insulin sensitivity, and lipid accumulation*. J Lipid Res, 2005. **46**(7): p. 1369-79.
238. Kitamoto, A., et al., *CDH13 Polymorphisms are Associated with Adiponectin Levels and Metabolic Syndrome Traits Independently of Visceral Fat Mass*. J Atheroscler Thromb, 2016. **23**(3): p. 309-19.
239. Rashid, S. and J. Genest, *Effect of obesity on high-density lipoprotein metabolism*. Obesity (Silver Spring), 2007. **15**(12): p. 2875-88.
240. Tyrberg, B., et al., *T-cadherin (Cdh13) in association with pancreatic beta-cell granules contributes to second phase insulin secretion*. Islets, 2011. **3**(6): p. 327-37.

241. Wang, C., et al., *Adiponectin sensitizes insulin signaling by reducing p70 S6 kinase-mediated serine phosphorylation of IRS-1*. J Biol Chem, 2007. **282**(11): p. 7991-6.
242. Gray, S.L., et al., *Leptin deficiency unmasks the deleterious effects of impaired peroxisome proliferator-activated receptor gamma function (P465L PPARgamma) in mice*. Diabetes, 2006. **55**(10): p. 2669-77.
243. Kim, J.Y., et al., *Obesity-associated improvements in metabolic profile through expansion of adipose tissue*. J Clin Invest, 2007. **117**(9): p. 2621-37.
244. Rubina, K.A., et al., *T-Cadherin Expression in Melanoma Cells Stimulates Stromal Cell Recruitment and Invasion by Regulating the Expression of Chemokines, Integrins and Adhesion Molecules*. Cancers (Basel), 2015. **7**(3): p. 1349-70.
245. Philippova, M., et al., *A guide and guard: the many faces of T-cadherin*. Cell Signal, 2009. **21**(7): p. 1035-44.
246. Petersen, M.C. and G.I. Shulman, *Roles of Diacylglycerols and Ceramides in Hepatic Insulin Resistance*. Trends Pharmacol Sci, 2017. **38**(7): p. 649-665.
247. Sampson, S.R. and D.R. Cooper, *Specific protein kinase C isoforms as transducers and modulators of insulin signaling*. Mol Genet Metab, 2006. **89**(1-2): p. 32-47.
248. Itani, S.I., et al., *Lipid-induced insulin resistance in human muscle is associated with changes in diacylglycerol, protein kinase C, and IkkappaB-alpha*. Diabetes, 2002. **51**(7): p. 2005-11.
249. Kao, A.W., et al., *Aldolase mediates the association of F-actin with the insulin-responsive glucose transporter GLUT4*. J Biol Chem, 1999. **274**(25): p. 17742-7.
250. Miles, L.A., et al., *Role of cell-surface lysines in plasminogen binding to cells: identification of alpha-enolase as a candidate plasminogen receptor*. Biochemistry, 1991. **30**(6): p. 1682-91.
251. Redlitz, A., et al., *The role of an enolase-related molecule in plasminogen binding to cells*. Eur J Biochem, 1995. **227**(1-2): p. 407-15.
252. Schoenenberger, A.W., et al., *Gender-Specific Associations between Circulating T-Cadherin and High Molecular Weight-Adiponectin in Patients with Stable Coronary Artery Disease*. PLoS One, 2015. **10**(6): p. e0131140.
253. Greenberg, A.S. and M.S. Obin, *Obesity and the role of adipose tissue in inflammation and metabolism*. Am J Clin Nutr, 2006. **83**(2): p. 461S-465S.
254. Southgate, R.J., et al., *PGC-1alpha gene expression is down-regulated by Akt-mediated phosphorylation and nuclear exclusion of FoxO1 in insulin-stimulated skeletal muscle*. FASEB J, 2005. **19**(14): p. 2072-4.
255. Coll, T., et al., *Palmitate-mediated downregulation of peroxisome proliferator-activated receptor-gamma coactivator 1alpha in skeletal muscle cells involves MEK1/2 and nuclear factor-kappaB activation*. Diabetes, 2006. **55**(10): p. 2779-87.
256. Li, X., et al., *Akt/PKB regulates hepatic metabolism by directly inhibiting PGC-1alpha transcription coactivator*. Nature, 2007. **447**(7147): p. 1012-6.

# Danksagung

Mein Dank gilt Herrn Prof. Al-Hasani für die Bereitstellung des Themas, das fortwährende Interesse an dieser Arbeit und die konstruktiven Diskussionen, welche maßgeblich zum Gelingen dieser Arbeit beigetragen haben. Außerdem bedanke ich mich für die Möglichkeit an nationalen und internationalen Kongressen teilzunehmen.

Herrn Prof. Feldbrügge möchte ich für die Übernahme des Koreferats und das Interesse an meiner Arbeit danken.

Darüber hinaus bedanke ich mich bei allen Mitgliedern der Plattform Proteomanalyse. Sonja möchte ich für die schöne Zeit im Büro, ihre lieben Geschenke (ja, auch für die „Notschublade bei Unterzuckerung“) und natürlich ihre fachliche Hilfe danken. Stefan danke ich für seine Betreuung und das offene Ohr für jegliche Themen. Birgit und Jörg möchte ich auch ganz herzlich danken für die guten Ideen und aktive Hilfe im Endspurt meiner Arbeit. Des Weiteren möchte ich Sylvia danken, die mir mit ihrer fröhlichen Art und ihrem stets offenen Ohr den Laboralltag versüßt hat. Auch Waltraud und Martina danke ich sehr für ihre Hilfe bei allen Fragen im und rund um das Labor. Ganz besonders danke ich auch Ulli für ihre stetige Hilfe im Labor und Geduld bei sich wiederholenden Fragen oder nötigen Erinnerungen.

Ein großer Dank gilt allen (ehemaligen) und aktuellen Studenten und Doktoranden der Pathobiochemie ohne die die Kaffee- und Mittagspausen nur halb so schön gewesen wären. Der „Gentleman's Coffeeclub“, die „ilf güldenen zwülf“ und die Freundschaften die aus eben jenen entstanden waren mir wahrscheinlich die größte Hilfe und Freude dieser Zeit.

Nicht zuletzt danke ich Mama, Papa und Andre, die immer an mich geglaubt haben und ohne deren Unterstützung ich diesen Weg nicht hätte gehen können.

Nicht genug kann ich wahrscheinlich meiner Freundin Carina danken, die täglich allen meinen Geschichten gelauscht, die damit verbundenen Launen ertragen und alles immer wieder ins rechte Licht gerückt hat. Danke!

# Eidesstattliche Erklärung

Ich versichere an Eides Statt, dass die Dissertation von mir selbständig und ohne unzulässige fremde Hilfe unter Beachtung der „Grundsätze zur Sicherung guter wissenschaftlicher Praxis an der Heinrich-Heine-Universität Düsseldorf“ erstellt worden ist. Die Dissertation wurde in der vorgelegten oder in ähnlicher Form noch bei keiner anderen Institution eingereicht. Ich habe bisher keine erfolglosen Promotionsversuche unternommen.

(Simon Göddeke)

Düsseldorf, den 09.04.2018